

Synthesis of Bio-Derived Polyesters

Marcell Nicholas Dering Haslewood

Master of Science by Research

University of York

Chemistry

March 2022

Abstract

Ring opening copolymerisation of epoxides and anhydrides (ROCOP) shows promise as a greener method of synthesising polyesters with wide ranging functionality, but it is understood that all studies have been conducted in extreme anhydrous conditions. Herein is reported the use of ROCOP under bench-top conditions to prepare polyesters from a range of monomers, including some entirely bio-derived, with molecular weights up to 11.7 kDa and narrow dispersities. Organoinitiator N-N'-dicyclohexylurea (DCU), a cheap by-product of peptide synthesis, was found to be comparably efficient to traditional organometallic initiator salph-Al , and was used to synthesise bio-derived copolymers of epichlorohydrin (ECH) and itaconic anhydride (IA) with two targets for post-polymerisation modification. These were cross-linked with multifunctional diamines and polythiols by aza- and thio-Michael addition and nucleophilic substitution to form high molecular weight insoluble thermoset polymeric resins. It has also been shown that bio-derived monomers with multiple active sites can also be reacted using ROCOP, creating high molecular weight crosslinked product from two polyunsaturated oils.

Table of Contents

Abstract	- p. 2
Table of Contents	- p. 3
List of Tables, Figures and Schemes	- p. 5
Acknowledgements and Declaration	- p. 7
1. Introduction	- p. 8
1.1. Background	- p. 8
1.2. Synthesis of Polyesters	- p. 9
1.3. ROCOP of Epoxides & Anhydrides	- p. 10
1.3.1. Organometallic Initiators	- p. 10
1.3.2. Organo-Initiators	- p. 16
1.3.3. Bio-Derived Monomers	- p. 17
1.3.4. Post-Polymerisation Modification	- p. 19
1.4. This Project	- p. 22
2. Experimental	- p. 24
2.1. Reagents	- p. 24
2.2. Characterisation	- p. 24
2.3. Salophen Initiator Synthesis	- p. 25
2.3.1. Ligand Synthesis	- p. 25
2.3.2. Aluminium Metalation	- p. 26
2.3.3. Chromium Metalation	- p. 27
2.4. General Polymerisation Procedure	- p. 28
2.4.1 Multi-Epoxy Polymerisation Procedure	- p. 30
2.5. Crosslinking Procedure	- p. 30

3. Results & Discussion	- p. 32
3.1. Polyester Synthesis	- p. 32
3.1.1. Control Experiments	- p. 32
3.1.2. Polymerisation Reactions	- p. 34
3.1.3. Discussion of Results	- p. 37
3.1.4. Mechanism	- p. 44
3.1.5. Multi-Epoxy Polymerisation	- p. 46
3.2. Crosslinking by PPM	- p. 48
3.2.1. Discussion of Results	- p. 50
4. Conclusion	- p. 57
5. Future Work	- p. 59
6. References	- p. 60
7. Appendices	- p. 66

List of Tables, Figures and Schemes

Tables

Table 1. Control reactions with ROCOP initiators	- p. 33
Table 2. The effectiveness of initiators A, B and C at ROCOP	- p. 35
Table 3. Multi-epoxide polymerisations	- p. 48
Table 4. Crosslinking reactions with amines and thiols	- p. 50
Table 5. Elemental analysis of cross-linked material	- p. 53
Table 6. Ideal elemental composition assuming 100% crosslinking	- p. 53

Figures

Figure 1. Potentially renewable polyesters and polycarbonates	- p. 10
Figure 2. Simplified initiation and propagation cycle of ROP and ROCOP	- p. 11
Figure 3. Common monomers used in ROCOP	- p. 13
Figure 4. Al-porphyrin and Zn-BDI complexes	- p. 14
Figure 5. Salen complexes and co-initiators	- p. 15
Figure 6. Organo-initiators	- p. 17
Figure 7. Bio-derived platform molecules	- p. 19
Figure 8. Examples of PPM upon polyesters	- p. 21
Figure 9. LIFDI-MS spectra for Initiators A & B	- p. 32
Figure 10. Initiators A, B & C	- p. 33
Figure 11. ¹ H NMR spectrum of ECH-PA copolymer	- p. 39
Figure 12. Typical side reactions of itaconate esters	- p. 40
Figure 13. ¹ H NMR spectrum of ECH-IA copolymer	- p. 41
Figure 14. ¹ H NMR spectrum of IA and crude ECH-IA copolymer	- p. 42

Figure 15. DSC of ECH-PA copolymer	- p. 43
Figure 16. Simplified initiation and propagation cycle of ROCOP	- p. 45
Figure 17. Possible chain structures of epoxidised macaw oil	- p. 47
Figure 18. Amines and thiols investigated for crosslinking	- p. 49
Figure 19. Thermal degradation curve of CLDA15	- p. 52
Figure 20. IR spectra of crosslinked materials	- p. 55

Schemes

Scheme 1. Generalised chain transfer reaction	- p. 12
Scheme 2. Synthesis of ligand salph-H ₂	- p. 25
Scheme 3. Synthesis of salph-AlCl	- p. 26
Scheme 4. Synthesis of salph-CrCl	- p. 27
Scheme 5. Generalised copolymerisation reaction	- p. 28
Scheme 6. Generalised crosslinking reaction	- p. 30
Scheme 7. Copolymerisation reactions performed during testing	- p. 35

Acknowledgements and Declaration

The author would like to thank Prof. Mike North and the North group, Dr. Tom Farmer and Dr. Dan Day for invaluable guidance and forbearance, Mr. Ryan E. Barker for running solid state ^{13}C NMR spectroscopy, Dr. Richard Gammons and the technicians in Green Chemistry for their patience and willingness to help, Dr. Phil Helliwell and the staff of the teaching laboratory for running ^1H and ^{13}C NMR spectroscopy and helping me find my feet in the midst of the pandemic, Mr. Karl Heaton for running mass spectrometry experiments and Dr. Graeme McAllister for running elemental analyses.

I declare that this thesis is a presentation of original work and I am the sole author. This work has not previously been presented for an award at this, or any other, University. All sources are acknowledged as references.

1. Introduction

1.1. Background

Crude oil is the most common feedstock on the planet for the chemical industry, and is an essential part of modern life. Many things we rely on and on which our economy is based are derived from it, including ubiquitous polymers such as polyethylene (PE), polystyrene (PS), polypropylene (PP) and polyvinyl chloride (PVC). However, despite our ingenious efforts to extract the last drops of it from the Earth's crust, it will run out. This depletion could occur arguably in the next hundred years, and some estimate the peak in global oil production, so-called 'peak oil', to occur in the next couple of decades¹.

Crude oil-derived non-biodegradable polymers fill our oceans^{2,3}, with between 4-12 million tons of plastic entering them in 2010 alone⁴, building up into floating islands of up to 250,000 tons. Crude oil-derived fumes are well on their way to creating an environment which is less biodiverse, and more at risk of flooding, drought, storms and wildfires⁵. It is the cause of our current environmental crisis, and we must eliminate our dependence on it. Production of common, crude-oil derived polymers uses a substantial part of worldwide oil and gas production, around 7%⁶, and a vast amount of current research is focussed on replacing them. Prominent in this race are aliphatic polyesters; they are usually biodegradable, degrading by hydrolysis to products that are typically benign⁷, and have the potential to be sourced from biomass in an entirely carbon neutral process^{8,9}. Some polyesters suitable for commercial uses such as packaging are also biocompatible, meaning they can also be used for medical applications—and in the case of polylactide (PLA) and polyhydroxybutyrate (PHB) (Fig. 1), they already are, for example for wound dressings or sutures which degrade *in vivo* in a non-toxic manner¹⁰⁻

¹². The development of novel means to prepare bio-derived polyesters is therefore useful on several fronts and the need, as we have seen, is imperative.

1.2. Synthesis of Polyesters

Polyesters are typically made through step-growth polycondensation, a process which requires high temperature and reduced pressure resulting in a correspondingly high energy usage to remove the small-molecule by-products and to run the reaction to the high conversions necessary to create high molecular weight polymers. Further drawbacks include side reactions such as undesired chain-cleavage *via* transesterification, which make the molecular weight and dispersity hard to control¹³.

In contrast, chain-growth ring-opening polymerisation (ROP) (Fig. 2, Scheme A) of cyclic esters (lactones) gives no small-molecule by-products, requires comparatively mild conditions as high-molecular-weight polymers can be obtained at lower conversions, and in some cases offers precise control over chain length, microstructure and dispersity *via* a living polymerisation¹⁴. Naturally, this makes this method highly appealing for future development and a wide range of initiators have been studied^{10,15}, with several types of polyester such as PLA and poly- ϵ -caprolactone (PCL) (Fig. 1) already being produced by ROP on an industrial scale. There are, however major drawbacks; only a limited range of lactone monomers are available, some require tedious steps to synthesise, transesterification occurs at higher conversions and the resulting polymers often have few options for post-polymerisation modification¹⁴.

An intriguing alternative to ROP is alternating ring-opening copolymerisation (ROCOP) (Fig. 2, Scheme B), which is often performed with epoxides and CO₂ to create polycarbonates such as polypropylene carbonate (PPC) (Fig. 1), or alternatively epoxides and anhydrides to create polyesters. The latter reaction has mild conditions,

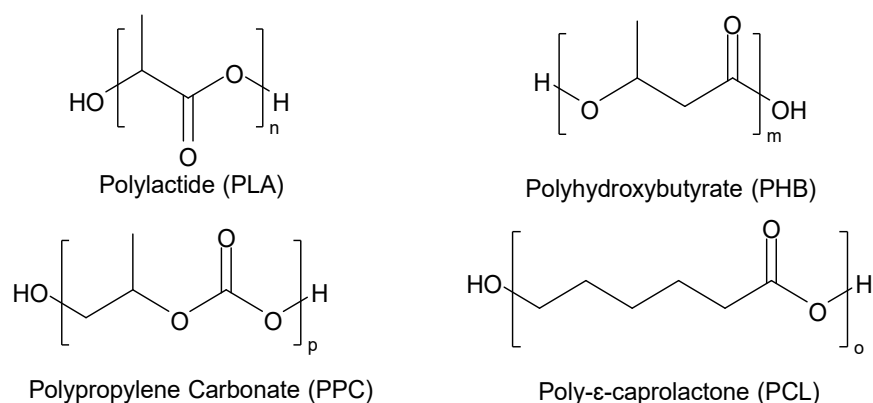


Figure 1 – Potentially renewable polyesters and polycarbonates

potential for a narrow dispersity and controllable chain length, as well as a wide range of monomers available as by-products from industrial processes or derivable from biomass^{8,16}. This immediately opens up many options for tuning properties, such as incorporating aromatic groups within an aliphatic polyester backbone, which is often difficult with polylactides. It also offers great potential for incorporating functional groups which could enable post-polymerisation modification in a facile manner.

1.3. ROCOP of Epoxides and Cyclic Anhydrides

1.3.1. Organometallic Initiators

ROCOP of epoxides and cyclic anhydrides was first demonstrated by Fischer in 1960 using dimethylbenzylamine, synthesising copolymers of 2.4-18.1 kDa¹⁷. Four years later, Tsuruta, Matsuura and Inoue demonstrated the first use of organometallic initiators for this reaction (ZnEt_2 , MgEt_2 , EtMgBr , CdEt_2 or $n\text{-BuLi}$) with a range of epoxides such as propylene oxide (PO), epichlorohydrin (ECH) and anhydrides such as norbornene anhydride (NA) and itaconic anhydride (IA)¹⁸ (Fig. 3). They also suggested an initiation step which has become the commonly accepted reaction mechanism following further research¹⁹, involving the activation by the Lewis acidic metal centre of

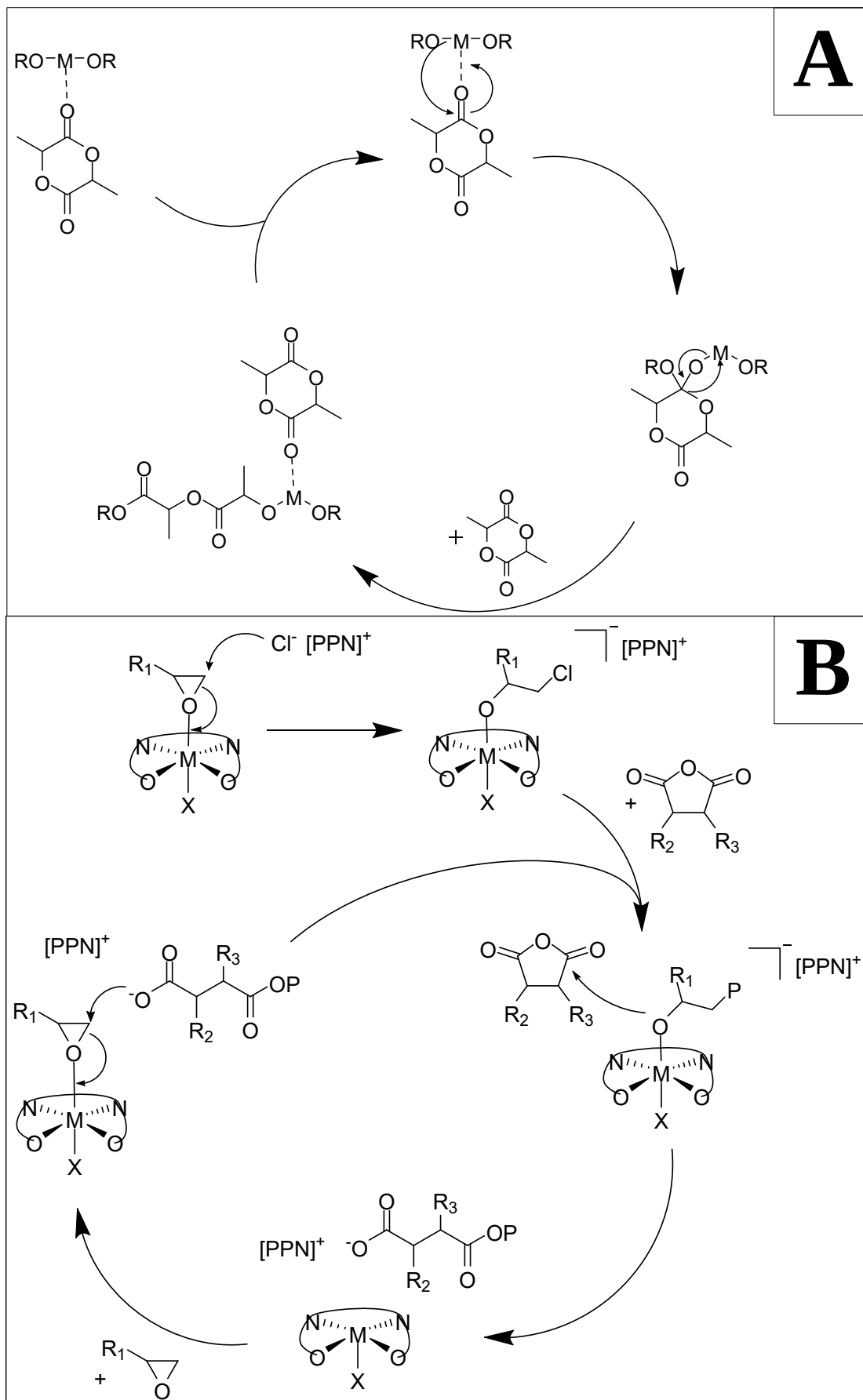
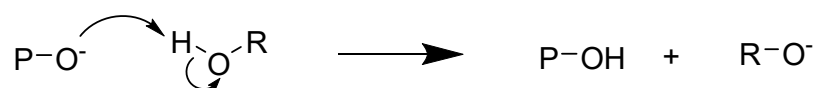


Figure 2 – Simplified initiation and propagation cycle of ROP and ROCOP with lactide and organometallic catalyst (eg SnOct_2) (Scheme A), and salophen initiator and PPNCl co-initiator (Scheme B), where X = halide, alkoxide or carboxylate and P = growing polymer chain

an epoxide monomer and its conversion into alkoxide, thus initiating propagation in an alternating fashion *via* alkoxide and carboxylate anions as identified by Fischer (Fig. 2, Scheme B). However, such early efforts were often hampered by low molecular weight products, a wide range of dispersity values, long reaction times – in the case of Tsuruta *et al.*, 7-9 days – and in some cases a high percentage of ether linkages compared to ester. Such wide variance from ideal molecular weights was identified to be due to the presence of hydroxyl—containing impurities, such as water or diacid, which undergo an unwanted chain-transfer reaction with the growing polymer chain in which the hydroxyl species is transferred to the propagating anion, terminating the growing polymer chain (Scheme 1). The former hydroxyl species becomes the new active anion, resulting in decreased molecular weights and a broad dispersity. For this reason, all ROCOP studies have been conducted in extreme anhydrous conditions, with the use of gloveboxes and extensive purification of reagents, in order to minimise the occurrence of chain transfer and maximise molecular weight of products.



Scheme 1 – Generalised chain transfer reaction in anionic polymerisation with a hydroxyl containing species R, where P is a growing polymer chain

Work proceeded slowly over the next decades with few notable advances, one exception being the usage by Aida and Inoue in 1985 of planar aluminium porphyrin initiators (Fig. 4) with tetraalkylammonium bromide co-initiators to copolymerise phthalic anhydride (PA) with various epoxides including PO, ethylene oxide (EO) and butylene oxide (BO)^{20,21}. Their pioneering work showed that the addition of a co-initiator increased the activity of organometallic complexes, and it could be argued that this was the first truly controlled reaction, with dispersities ranging only from 1.08-1.16 and no

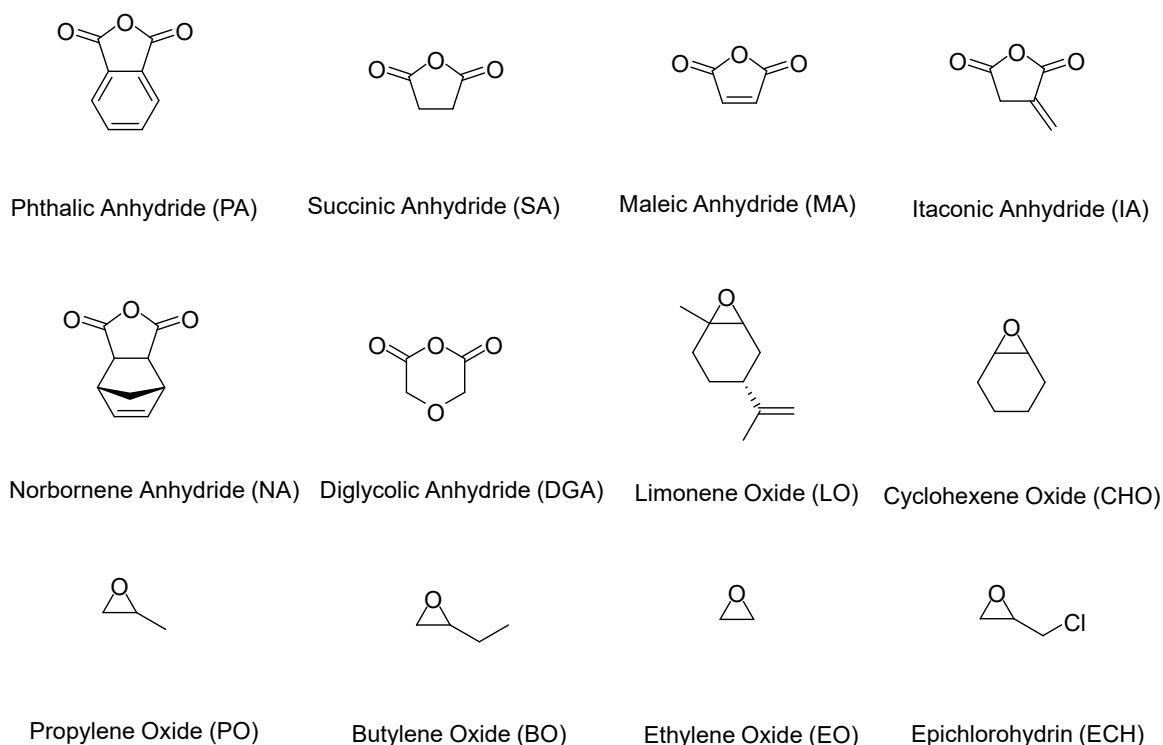


Figure 3 – Common monomers used in ROCOP

ether linkages. However, molecular weights remained under 4 kDa and long reaction times of 4-16 days were a persistent problem.

The next major development occurred in 2007, when Coates *et al.* used a zinc β -diiminato (BDI) complex (Fig. 4), which was already known to be active in epoxide- CO_2 copolymerisation reactions, and applied it to a wide range of epoxides and anhydrides including cyclohexene oxide (CHO), diglycolic anhydride (DGA) and the renewably-sourced limonene oxide (LO)²². They created the first high molecular weight epoxide-anhydride copolymer, with a molecular weight in excess of 55 kDa with some promising properties, including a high decomposition temperature around 290 °C.

Since then, the focus has shifted onto N,N'-bis(salicylidene)ethylenediamine, or salen complexes and their derivatives. The activity of these versatile initiators had already been recognised for polylactide²³, polyether²⁴ and polycarbonate²⁵ syntheses as well as many other reactions. Their first reported use for epoxide-anhydride copolymerisation

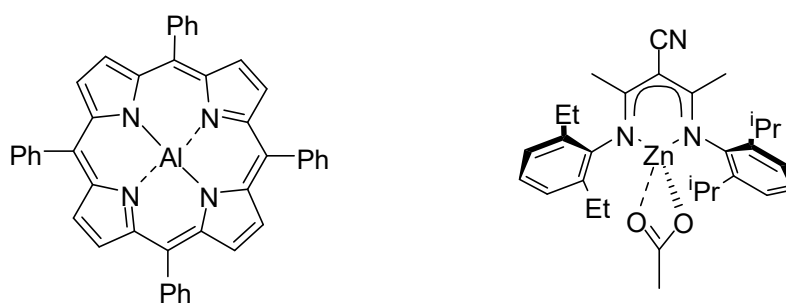
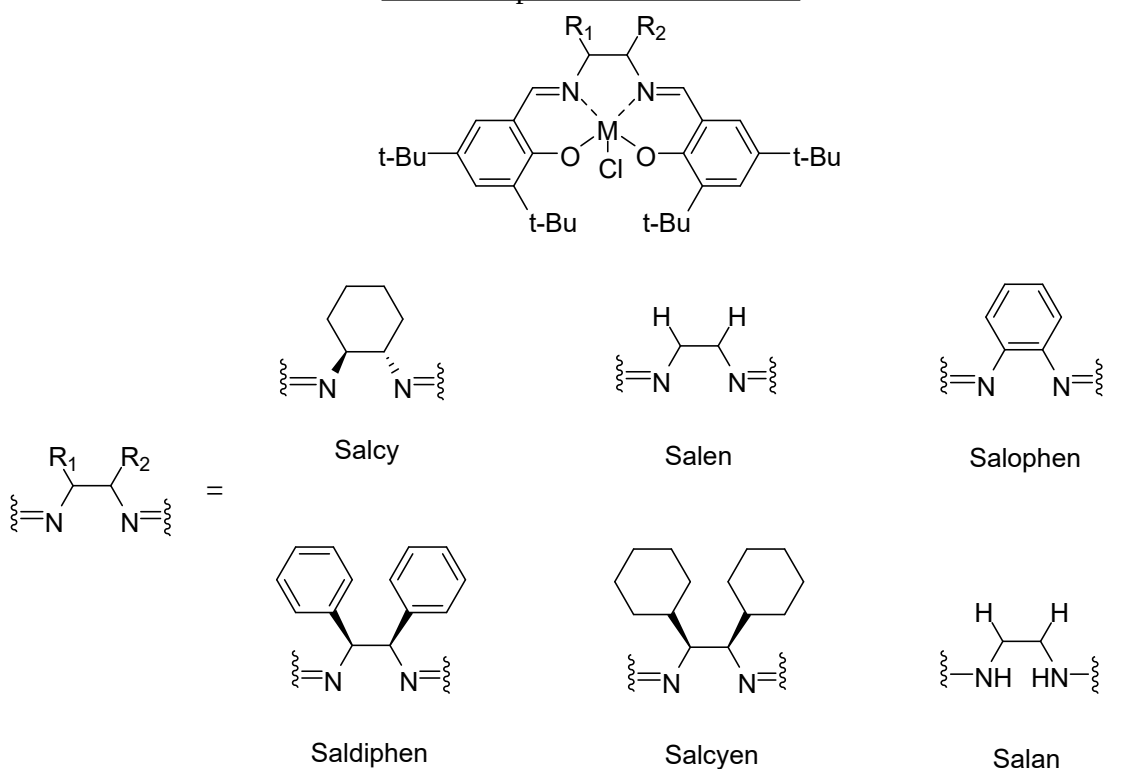


Figure 4 – Al-porphyrin (left) and Zn-BDI (right) metal complexes

came in 2011²⁶, and later that year Coates *et al.* compared the activity and selectivity of cobalt and chromium N,N'-bis(salicylidene)cyclohexanediamine (salcy) complexes (Fig. 5) with Zn-BDI and Al-porphyrin complexes and found a significantly higher activity in the copolymerisation of PO and maleic anhydride (MA) with negligible ether linkages using the chromium salcy complex²⁷. Since then, a wide range of metal salen complexes have been trialled in epoxide/anhydride copolymerisation—including aluminium^{28,29}, cobalt^{30,31}, chromium^{26,27}, manganese^{32,33} and iron³⁴—along with a similarly comprehensive range of salen derivatives. Duchateau *et al.* compared the activity of chromium, aluminium and cobalt salen derivatives with various diimine linkers, including salen, salophen, saldiphen and salcyen complexes (Fig. 5), and found that chromium salophen complexes exhibited the highest activity³⁰. This is likely because the aromatic ring in the backbone conveys more rigidity to the complex than other salen derivatives, and prevents it deforming and thus resulting in lower activity. The effect of substituents in the salen backbone has also been the subject of study, with both the diimine linkers and phenol rings coming under scrutiny. According to the mechanism proposed by Fieser *et al.* (Fig. 2, Scheme B), a carboxylate anion must dissociate from the metal centre for an epoxide to bind in its place and be ring-opened, thus propagating the reaction¹⁹. It then follows that the more Lewis acidic the metal, the slower this dissociation becomes, and the slower the reaction. Unsurprisingly, it has

Salen complexes and derivatives



Co-initiators

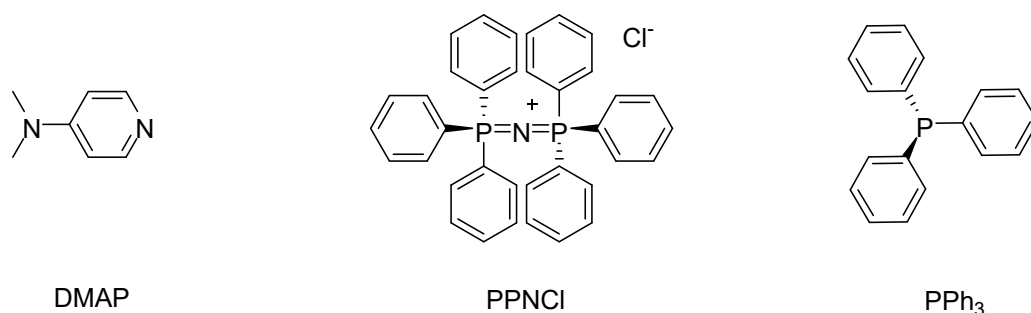


Figure 5 – Salen complexes and co-initiators

been found that electron-withdrawing substituents on the phenol moieties reduces activity by decreasing electron density at the metal centre, though it does reduce the rates of transesterification and epimerization side reactions²⁹. Conversely, electron donating substituents such as the commonly used tert-butyls in positions 3 and 5 increase the rate of reaction, though it has also been noted in a study by Darensbourg *et al.* that replacing tert-butyl substituents with more highly electron donating methoxy substituents decreases the solubility of the salen complex and hence it's overall activity,

even though it would increase the electron density of the metal centre³⁵. They also showed that sterically encumbering substituents on the diimine linker negatively affect activity.

Like the porphyrin initiator used by Aida and Inoue, it has been shown that a co-initiator is necessary when using salen-type initiators for ROCOP²⁶. Various co-initiators have been investigated including N-heterocyclic nucleophiles such as DMAP, phosphines such as PPh₃, and onium salts (Fig. 5); the latter have proven to be most effective, and most widely used is PPNCl, which is both highly active, widely available and non-interfering, unlike DMAP which can cause crosslinking when double bonds are present, for example in MA^{30,36}.

1.3.2. Organo-Initiators

Organo-initiation has been a relatively recent development in ROCOP, with fewer than 20 papers and one notable review having been published on the topic since its inception³⁷. Initially PPNCl (Fig. 5), the commonly-used co-initiator with metal complex initiators, was found to initiate ROCOP itself, though at lower rates compared to metal-initiated copolymerisation^{38,39}, by activation of the epoxide to the PPN⁺ cation and initiation by the chloride anion. However, its activity was discovered to markedly increase if combined with a Lewis acid such as triethylborane which took the role of the monomer activator, with the PPN⁺ cation returning to the role of large positively-charged counterion that it fills in metal-initiated systems (Fig. 2, Scheme B). The resulting system proved to be both highly selective and highly active⁴⁰, with TOF values of up to 330 h⁻¹. Since this discovery, organoboranes, onium salts and phosphazene bases (Fig. 6) have been explored in various Lewis acid-Lewis base pairings, with further high activities being achieved^{41,42}.

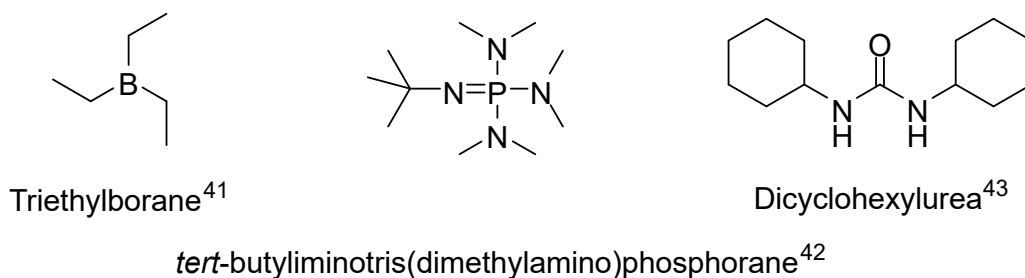


Figure 6 – Organo-initiators: boranes, phosphazenes and DCU

The most interesting development in this area has been the findings of Lin *et al.*⁴³ that if triethylborane is replaced with N,N'-dicyclohexylurea (DCU) (Fig. 6), a widely available by-product of organic reactions including Steglich esterification⁴⁴ and peptide synthesis coupling reactions⁴⁵, the activity of the system is favourably impacted, with TOF values of up to 456 h⁻¹ and high molecular weight polymers of up to 34.6 kDa produced. DCU had previously been known to be active in lactide ROP⁴⁶ in which it initiates the reaction by activating monomers with H-bond donation, and it is surmised that it acts in a similar way in ROCOP. This level of activity is comparable to the most active metal-based initiators, and the repurposing of a cheap, previously underutilised by-product has promising implications for greener pathways to polyester synthesis *via* ROCOP.

1.3.3. Bio-Derived Monomers

Due to the widely-recognised potential offered by ROCOP to replace non-renewable polyesters, considerable work has been undertaken in the area of bio-derived monomers. Of the wide range of epoxides this reaction has been demonstrated with, terpene- and glycerol-derived epoxides have been the most commonly used. Terpenes, such as limonene which can be extracted from citrus peels⁸ and α -pinene from pine oil⁴⁷, all feature double bonds which can be epoxidized (Fig. 7). In their pioneering 2007 work, Jeske *et al.* copolymerised LO with DGA to create high molecular weight polymers of

up to 36 kDa²², and terpene-based epoxides have featured heavily in ROCOP literature since^{28,32,48}.

Renewably sourced glycerol has seen a jump in supply as it is a by-product from the production of bio-diesel from feedstock such as rapeseed oil, which has triggered great interest in potential uses for this bio-derived material⁴⁹. It can be converted into epichlorohydrin by chlorinating using HCl then ring-closing by addition of a base, which is considerably more atom-economical than its industrial production from propene, generating only one equivalent of waste chloride instead of three⁵⁰. ECH itself has been used as a monomer for ROCOP^{18,42}, but it can also be converted into other monomers such as eugenyl glycidyl ether (EGE) or allyl glycidyl ether (AGE) by reaction with eugenol or allyl alcohol, also potentially renewably-sourced materials^{51,52}. Longer chain molecules featuring double bonds such as those derived from vegetable oils or sugars can also be epoxidized and used as monomers, though this is as of yet a mostly unexplored area of ROCOP. Takasu *et al.* demonstrated the epoxidization of carbohydrate-derived alkenes with pendant sugars, and their copolymerisation with potentially renewable succinic anhydride, to form low molecular weight polymers of up to 4.2 kDa⁵³. In addition, the production of 1,4-cyclohexadiene has been reported as a side product from olefin metathesis of polyunsaturated fatty acids, and this has been selectively epoxidized and hydrogenated to form cyclohexene oxide, implying that a more renewable process to form CHO could be viable⁵⁴.

Diacids such as succinic and itaconic acid (Fig. 7) can be isolated from the fermentation products of cheap carbohydrates such as glucose^{55,56}, which in the case of the latter is the preferred form of industrial production over the pyrolysis of citric acid⁵⁷. They can then be cyclised to form their respective anhydrides either by dehydration, or intriguingly by metal salens as demonstrated by Robert *et al.*²⁸ They reported a one-pot system in which

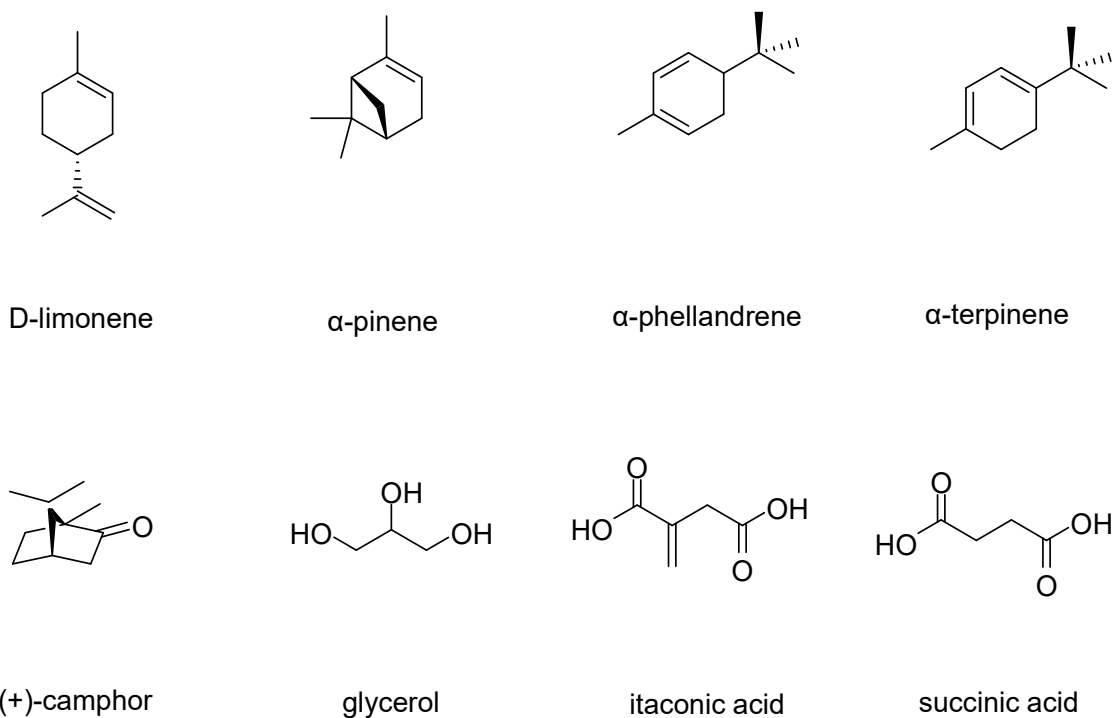


Figure 7 – Bio-derived platform molecules

renewable monomers such as camphoric acid were cyclised and immediately copolymerised *in situ* with renewable epoxides such as LO, which takes advantage of the versatility of salen initiators to present a promising route to atom-economical, green polymer synthesis.

Finally, terpenes have been a fruitful source of bio-derived anhydrides as well as epoxides, with bi- and tricyclic anhydrides being produced from renewable sources such as (+)-camphor, α -terpinene and α -phellandrine (Fig. 7) and subsequently polymerised to produce copolymers with T_g values of up to 109 °C^{28,58}. Interestingly, camphorate esters have also been used to partially replace non-renewable terephthalate units in PET with no noticeable decrease in physical properties⁵⁹.

1.3.4. Post-Polymerisation Modification

Post-polymerisation modification (PPM) allows for secondary groups to be introduced into an existing polymeric structure, thereby modifying its properties in desirable ways⁶⁰. Insoluble long chain polymers can be made soluble by the addition of hydroxyl

groups onto the backbone, or pliable, amorphous polymers can be made more rigid, such as the crosslinking of polyisoprene with sulphur i.e. the vulcanisation of rubber. To perform PPM, the requisite functional groups need to be present in the polymer and conditions need to be found such that PPM reactions take place without affecting the chain length. The first caveat can be overcome by the wide range of functionalised monomers available for ROCOP, but the second can be more difficult due to the susceptibility of polyesters to hydrolytic degradation. Several methods in particular have been shown to successfully circumvent this, and have had significant interest in recent years: thiol-ene click reactions, aza-Michael additions and olefin cross-metathesis (Fig. 8).

Thiol-ene click chemistry has been a major area of development into PPM of anhydride and epoxide copolymers as it is facile, extremely rapid and takes place under mild reaction conditions. It involves linking thiols with double bonds, usually initiated by radicals from a source such as azobisisobutylnitrile (AIBN), or by UV radiation. The primary receptor used in PPM of ROCOP products for thiol-ene click chemistry has been NA due to its electron-rich, available double bond^{38,61}, though it has also been demonstrated upon pendant vinyl groups with more limited effectiveness⁶². This type of PPM has successfully been employed to incorporate hydroxyl and amine functionality onto polyester chains, thus improving the molecular weight and changing its properties by making it water-soluble, and graft aromatic rings onto the polymeric backbone and thus improve its rigidity and T_g .

Aza-Michael additions onto electron-deficient double bonds are another promising route into post-polymerisation modification, with the double bond in itaconic anhydride being the most suitable target amongst bio-based monomers despite long reaction times (up to 3 days)⁶³. This is due to a side reaction in which amines, instead of adding onto the

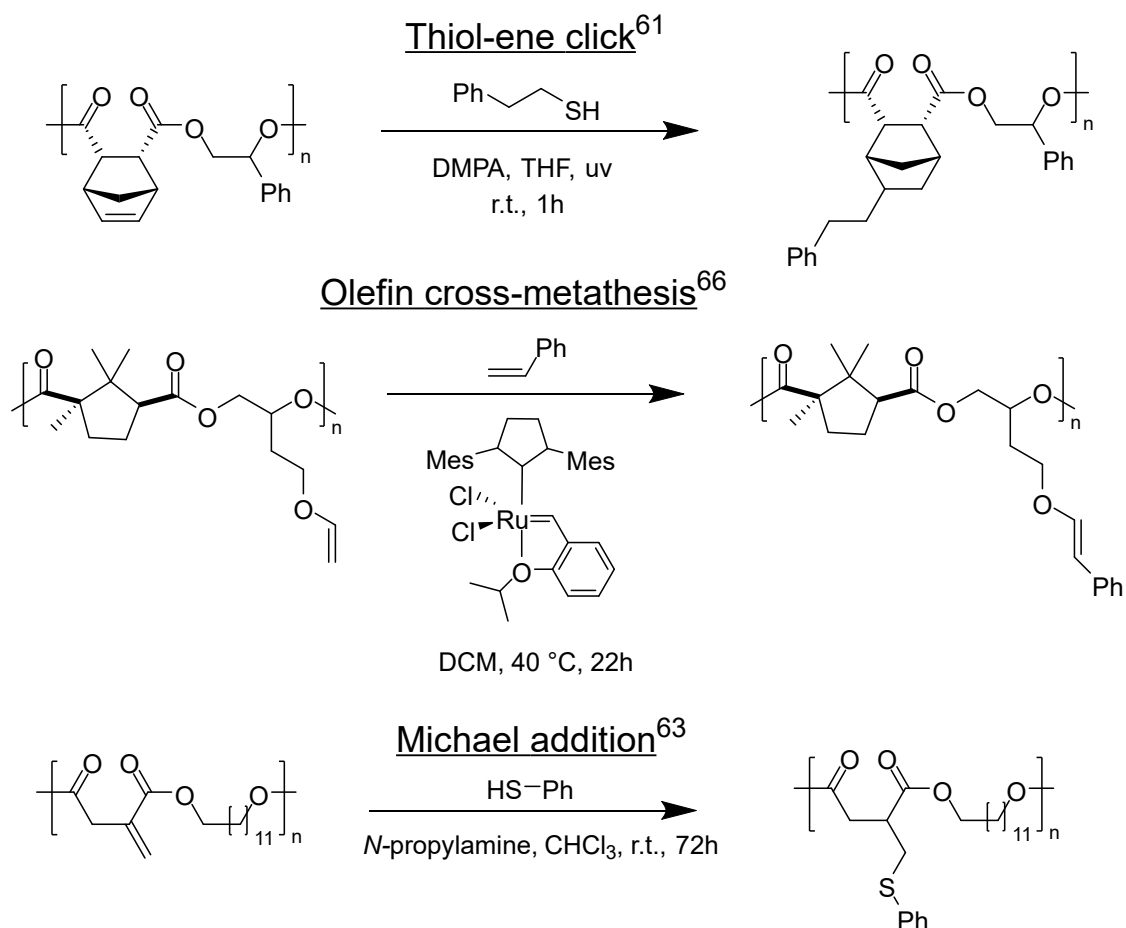


Figure 8 – Examples of PPM upon polyesters

double bond, convert itaconate esters into their less reactive mesaconate regioisomer⁶⁴. Using a strong base such as triazabicyclodecene (TBD) has completed the reaction in 1 minute, however strong bases also degrade the polyester backbone as a side reaction⁶⁵; in addition, the aza-Michael addition using TBD was performed on a maleate ester, so it is possible that adding a strong base to an itaconate ester could speed its regioisomerisation.

Hoveyda-Grubbs second and third generation catalysts have also been used to perform PPM on a range of polyesters by cross-metathesis, including introducing functionality to those featuring pendant vinyl groups⁶⁶. This has shown to be effective although reaction times were long, up to three days, to reach high conversions.

Branching and cross-linking using PPM has also been demonstrated on polyesters using several of these methods, including on some polymers created partially or fully from bio-derived materials. Multiple consecutive aza- or thio-Michael reactions using di- or poly-amines or thiols can create crosslinking between polymer chains to form an insoluble resin, however using a secondary diamine of a certain length can cause an intramolecular cyclisation to occur, forming a cyclic lactam⁶⁷. Nevertheless, Michael addition has been effectively put to use by Hoffman *et al.*⁶⁸ on partly bio-derived copolymers of itaconate esters and polyethylene glycol (PEG), cross-linked by both linear and branched multi-amines to form hydrogels. Crosslinking using radicals to link double bonds incorporated from bio-derived IA has also been demonstrated, with Mehtiö *et al.* using radicals generated from peroxides to rapidly form crosslinked gels with up to 77% crosslinked material by weight⁶⁹. However, this comes with obvious downsides; peroxides are generally toxic and dangerous to store and use safely. Grubbs' 3rd generation catalyst has also been successfully used to crosslink NA-containing polymers by cross-metathesis⁶¹, albeit at much longer reaction times than other methods mentioned.

Interestingly, we were unable to find any substantial discussion of PPM *via* nucleophilic substitution onto ECH; surface modification of PVC *via* nucleophilic substitution is fairly well-known^{70,71}, but this oversight seems to provide as yet unexplored potential for bio-derived crosslinking.

1.4. This Project

To our knowledge, all referenced literature on ROCOP thus far was performed inside a glovebox. However, this is sub-optimal when it comes to real-world applications, as gloveboxes are expensive, limited in capacity and wasteful in energy and inert gases. The aim of this project was to test the viability of this reaction outside a glovebox, using

only bench-top equipment to ensure as dry an atmosphere as possible. We decided to use two metal-based initiators known to be effective, salph-AlCl and salph-CrCl , and compare them with the novel organo-initiator DCU presented by Lin *et al.*⁴³ to see if this promising, greener initiator remained comparable in activity in conditions subject to less rigorous water removal, as might be the case were this reaction to be scaled up to industrial level. We also aimed to use bio-derived monomers in this reaction, and then to test, and look for ways to enhance, their properties by PPM to determine their viability in replacing non-renewably sourced polymers.

2. Experimental

2.1. Reagents

Phthalic anhydride (Sigma-Aldrich), itaconic anhydride (Sigma-Aldrich), cyclohexene oxide (Sigma-Aldrich), epichlorohydrin (Sigma-Aldrich), 1,2-diaminobenzene (Sigma-Aldrich), N,N'-dicyclohexylurea (Sigma-Aldrich), chromium (II) chloride (Sigma-Aldrich), silica (60 Å, Sigma-Aldrich), ethanol (Sigma-Aldrich), chloroform (Sigma-Aldrich), dichloromethane (Sigma-Aldrich), ammonium chloride (Sigma-Aldrich), succinic anhydride (Merck), diethylaluminium chloride (Acros Organics), 3,5-di-tert-butylsalicylaldehyde (Apollo Scientific), bis(triphenylphosphorylidene)ammonium chloride (Alfa Aesar), dimethylformamide (VWR), methylbis(3-methylaminopropyl)amine (Sigma-Aldrich), piperazine (Sigma-Aldrich), 2,2'-(ethylenedioxy)diethanethiol (Sigma-Aldrich), pentaerythritol tetrakis(3-mercaptopropionate) (Sigma-Aldrich), L-Cystine dimethyl ester dihydrochloride (Sigma-Aldrich) were used as received. Hexane, toluene, tetrahydrofuran were purified with the aid of an Innovative Technologies anhydrous solvent engineering system. Epoxidised macaw palm oil and baru nut oil were reused from a previous project⁷².

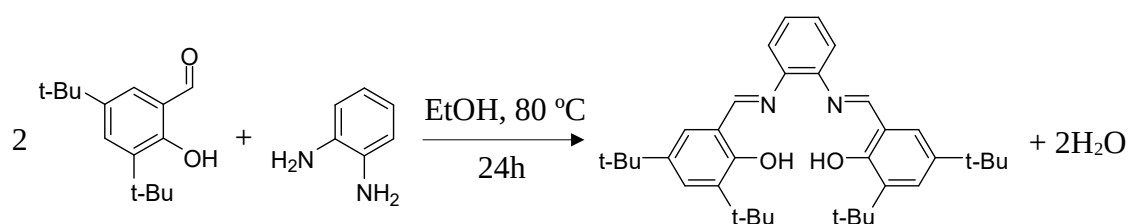
2.2. Characterisation

Liquid state ¹H and ¹³C NMR spectra were acquired on a Bruker AVIII 300 NB spectrometer or a JEOL ECS400 spectrometer at 300 MHz and 75 MHz or 400 MHz and 100 MHz respectively, and solid state ¹³C NMR spectra were acquired on a Bruker AVIII HD 400 WB spectrometer at 100 MHz. Infrared spectra were acquired on a Perkin-Elmer Spectrum 400 FTIR spectrometer. UV/visible absorption spectra were acquired on a Thermo Scientific GENESYS 180 UV-vis spectrophotometer. Mass

spectrometry measurements were performed on a Bruker compact time-of-flight mass spectrometer (ESI) or a JEOL AccuTOF GCx plus time-of-flight mass spectrometer (LIFDI). DSC spectra were acquired using a TA Instruments Q2000 modulated Differential Scanning Calorimeter. TGA spectra were acquired using a Stanton Redcroft STA 625 or a Netzsch STA 409 instrument. Melting points were measured using a Stuart SMP30 Melting Point apparatus. SEC was carried out using a set (PSS SDV High) of 3 analytical columns (300 x 8 mm, particle diameter 5 μm) of 1000, 105 and 106 \AA pore sizes, plus guard column, supplied by Polymer Standards Service GmbH (PSS) installed in a PSS SECurity SEC system. Elution was with THF at 1 ml/min with a column temperature of 30 $^{\circ}\text{C}$ and detection by refractive index. 20 μL of a 1 mg/ml sample in THF, with a small quantity of toluene added as a flow marker, was injected for each measurement and eluted for 45 minutes. Calibration was carried out in the molecular weight range 400–2x10⁶ Da using ReadyCal polystyrene standards supplied by Sigma Aldrich, and referenced to the toluene peak.

2.3. Salophen Initiator Synthesis

2.3.1. Ligand Synthesis



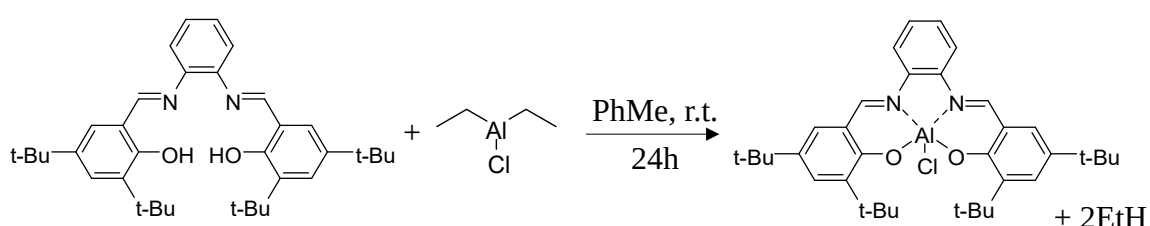
Scheme 2 – The synthesis of ligand salph-H₂

To 3,5-di-tert-butylsalicylaldehyde (1.030 g, 4.4 mmol) dissolved in minimal ethanol (~20 mL) was added 1,2-diaminobenzene (0.230 g, 2.13 mmol) and the resulting yellow solution was stirred at reflux overnight then left to cool to r.t. The resulting orange

solution was left in the fridge overnight to crystallise and the resulting solid was filtered *in vacuo* and washed with cold ethanol to obtain yellow crystals of salph-H₂ ligand intermediate (0.898 g, 78%).

¹H NMR (300 MHz, CDCl₃, ppm): δ 1.32 (s, 18H, CCH₃), 1.43 (s, 18H, CCH₃), 7.20-7.25 (m, 4H, PhH), 7.28-7.34 (m, 2H, PhH), 7.44 (d, 2H, *J* = 2.4 Hz, PhH), 8.66 (s, 2H, HC=N), 13.52 (s, 2H, OH)⁷³.

2.3.2. Aluminium Metalation



Scheme 3 – The synthesis of salph-AlCl

To salph-H₂ (0.370 g, 0.684 mmol) dissolved in minimal anhydrous toluene (~15 mL) in an oven-dried reaction vessel was added diethylaluminum chloride (0.9 M, 0.770 mL, 0.693 mmol) dropwise with stirring under an atmosphere of dinitrogen. The reaction mixture was stirred overnight at r.t. under inert atmosphere and the resulting solid was filtered *in vacuo* and washed with hexanes to obtain a yellow solid of Initiator A, salph-AlCl (0.277 g, 67.4%, m.p. = 285-290 °C [dec.]).

¹H NMR (300 MHz, CDCl₃, ppm): δ 1.35 (s, 18H, CCH₃), 1.60 (s, 18H, CCH₃), 7.24 (d, 2H, *J* = 2.6 Hz, PhH), 7.42 (dd, 2H, *J* = 6.2 Hz, 3.4 Hz, PhH), 7.68 (d, 2H, *J* = 2.6 Hz, PhH), 7.77 (dd, 2H, *J* = 6.2 Hz, 3.4 Hz, PhH), 8.97 (s, 2H, HC=N).

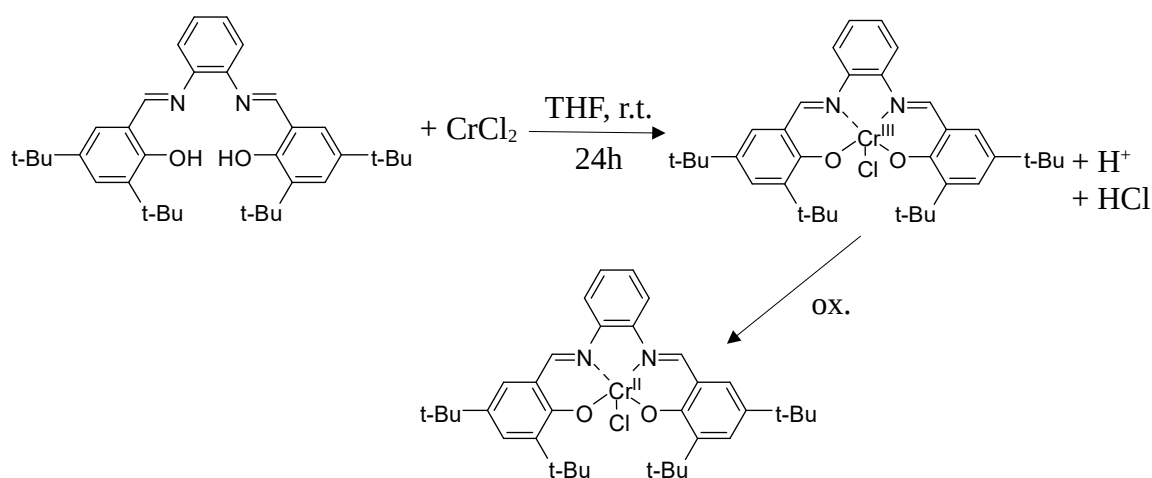
¹³C NMR (75 MHz, CDCl₃, ppm): δ 29.8 (CH₃), 31.3 (CH₃), 34.1 (CH₃), 35.7 (CCH₃), 115.4 (Ar), 118.5 (Ar), 128.1 (Ar), 128.2 (Ar), 133.1 (Ar), 137.8 (Ar), 139.7 (Ar), 141.6 (Ar), 164.4 (C=N).

IR (KBr, cm^{-1}): 2948, 2904, 2865, 1613, 1583, 1555, 1538, 1466, 1440, 1411, 1385, 1359, 1318, 1262, 1199, 1183, 1135, 872, 846, 786, 743⁷⁴.

ESI-MS (m/z): Calculated for $\text{C}_{36}\text{H}_{46}\text{AlN}_2\text{O}_2 = 565.3369$; measured = 565.3392 $[\text{M}]^+$, 583.3491 $[\text{M}+\text{NH}_4]^+$, 597.3641 $[\text{M}+\text{CH}_3\text{OH}]^+$; error = 2.3 mDa.

LIFDI-MS (m/z): Calculated for $\text{C}_{36}\text{H}_{46}\text{AlClN}_2\text{O}_2 = 600.30577$; measured = 600.30656 $[\text{M}]^+$; error = 0.79 mDa.

2.3.3. Chromium Metalation



Scheme 4 – The synthesis of salph-CrCl

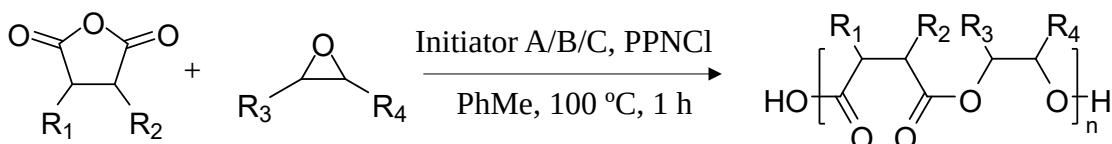
To salph-H₂ (1.273 g, 2.35 mmol) was added CrCl₂ (0.318 g, 2.59 mmol) under an atmosphere of dinitrogen in an oven-dried reaction vessel, and the reaction mixture was dissolved in anhydrous THF (50 mL) and stirred for 24h. The resulting dark brown solution was opened to air and stirred for a further 24h. The reaction mixture was poured into diethyl ether (200 mL), washed with NH₄Cl (3 x 150 mL), brine (3 x 150 mL) dried with MgSO₄, then filtered *in vacuo*. The remaining solvent was removed *in vacuo* and solids washed in hexane to give dark red solid of Initiator B, salph-CrCl (0.670 g, 45.6%, m.p. = 280-285 °C [dec.]).

IR (KBr, cm^{-1}): 2952, 2904, 2865, 1603, 1579, 1524, 1460, 1425, 1387, 1357, 1325, 1256, 1195, 1171, 1131, 870, 838, 784, 751⁷³.

ESI-MS (m/z): Calculated for $C_{36}H_{46}CrN_2O_2 = 590.2959$; measured = 590.2964 $[M]^+$; error = 0.5 mDa.

LIFDI-MS (m/z): Calculated for $C_{36}H_{46}ClCrN_2O_2 = 625.26404$; measured = 625.26208 $[M]^+$; error = 2.66 mDa.

2.4. General Polymerisation Procedure



Scheme 5 – Generalised copolymerisation reaction

All polymerisation reactions were performed at 100 °C for 1 hour with a $[initiator]_0$: $[co-initiator]_0$: $[epoxide]_0$: $[anhydride]_0$ ratio of 1:1:250:250 where 1 = 20 μ mol unless stated otherwise.

To an oven-dried 5 mL sample vial were added initiator, co-initiator and anhydride and the vessel was sealed and purged with dinitrogen. Epoxide was added, along with toluene (1 mL) if reaction was performed in solution, and after equilibration at the desired temperature, polymerisation started. After the desired reaction time, or when viscosity had increased to a point where stirring was no longer effective, the reaction was removed from heat, exposed to air and an aliquot was taken for 1H NMR analysis. The polymer was purified by dissolving in minimal dichloromethane and precipitating into a 10-fold excess of cold methanol or hexane twice. Liquids were decanted and the resulting polymer dried under vacuum to a constant weight.

CHO-PA: 1H NMR (300 MHz, $CDCl_3$, ppm): δ 1.51 (br, CH_2), 1.76 (br, CH_2), 2.23 (br, CH_2), 5.15 (br, 2H, OCH), 7.30-7.80 (m, 4H, ArH).

^{13}C NMR (75 MHz, CDCl_3 , ppm): δ 23.4 (CH_2), 29.9 (CH_2), 74.7 (OCH), 128.9 (Ar), 131.0 (Ar), 132.1 (Ar), 166.7 ($\text{C}=\text{O}$)⁴³.

IR (KBr, cm^{-1}): 2932, 2860, 1717, 1596, 1578, 1449, 1321, 1254, 1115, 1064, 1022, 986, 958, 917, 842, 737, 704.

CHO-SA: ^1H NMR (300 MHz, CDCl_3 , ppm): δ 1.34 (br, CH_2), 1.70 (br, CH_2), 1.99 (br, CH_2), 2.59 (br, 4H, COCH_2), 4.81 (br, 2H, OCH).

^{13}C NMR (75 MHz, CDCl_3 , ppm): δ 23.3 (CH_2), 29.1 (CH_2), 30.0 (COCH_2), 73.7 (OCH), 171.7 ($\text{C}=\text{O}$)⁴³.

IR (KBr, cm^{-1}): 2938, 2860, 1724, 1411, 1352, 1238, 1208, 1138, 1028, 1007, 845.

CHO-IA: ^1H NMR (300 MHz, CDCl_3 , ppm): δ 1.27 (br, CH_2/CH_3), 1.69 (br, CH_2), 2.00 (br, CH_2), 2.50-3.50 (br, COCH_2), 4.50-5.00 (br, OCH), 5.65-5.95 (br, $\text{C}=\text{CH}$ (cit.)/ $\text{C}=\text{CH}_2$), 6.30 (br, $\text{C}=\text{CH}_2$).

No satisfactory ^{13}C NMR obtained – see Appendices.

IR (KBr, cm^{-1}): 2927, 2860, 1766, 1724, 1650, 1449, 1264, 1174, 1092, 1030, 914, 845, 729.

ECH-PA: ^1H NMR (300 MHz, CDCl_3 , ppm): δ 3.73-3.92 (br, 2H, CH_2Cl), 4.60 (br, 2H, $\text{CH}_2\text{CH}(\text{CH}_2\text{Cl})$), 5.54 (br, 1H, $\text{CH}_2\text{CH}(\text{CH}_2\text{Cl})$), 7.64 (dq, 4H, $J = 56.7, 4.7$ Hz, ArH).

^{13}C NMR (75 MHz, CDCl_3 , ppm): δ 42.1 ($\text{CH}(\text{CH}_2\text{Cl})\text{CH}_2$), 63.4 ($\text{CH}(\text{CH}_2\text{Cl})\text{CH}_2$), 71.5 ($\text{CH}(\text{CH}_2\text{Cl})\text{CH}_2$), 129.2 (Ar), 131.1 (Ar), 131.6 (Ar), 166.4 ($\text{C}=\text{O}$)⁷⁵.

IR (KBr, cm^{-1}): 2960, 1722, 1599, 1579, 1488, 1446, 1349, 1318, 1248, 1115, 1066, 985, 737, 701.

ECH-SA: ^1H NMR (300 MHz, CDCl_3 , ppm): δ 2.67 (s, 4H, CH_2), 3.59-3.78 (m, 2H, CH_2Cl), 4.16-4.49 (m, 2H, $\text{CH}_2\text{CH}(\text{CH}_2\text{Cl})$), 5.24 (m, 1H, $\text{CH}_2\text{CH}(\text{CH}_2\text{Cl})$).

^{13}C NMR (75 MHz, CDCl_3 , ppm): δ 28.8 (CH_2), 28.9 (CH_2), 42.2 (CH_2Cl), 62.7 ($\text{CH}_2\text{CH}(\text{CH}_2\text{Cl})$), 70.8 ($\text{CH}_2\text{CH}(\text{CH}_2\text{Cl})$), 171.4 ($\text{C}=\text{O}$), 171.7 ($\text{C}=\text{O}$)⁷⁵.

IR (KBr, cm^{-1}): 2964, 1732, 1409, 1363, 1240, 1207, 1141, 1058, 1030, 1000, 832, 800, 753, 695.

ECH-IA: ^1H NMR (300 MHz, CDCl_3 , ppm): δ 1.96-2.18 (m, $\text{CH}_3/\text{O}=\text{CCH}_2$), 3.55-3.83 (br, CH_2Cl), 4.15-4.55 (br, OCH_2), 5.15-5.40 (br, $\text{OCH}(\text{CH}_2\text{Cl})$), 5.75-5.85 (br, $\text{C}=\text{CH}_2$), 5.85-5.95 (br, $\text{C}=\text{CH}$ (cit.)), 6.30-6.40 (br, $\text{C}=\text{CH}_2$).

No satisfactory ^{13}C NMR obtained – see Appendices.

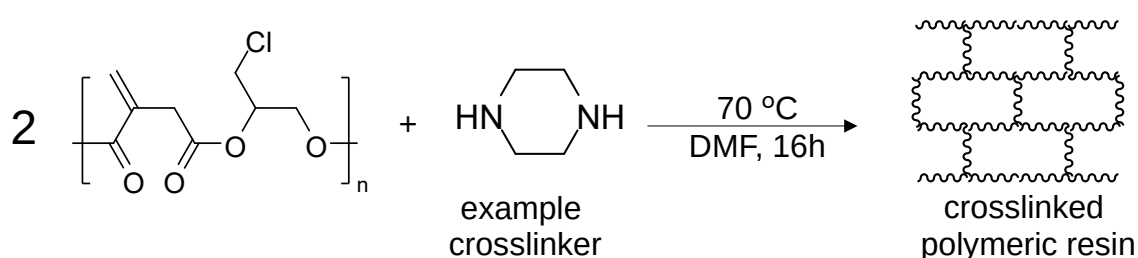
IR (KBr, cm^{-1}): 3515, 2964, 1764, 1724, 1651, 1442, 1345, 1252, 1157, 1123, 1062, 1034, 975, 925, 751, 703.

2.4.1. Multi-Epoxy Polymerisation Procedure

Polymerisation reactions were performed at 100 °C for 1 hour, for entries BMEPA1-BMEPA6 with a $[\text{initiator}]_0 : [\text{co-initiator}]_0 : [\text{epoxide}]_0 : [\text{anhydride}]_0$ ratio of 1:1:250:250 where 1 = 20 μmol and subsequently with $[\text{initiator}]_0 : [\text{co-initiator}]_0 : [\text{epoxide}]_0 : [\text{anhydride}]_0$ ratio of 1:1:250:1000 where 1 = 10 μmol .

To an oven-dried 15 mL sample vial were added initiator, co-initiator, epoxide and anhydride and the vessel was sealed and purged with dinitrogen. After equilibration at the desired temperature, polymerisation started. After the desired reaction time, or when viscosity had increased to a point where stirring was no longer effective, the reaction was removed from heat and exposed to air. Reaction mixture was purified by washing with excess DCM (100 mL) and filtration *in vacuo*, then drying to a constant weight.

2.5. Crosslinking Procedure



Scheme 6 – Generalised crosslinking reaction

All crosslinking reactions were performed at 70 °C for 16 hours with a [difunctional crosslinker]₀ : [polymer repeat units]₀ stoichiometric ratio of 1 : 2 or [tetrafunctional crosslinker]₀ : [polymer repeat units]₀ ratio of 1 : 4, where 1 = 0.490 mmol unless stated otherwise.

To an oven-dried 5 mL sample vial were added polymer and cross-linker and the vessel was sealed and purged with dinitrogen. If the reaction was performed in solution, dimethylformamide (0.1 mL) was added and after equilibration at the desired temperature, the reaction began. After the desired reaction time, the reaction was removed from heat and exposed to air. Unreacted polymer was removed by adding 5 mL of dichloromethane and stirring overnight, then decanting the solute and drying under vacuum until a constant weight to give the yield of insoluble crosslinked product by mass.

MMAPA crosslinked material: IR (KBr, cm⁻¹): 3468, 2948, 2793, 2472, 1730, 1623, 1458, 1375, 1157, 1052, 844, 747.

Piperazine crosslinked material: IR (KBr, cm⁻¹): 3400, 2956, 2821, 2472, 1730, 1619, 1438, 1375, 1155, 1048, 1002, 747.

EDDET crosslinked material: IR (KBr, cm⁻¹): 3468, 2920, 2865, 1730, 1659, 1440, 1353, 1246, 1155, 1108, 1062, 925, 751.

PETMP crosslinked material: IR (KBr, cm⁻¹): 3484, 2960, 1728, 1387, 1353, 1232, 1145, 1050, 1014, 929, 753.

3. Results & Discussion

3.1. Polyester Synthesis

In order to show that both metal-initiated and organo-initiated ROCOP are effective outside of a glovebox with a range of monomers, aluminium complex Initiator A and chromium complex Initiator B (Fig. 10) were first synthesised according to literature methods^{35,74,76} and their structures confirmed with NMR and IR spectroscopy, ESI-MS and LIFDI-MS (Fig. 9).

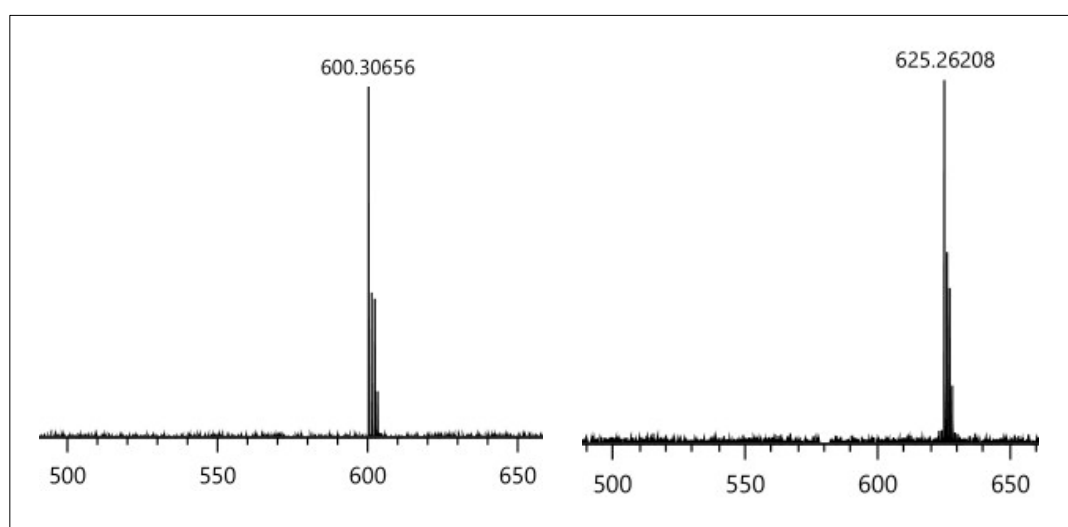


Figure 9 – LIFDI-MS spectra for *salph-AlCl* (left, calc. mass = 600.30577 Da) and *salph-CrCl* (right, calc. mass = 625.26454 Da)

3.1.1. Control Experiments

Initiators A and B, along with an organo-initiator Initiator C, *N,N'*-dicyclohexylurea (DCU) (Fig. 10), were then used for a series of control experiments. Reactions were run with PA and CHO as model monomers with no initiators, and one equivalent only of co-initiator and Initiators A, B and C (Table 1). No activity was present with no initiator, and very little activity was evident with Initiators A, B and C alone, showing that each required the presence of the co-initiator in order for significant polymerisation to occur.

Interestingly, some polymerisation did occur with co-initiator only in accordance with the observations of Han *et al.*³⁸ (Table 1, CTRL2), though it showed a 15% lower anhydride conversion compared to the lowest conversion of the same monomers in the presence of both initiator and co-initiator.

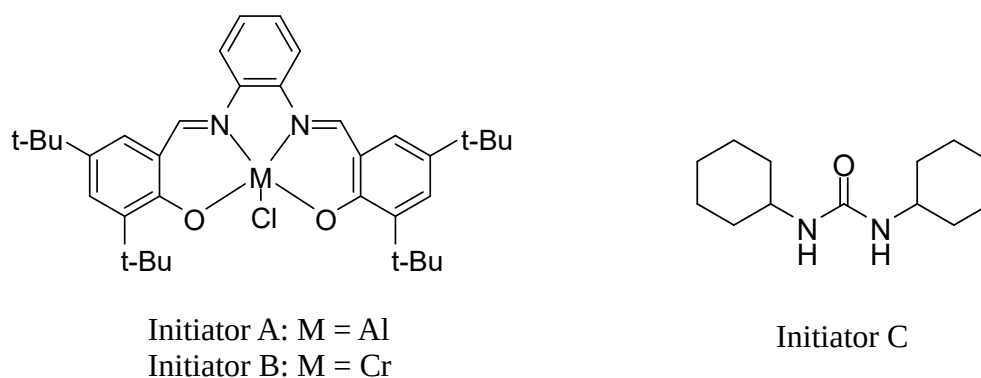


Figure 10 – Initiators A, B and C

Table 1: Control reactions

Entry	Initiator	Ratio ^a	Epoxide	Anhydride	Anh. conv. (%) ^b	Ether (%) ^c
CTRL1	-	0:0:250:250	CHO	PA	-	-
CTRL2	-	0:1:250:250	CHO	PA	48	12
CTRL3	A	1:0:250:250	CHO	PA	-	-
CTRL4	B	1:0:250:250	CHO	PA	9	48
CTRL5	C	1:0:250:250	CHO	PA	19	18
CTRL6	A	1:1:250:0	ECH	-	-	-
CTRL7	B	1:1:250:0	ECH	-	-	-
CTRL8	C	1:1:250:0	ECH	-	-	-

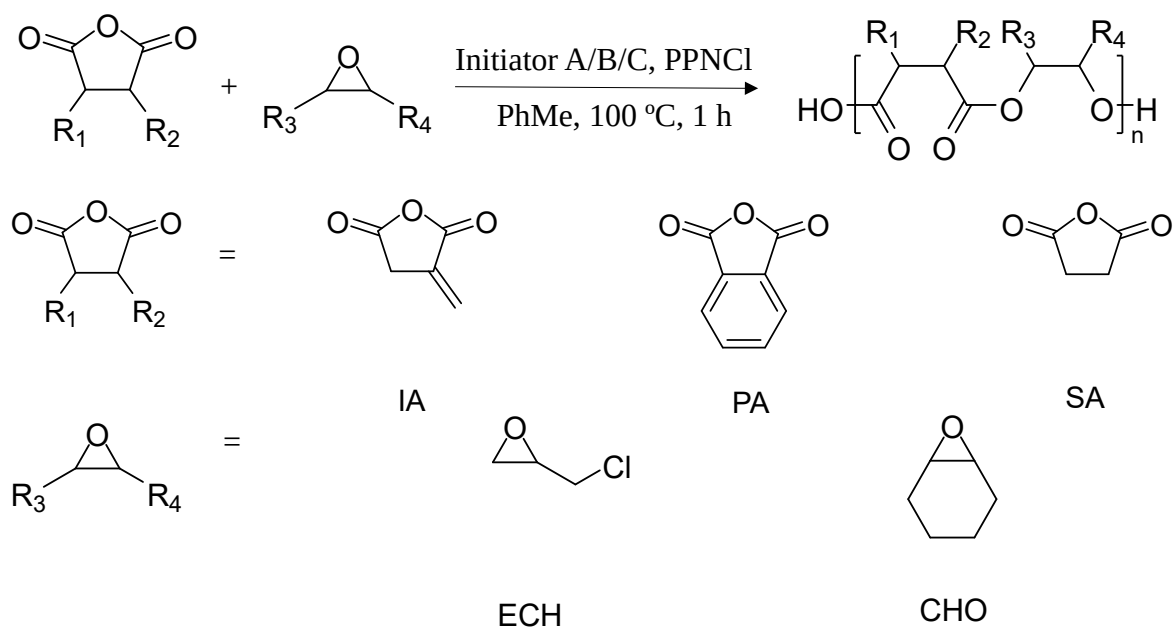
Reaction conditions: 100 °C, 1h, bulk. ^a Molar ratio [initiator]₀ : [PPNCl]₀ : [epoxide]₀ : [anhydride]₀ where 1 = 20 μmol. ^b Determined from ¹H NMR spectra in CDCl₃ by integrating the resonances for PA (7.87-8.07 ppm) with those for the ester -CH- groups (5.15 ppm). ^c Determined from ¹H NMR spectra in CDCl₃ by integrating the -CH- resonances for ester (5.15 ppm) with those for ether (3.45-3.70 ppm).

Control experiments with initiator, co-initiator and ECH without anhydride were also run to verify the observation of Zhang *et al.* that ECH does not form polyether under ROCOP conditions⁴². No self-propagation was observed, implying ECH-anhydride copolymerisations could potentially be performed using excess ECH as solvent without the risk of polyether formation once all anhydride had reacted.

3.1.2. Polymerisation Reactions

The effectiveness of the three initiators outside a glovebox were then evaluated through comparative testing using PPNCl as co-initiator. They were tested with a range of epoxides – CHO, ECH – and cyclic anhydrides – PA, SA and IA – with the aim of creating entirely bio-derived polymers. The experiments were performed at 100 °C with equimolar amounts of monomers based on the conditions used by Nejad *et al.*³⁰, both in bulk and toluene (1 mL) in order to compare the effect of solvent upon the reaction. Reaction vessels were oven-dried overnight, solid reagents were added then the atmosphere purged with N₂ before addition of liquids. Reactions were run for 60 mins, or until viscosity increased to such a degree that stirring became ineffective. Polymerisations involving IA were repeated for 120 mins due to its decreased ring strain, and hence comparative lack of reactivity compared to PA.

¹H NMR spectroscopy was used to determine the conversion of starting materials and the content of ester to ether linkages where possible. The molar mass and dispersity of the polymers were measured by GPC analysis using a polystyrene reference standard.



Scheme 7 – Copolymerisation reactions performed during comparative testing

Table 2: The effectiveness of Initiators A, B and C at ROCOP outside a glovebox

Entry	Initiator	Medium	Epoxide	Anhydride	<i>t</i> (min)	Anh. Conv. (%) ^a	Ether (%) ^b	<i>M_n</i> (kDa) ^c	<i>D_w</i> ^c	<i>M_n</i> (kDa) lit values
CHOPA11	A	bulk	CHO	PA	15	64	24	1.32	1.09	11.0 ^{30, k}
CHOPA12	A	toluene	CHO	PA	60	62	5	1.68	1.08	13.4 ^{30, l}
CHOPA21	B	bulk	CHO	PA	15	76	10	0.65	1.12	13.6 ^{30, k}
CHOPA22	B	toluene	CHO	PA	60	79	14	1.76	1.04	12.4 ^{30, l}
CHOPA31	C	bulk	CHO	PA	30	66	22	0.57	1.16	8.9 ^{43, h}
CHOPA32	C	toluene	CHO	PA	60	63	17	1.56	1.08	5.2 ^{43, i}
CHOSA11	A	bulk	CHO	SA	60	45	24	- ^d	- ^d	2.3 ^{30, j}
CHOSA12	A	toluene	CHO	SA	60	51	17	- ^d	- ^d	1.6 ^{30, l}
CHOSA21	B	bulk	CHO	SA	45	82	10	2.27	1.00	1.3 ^{30, j}
CHOSA22	B	toluene	CHO	SA	60	93	5	2.28	1.00	1.6 ^{30, l}

CHOSA31	C	bulk	CHO	SA	60	62	36	2.17	1.00	3.3 ^{43, h}
CHOSA32	C	toluene	CHO	SA	60	30	25	2.18	1.00	2.5 ^{43, i}
CHOIA13	A	bulk	CHO	IA	45	79	- ^e	- ^d	- ^d	- ^q
CHOIA14	A	toluene	CHO	IA	120	99	- ^e	3.29	2.16	- ^q
CHOIA23	B	bulk	CHO	IA	45	96	- ^e	4.37	1.51	- ^q
CHOIA24	B	toluene	CHO	IA	120	>99	- ^e	7.37	2.53	- ^q
CHOIA33	C	bulk	CHO	IA	45	92	- ^e	1.38	2.28	- ^q
CHOIA34	C	toluene	CHO	IA	120	90	- ^e	1.45	2.27	- ^q
ECHPA11	A	bulk	ECH	PA	30	90	- ^f	5.89	1.26	21.0 ^{75, n}
ECHPA12	A	toluene	ECH	PA	60	89	- ^f	6.35	1.37	21.0 ^{75, n}
ECHPA21	B	bulk	ECH	PA	15	90	- ^f	11.7	1.80	21.0 ^{75, n}
ECHPA22	B	toluene	ECH	PA	60	97	- ^f	8.93	1.31	21.0 ^{75, n}
ECHPA31	C	bulk	ECH	PA	45	69	- ^f	5.41	1.21	8.2 ^{42, o}
ECHPA32	C	toluene	ECH	PA	60	78	- ^f	7.67	1.26	8.2 ^{42, o}
ECHSA11	A	bulk	ECH	SA	60	97	- ^f	1.02	1.13	20.0 ^{75, m}
ECHSA12	A	toluene	ECH	SA	120	91	- ^f	1.06	1.19	12.0 ^{77, l}
ECHSA21	B	bulk	ECH	SA	60	95	- ^f	1.53	1.64	20.0 ^{75, m}
ECHSA22	B	toluene	ECH	SA	120	>99	- ^f	1.51	1.38	12.0 ^{77, l}
ECHSA31	C	bulk	ECH	SA	60	96	- ^f	0.99	1.12	11.4 ^{42, p}
ECHSA32	C	toluene	ECH	SA	120	89	- ^f	1.21	1.26	11.4 ^{42, p}
ECHIA11	A	bulk	ECH	IA	120	90	- ^f	1.30	1.01	- ^q
ECHIA12	A	toluene	ECH	IA	120	38	- ^f	1.41	1.05	- ^q
ECHIA21	B	bulk	ECH	IA	120	99	- ^f	- ^g	- ^g	- ^q
ECHIA22	B	toluene	ECH	IA	120	>99	- ^f	2.23	1.29	- ^q

ECHIA31	C	bulk	ECH	IA	120	60	- ^f	1.68	1.15	- ^g
ECHIA32	C	toluene	ECH	IA	120	29	- ^f	1.61	1.14	- ^g

Reaction conditions: 100 °C, 1:1:250:250 ratio of [initiator]₀ : [cocatalyst]₀ : [epoxide]₀ : [anhydride]₀ where 1 = 20 μmol unless stated otherwise. ^a CHOPA polymers: Determined from ¹H NMR spectra in CDCl₃ by integrating the resonances for PA (7.87-8.07 ppm) with those for the ester -CH- groups (5.15 ppm). CHOSA polymers: Determined from ¹H NMR spectra in CDCl₃ by integrating the resonances for SA (3.00 ppm) with those for the succinate -CH₂-CH₂- (2.51 ppm). CHOIA polymers: Determined from ¹H NMR in CDCl₃ by integrating the resonance for citraconic anhydride C=CH (6.66 ppm) with one of those for the ester C=CH₂ group and the citraconate C=CH (5.80-6.05 ppm). ECHPA polymers: Determined from ¹H NMR spectra in CDCl₃ by integrating the resonances from PA (7.87-8.07 ppm) with those for phenylene in the polymer (7.54-7.87 ppm). ECHSA polymers: Determined from ¹H NMR in CDCl₃ by integrating the resonance from SA (3.00 ppm) with those for the succinate -CH₂-CH₂- (2.70 ppm). ECHIA polymers: Determined from ¹H NMR spectra in CDCl₃ by integrating the resonance for citraconic anhydride C=CH (6.64 ppm) with one of the resonances for the itaconate ester C=CH₂ (5.94 ppm) and that of the citraconate ester C=CH (5.91 ppm). ^b Determined from ¹H NMR spectra in CDCl₃ by comparing the resonances for the -CH- groups for the ester (5.15 ppm) with those for the ether (3.45-3.70 ppm). ^c Measured using GPC analysis. ^d Polymers did not precipitate during purification, and could not be analysed by GPC. ^e Ether linkage content could not be determined due to overlap with itaconate -CH- groups. ^f No ether formed. ^g Polymer formed was insoluble, and could not be analysed by GPC. ^h Reaction carried out at 110 °C at a ratio of 1:1:200:100 where 1 = 0.05 mmol. ⁱ Reaction carried out at 110 °C at a ratio of 1:1:100:100 where 1 = 0.05 mmol in xylene. ^j Reaction carried out at a ratio of 1:1:250:250 where 1 = 10 μmol at 110 °C for 150 min. ^k Reaction carried out at a ratio of 1:1:250:250 where 1 = 10 μmol at 130 °C for 150 min. ^l Reaction carried out at a ratio of 1:1:250:250 where 1 = 10 μmol at 110 °C for 300 min. ^m Reaction carried out using binuclear Cr-salan with no co-initiator at a ratio of 1:400:400 where 1 = 0.75 mmol for 24h. ⁿ Reaction carried out using Co-salicy and PPNNNO₃ at a ratio of 1:1:800:400 where 1 = 0.01 mmol at 30 °C for 5 h. ^o Reaction carried out using Co-salicy and PPNNNO₃ at a ratio of 1:1:400:400 where 1 = 0.01 mmol at 30 °C for 2.5 h in THF. ^p Reaction carried out at a ratio of [1,4-benzenedimethanol (BDM)]₀ : [tert-butyliminotris(dimethylamino)phosphorane (t-BuP₁)]₀ : [epoxide]₀ : [anhydride]₀ of 1:0.5:100:50 where 1 = 0.05 mmol at 60 °C for 6 h. ^q Reaction carried out at a ratio of [BDM]₀ : [t-BuP₁]₀ : [triethylborane]₀ : [epoxide]₀ : [anhydride]₀ of 1:0.5:0.25:100:40 where 1 = 0.05 mmol at 25 °C for 48 h. ^r No ROCOP reaction between these monomers found.

3.1.3. Discussion of Results

From comparative testing results it can be seen that all initiators are effective in creating poly(ester-ether) copolymers outside of a glovebox environment with ECH, CHO, IA, SA and PA. Initiator B is consistently the most active, but metal-free Initiator C is comparable in activity to Initiator A, which is promising as a greener method of polyester synthesis *via* ROCOP considering its wide commercial availability.

Bio-derived monomers were also successfully utilized for polymer synthesis. These were copolymerised to create an entirely bio-derived polymer and this reaction was scaled up to gram scale, performing the reaction in bulk to minimise solvent use in accordance with the principles of green chemistry. Its scalability beyond this level could not be determined however due to time constraints.

As expected, when using an anhydride with decreased ring strain, longer reaction times were necessary to obtain higher conversions. The highly strained PA was noticeably faster to become completely viscous and produced the highest molecular weight

copolymers within 1 hour when paired with ECH, whereas SA and IA are less strained and hence reacted more slowly. When scaling up the ECH-IA copolymerisation, 4 hours was found to be the optimal reaction time as leaving it longer resulted in an insoluble polymeric material, almost certainly due to side reactions such as radical cross-linking. The effect of the addition of solvent on the system was investigated and was found to be a hindrance at shorter reaction times with a less reactive reaction system due to dilution factors, but at longer reaction times when viscosity of the reaction mixture is the limiting factor it is beneficial to conversion rates.

The largest molecular weight polymer produced in the course of monomer testing was an 11.7 kDa copolymer of ECH and PA (Table 2, ECHPA21), measured using GPC against a polystyrene standard, which though the highest achieved in this study was close to half the 20.0 kDa copolymer achieved using the same monomers with a Cobalt salicy catalyst by DiCiccio *et al.*⁷⁵ However, there were instances where the molecular weight achieved improved upon comparable reactions in literature, notably between CHO and SA; results achieved in this study using a Cr salophen catalyst achieved higher molecular weights than comparable reactions performed by Nejad *et al.*, despite a lack of comparable water removal techniques (Table 2, CHOSA22).

In general, the vast majority of products were short-chain polymers, with most being under 3 kDa. This is due to the presence of trace amounts of water in the reaction vessel, which then acts as a chain transfer agent (CTA), lowering molecular weights. This could come from trace amounts of water in reagents, incomplete N₂ purging, or the presence of diacid from anhydrides which can also act as a CTA. That this is occurring can be seen from the fact that polymer chain lengths are far from their ideal values, and the presence of hydroxyl chain ends in NMR spectra, visible as peaks d, e, and g on the ¹H NMR spectrum of an ECH-PA copolymer in Figure 11. The presence of adventitious

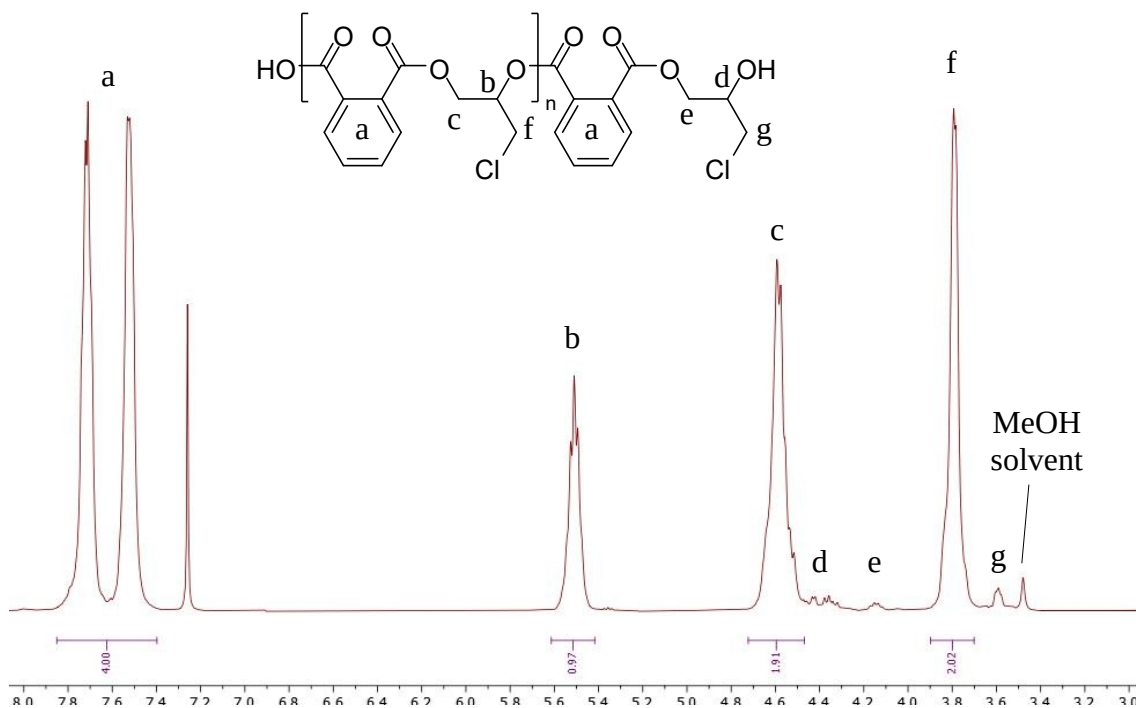


Figure 11 – ^1H NMR spectrum of ECH-PA copolymer

water is a problem in ROCOP even when gloveboxes and rigorous reagent purification methods are used.³¹

Selectivity was generally good, usually with a small (<25%) amount of polyether detected, due to the propensity of CHO to homopolymerise. The percentages calculated in Table 2 are also likely to be inflated, as polyether signals fall in the same area as those produced by hydroxy-terminated chain ends. However as Zhang *et al.* observed⁴², ECH does not produce polyether during ROCOP and as can be seen in Figure 11, there are no polyether signals present in their expected position around 3.5 ppm.

However due to their unsaturation, itaconate esters are often prone to side reactions such as radical crosslinking, regioisomerisation and Ordelt saturation, an oxo-Michael addition (Fig. 12) which occurs onto the double bond when a growing polymer chain is hydroxyl terminated. Similarly to Takasu *et al.* in their pioneering use of IA in ROCOP⁷⁸, evidence of all these side reactions was observed during polymerisation of

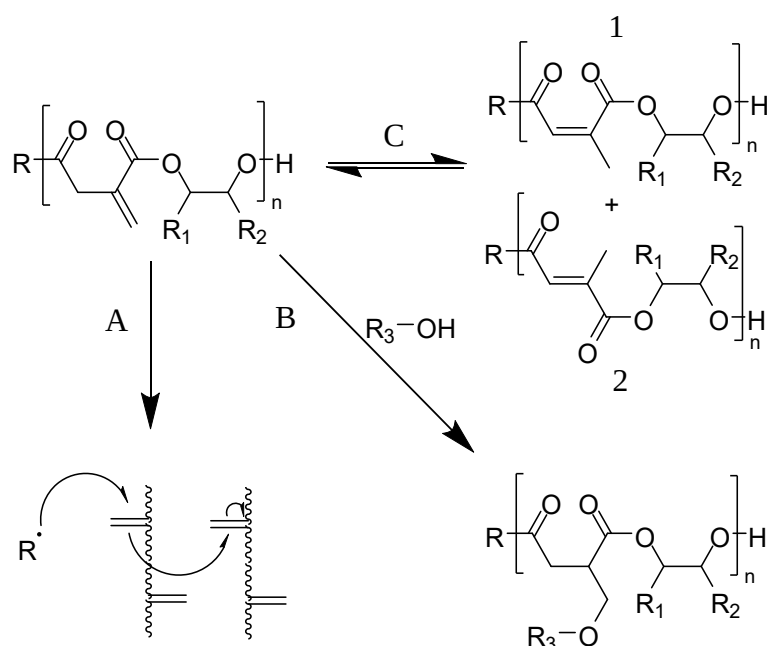


Figure 12 – Typical side reactions of itaconate esters, as shown by Farmer *et al.*⁶⁴ : Radical cross-linking (Scheme A), Ordel's saturation (Scheme B) and regioisomerisation (Scheme C) to mesaconate (1) and citraconate (2) isomers.

itaconic anhydride.

Firstly, when reaction times were extended beyond 5-6 h during scale-up, gelation of the reaction mixture was observed and a soft, rubbery insoluble resin was extracted typical of directly crosslinked itaconate polyesters⁷⁹ created by radical crosslinking. Secondly, OH-terminated chains were sometimes visible in various ¹H NMR spectra (Fig. 11), suggesting that Ordel's saturation could take place. Furthermore, both ¹H and ¹³C NMR spectra of itaconate polyesters showed indistinct peaks, and integration ratios of saturated groups in ¹H NMR spectra were often significantly larger than predicted (Fig. 13), with both of these side reactions as a probable cause. Also observable on ¹H NMR spectra is regioisomerisation in the olefinic region, with additional peaks present other than those of the itaconate double bond at 6.35 ppm and 5.80 ppm. In their comprehensive study of itaconate regioisomerisation, Farmer *et al.*⁶⁴ found that when regioisomerisation occurred it was primarily the mesaconate isomer produced, with

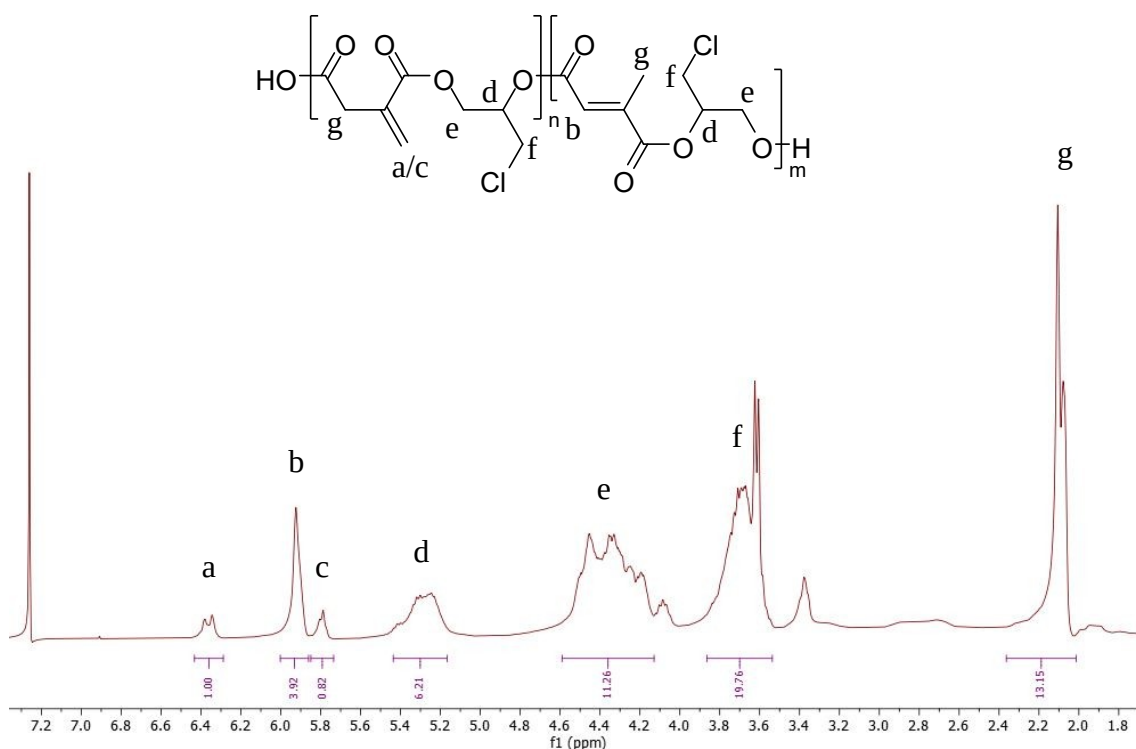


Figure 13 – ^1H NMR spectrum of ECH-IA copolymer showing itaconate double bond Hs (a/c) and proposed citraconate isomer (b). Proportionally, saturated CH/CH₂/CH₃ signals (d-g) are larger than expected and are wide and indistinct, suggesting other side reactions have occurred

negligible amounts of the citraconate variant detectable (Fig. 12). However as can be seen in Fig. 13, no mesaconate olefinic signal is observed at 6.70 ppm, with the isomeric signal found at 5.92 ppm similar to the olefinic signal observed for dimethyl citraconate (5.85 ppm)⁸⁰. This would suggest that the major isomer produced in ROCOP of itaconic anhydride is exclusively the citraconate ester, and in greater proportions than the desired itaconate product. This unfavourable ratio of product to isomer could be because the exo-type double bond present in itaconate esters are prone to cross-linking side-reactions, whereas the endo-type double bond in citraconate esters are less reactive to such reactions due to steric hindrance, and as such more of this isomer remains in the product.

In addition, it appears that significant regioisomerisation of itaconic anhydride starting material occurred during the course of the reaction, with all unsaturated signals from

unreacted anhydride detectable around 6.65 ppm showing a quartet characteristic of citraconic anhydride instead of a triplet from itaconic anhydride (Fig. 14). This suggests that citraconic anhydride is also less reactive in ROCOP than its itaconate form, possibly because the double bond's position in citraconic anhydride means that it can delocalise to both carbonyl groups and decrease both of their electrophilicities and thus their reactivity.

Since most polymers produced were of short chain lengths, purification became a time-consuming chore. The usual method of purification involves the dissolution of the polymer in DCM/chloroform and precipitation into cold methanol, which is effective in removing both unreacted epoxide and anhydride. However, it was found that short-chain polymers are often still too polar to precipitate out of solution into methanol. A range of

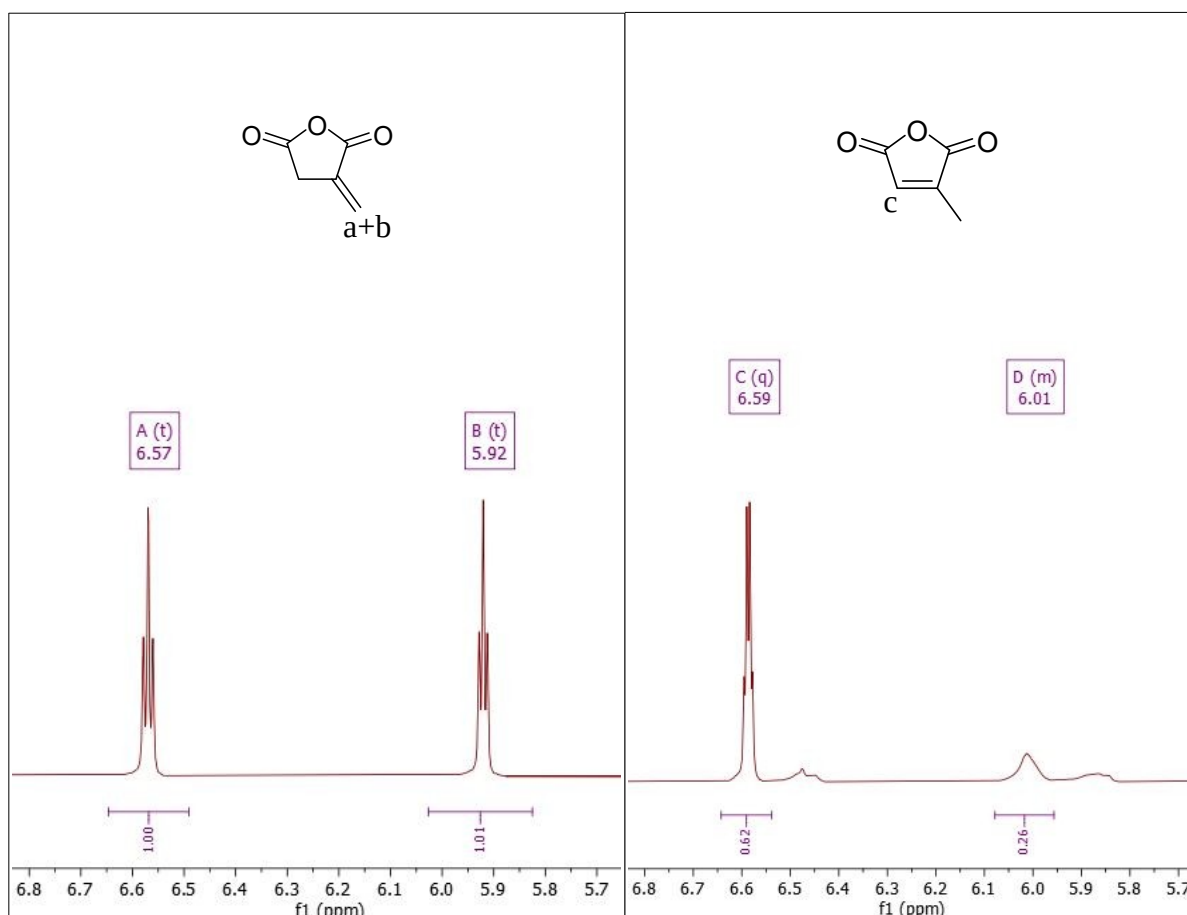


Figure 14 – ^1H NMR spectrum of IA (left) and crude ECH-IA copolymer (right), showing triplet splitting pattern in vinylic protons present in IA compared to quartet splitting pattern present in unreacted citraconic anhydride in reaction mixture

techniques were unsuccessfully attempted to solve this problem, including trying to find an alternative solvent that would preferentially precipitate out polymer while retaining anhydride in solution such as isopropanol and ether, and ring-opening unreacted anhydride by liquid-liquid extraction using 1M sodium carbonate (5 mL), which also affected the polymer chain length by hydrolysing the ester backbone.

Due to time pressure, a full range of physical testing was not run on all polyesters, however DSCs were obtained for all copolymers (Fig. 15). These, with a few exceptions, showed T_g values of 30-50 °C and T_m values of 110 °C, a relatively low glass transition temperature similar to that of industrially produced nylons used for films and packaging such as nylon-6 and nylon-12⁸¹, albeit with a much lower melting point. Notable outliers include ECH-SA copolymers, all of which had low T_g values of -10 to 0 °C, which is unsurprising given the lack of rigidity or sterically demanding groups along the polymer backbone, and CHO-PA copolymers which had T_g values

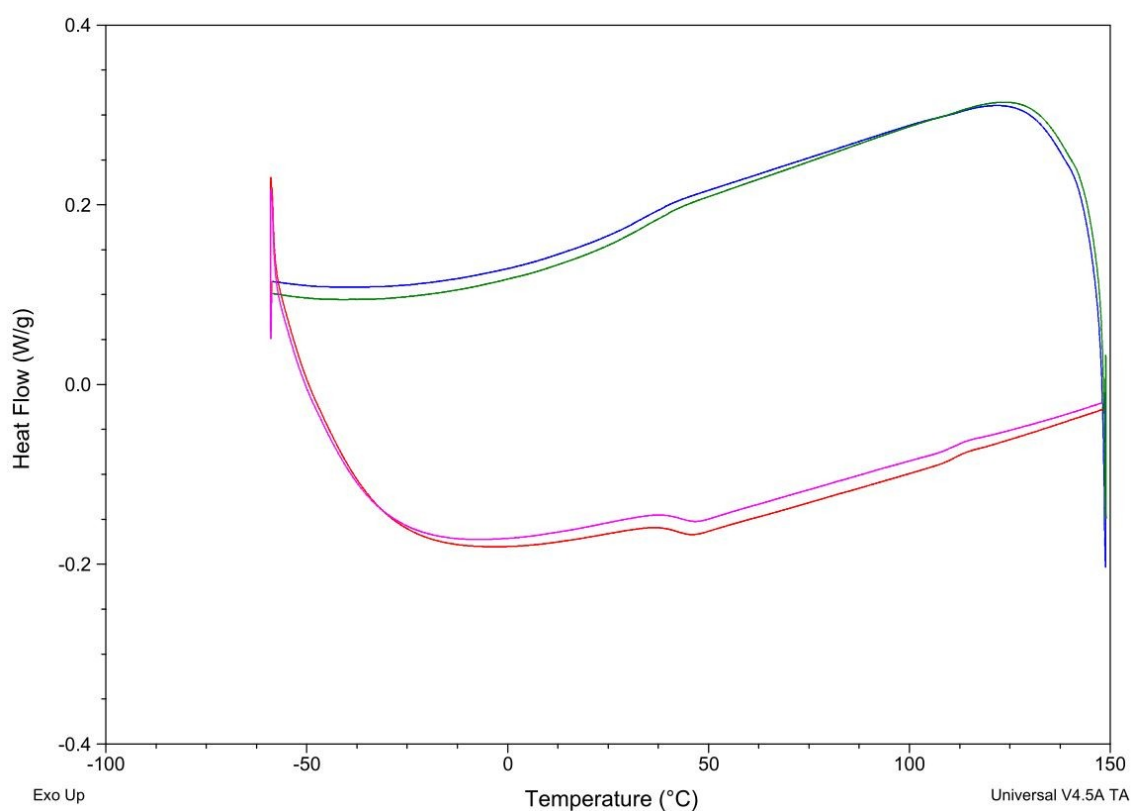


Figure 15 – DSC of ECH-PA copolymer, showing a T_g of 50 °C and a T_m of 110 °C

reaching to 110 °C. This is due to the rigidity of the backbone featuring aromatic rings, and though it was the highest T_g value measured it was still significantly lower than examples from Proverbio *et al.* who recorded T_g values of up to 140 °C³³. Glass transition temperatures observed are within 10 °C of literature values for CHO-SA²², ECH-SA⁷⁵ and ECH-PA⁷³ – few examples of itaconic anhydride in ROCOP could be found in literature, though one notable example, that of Takasu *et al.*, produced poly-IA-co-epoxybutane with glass transition temperatures recorded between -10 and 10 °C, substantially lower than those observed in this study⁷⁸. As a completely aliphatic polyesters, it might be expected that, for example, ECH-IA polymers might have a similar T_g to those produced by Takasu *et al.*; a degree of crosslinking from spontaneous side reactions is likely the explanation for these elevated T_g values.

3.1.4. Mechanism

With no water present, metal-initiated ROCOP is initiated from chloride ions from the metal complex or PPNCl after activation of the epoxide monomer by the Lewis acidic metal centre, according to the mechanism proposed by Fieser *et al.*¹⁹ (Fig. 16, Scheme A). They theorised that the rate limiting step is the spontaneous dissociation of carboxylate anion of the growing polymer chain to allow the metal centre to activate the next monomer for the propagation cycle to continue. Organo-initiation functions in a similar way, with a Lewis acid activating monomers and Lewis base initiating polymerisation, according to the mechanism of Kummari *et al.*⁸²

In the case of DCU however, it has been proposed by Lin *et al.*⁴³ that DCU acts as a H-bond donor as opposed to a Lewis acid (Figure 16, Scheme B), though as DCU's efficacy is a recent discovery it has not yet been elucidated whether the mechanism of reaction uses both H-bonds per catalytic cycle or one; Figure 16 shows the proposed mechanism using two H-bonds, one to interact with the growing polymer chain and the

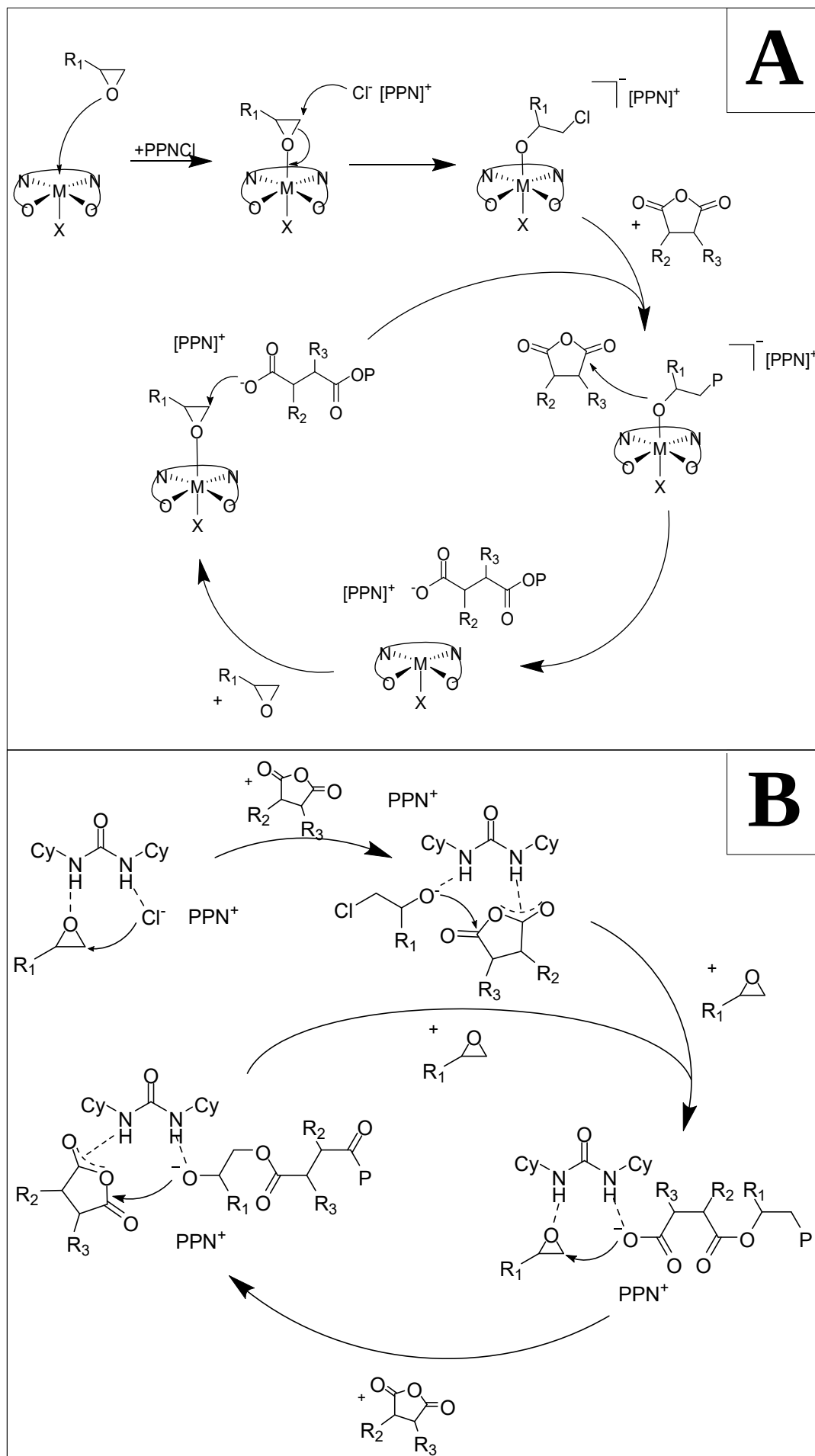


Figure 16 – Simplified initiation and propagation cycle of ROCOP with: salophen initiator and PPNCl co-initiator (Scheme A), where X = halide, alkoxide or carboxylate and P = growing polymer 45 chain, and DCU and PPNCl co-initiator (Scheme B).

other to activate the next monomer and thus speed propagation. This, if accurate, would be an improvement over initiation by a single centre as it removes the rate-limiting dissociation step.

The presence of hydroxyl chain ends in NMR spectra was commonly observed (Fig. 11, peaks d-g), meaning that chain transfer with water was undoubtedly occurring; as DCU also uses PPNCl as a co-initiator, all polymer chains in the complete absence of water should be chloride-terminated.

3.1.5. Multi-Epoxy Polymerisation

After finding during monomer testing that short-chain polymers were common, we set out to find ways of increasing the molecular weight of polymers obtainable by this method, namely by crosslinking. We decided to try two methods of producing high-molecular weight, crosslinked polymers; firstly, by copolymerising bio-derived monomers with multiple active sites and secondly, by post-polymerisation modification of existing polymers.

In a previous project⁷², vegetable oil produced from baru nut and macaw palm fruits were obtained and found to contain 4 and 3.5 double bonds per triglyceride molecule respectively (Fig. 17). They were then epoxidized to create long-chain fatty acid-derived multi-epoxides. These materials were first tested with all initiators in bulk at a 1:1 ratio $[\text{epoxide}]_0 : [\text{PA}]_0$ under the same conditions as previous comparative testing and the results washed with excess DCM to remove any soluble material. The results showed greater yields by mass of cross-linked polymer from the epoxidized macaw oil (Table 3, BMEPA1-3) so this was chosen to be reacted at a 1:4 ratio $[\text{epoxide}]_0 : [\text{PA}]_0$ to potentially fully react all epoxides in the long-chain monomer. This reaction successfully created a partially bio-derived insoluble crosslinked polymeric resin, as tested in chloroform and THF, in the form of a soft, rubbery gel-like material. These

were then tested by DSC, with no observed transitions between -60 °C and 150 °C suggesting that the resulting polymer had some degree of chemical crosslinking, and TGA found that this insoluble polymeric material had a T_{D10} of 311 °C, indicating decent thermal stability. Due to limited time, no further physical analysis was able to be completed. Solid state ^{13}C NMR spectra showed that the materials had residual epoxide peaks in the 55-60 ppm range indicating a lack of complete reaction, but materials created using DCU had the smallest such peak, suggesting it was the most effective initiator for crosslinking multi-epoxides using ROCOP.

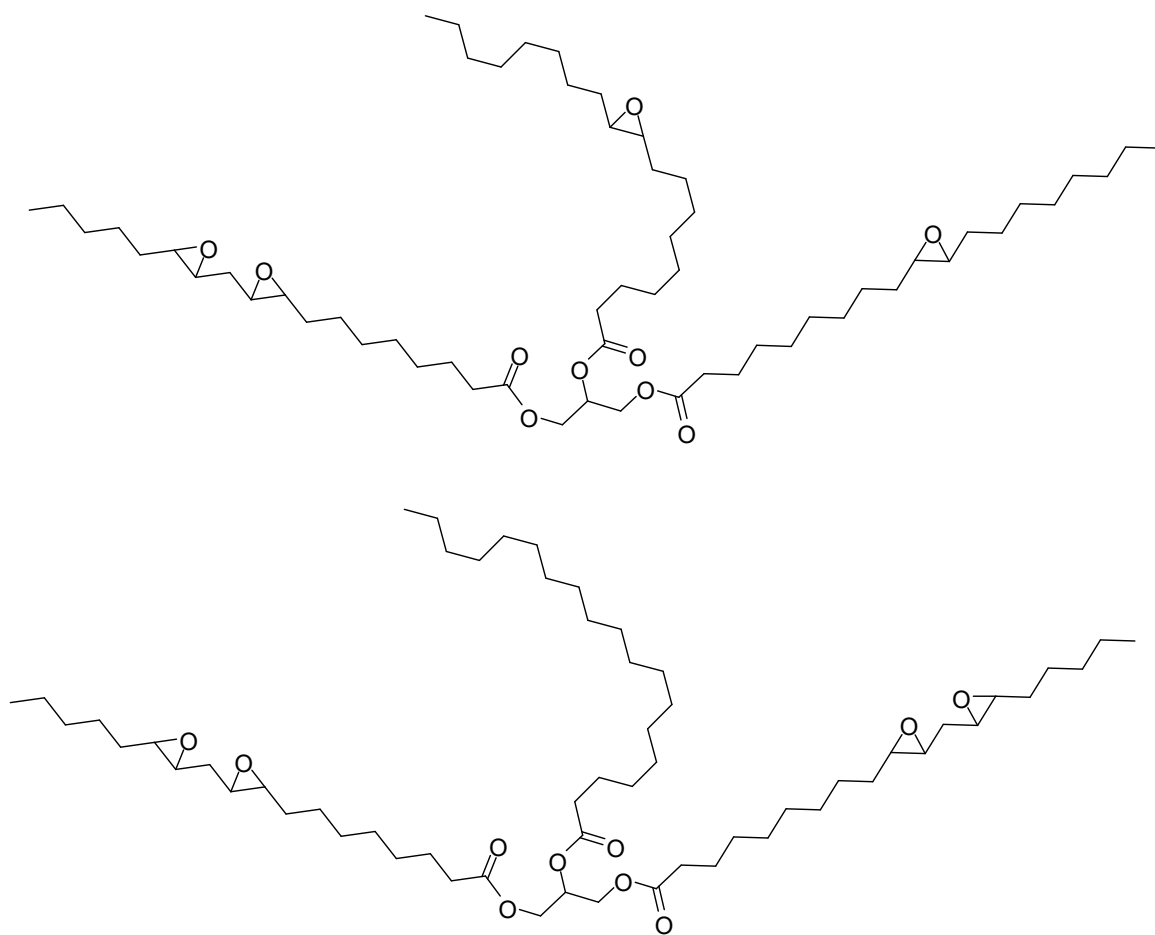


Figure 17 – Possible chain structures of epoxidised macaw oil⁷²

Table 3: The synthesis of crosslinked polymers

Entry	Ratio ^a	Initiator	Epoxide	Yield (%)
BMEPA1	1:1:250:250	A	macaw oil	56.4
BMEPA2	1:1:250:250	B	macaw oil	72.8
BMEPA3	1:1:250:250	C	macaw oil	57.3
BMEPA4	1:1:250:250	A	baru oil	32.8
BMEPA5	1:1:250:250	B	baru oil	44.2
BMEPA6	1:1:250:250	C	baru oil	- ^b
BMEPA7	1:1:250:1000	A	macaw oil	39.4
BMEPA8	1:1:250:1000	B	macaw oil	49.4
BMEPA9	1:1:250:1000	C	macaw oil	38.2

^a Ratio of [initiator]₀ : [PPNCl]₀ : [epoxide]₀ : [anhydride]₀. BMEPA1-6: 1 = 20 μmol, BMEPA7-9: 1 = 10 μmol. ^b No insoluble material produced.

3.2. Crosslinking by PPM

Another method of cross-linking is by using PPM to link already formed polymers into a network using difunctional crosslinkers, essentially treating the polymers as macromonomers. The entirely bio-derived polyester formed with epichlorohydrin and itaconic anhydride is a very suitable starting material for this sort of reaction, having two functional groups which could be the target of crosslinking by PPM – the pendant alkyl chloride group from ECH and electron-poor double bond from IA. Amine and thiol groups have the ability to react with either PPM target, either by nucleophilic substitution or Michael addition, so our goals were firstly to see if an insoluble high

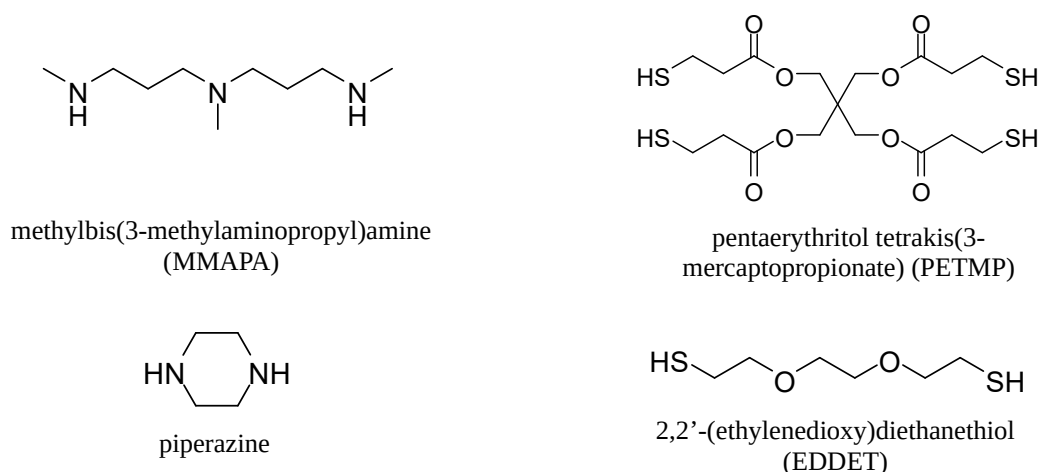


Figure 18 – Amines and thiols investigated for cross-linking by PPM

molecular weight material could be created by crosslinking using diamines and dithiols and if successful, to evaluate its properties and see whether it could be discerned which method of crosslinking was dominant. We used two diamines which were already in stock for another project, a linear diamine methylbis(3-methylaminopropyl)amine (MMAPA) and piperazine which though smaller, has greater availability at its Ns, and compared them to two high molecular weight thiols to avoid a stench, a linear dithiol 2,2'-(ethylenedioxy)diethanethiol (EDDET) and a tetrathiol pentaerythritol tetrakis(3-mercaptopropionate) (PETMP) (Fig. 18). Comparing with diol crosslinkers was ruled out due to the potential for transesterification and degradation of the polymer backbone. The method proposed by Hoffmann *et al.* was used; all reactions were conducted at 70 °C in bulk and with the addition of 0.1 mL DMF⁶⁸ to determine the effect of solvent upon the reaction. The reaction vessel was kept airtight and purged with N₂ beforehand, firstly to avoid any chance of the dithiols oxidising and secondly to avoid a stench upon heating, and all reactions were run overnight. The yield of the resulting insoluble polymeric resins was determined by removal of the unreacted polymer by dissolving in DCM and agitation overnight, with the resulting material being dried, mass determined

and compared to the initial mass of reaction mixture before purification. In order to determine whether crosslinking would occur spontaneously under these conditions, control reactions were performed without crosslinkers but otherwise identical reaction conditions. After purification and solubility testing, the control reaction in bulk showed no evidence of reactivity, but in solution an insoluble crosslinked material was made with 7% yield by mass. This is further evidence for the spontaneous occurrence of side reactions upon the heating of itaconate esters such as radical cross-linking, but suggests that the addition of crosslinkers is necessary to achieve high yields of insoluble material.

3.2.1. Discussion of Results

Table 4: Crosslinking reactions with amines and thiols

Entry	Cross-Linker	Medium	Insolubles Yield (%) ^a	T _{D10} (° C)
CLDA12	MMAPA	bulk	77	177
CLDA13	MMAPA	solution	83	167
CLDA16	piperazine	bulk	90	- ^c
CLDA15	piperazine	solution	95	183
CLDT9	EDDET	bulk	30	- ^b
CLDT10	EDDET	solution	39	- ^b
CLDT11	PETMP	bulk	1	- ^b
CLDT12	PETMP	solution	79	280

^a Yield of insoluble material calculated by mass compared to mass of reaction mixture. ^b Too little insoluble material produced to test thermal stability. ^c Not tested due to poor quality of material – see elemental analysis.

Solubility testing confirmed that all crosslinkers do form insoluble thermoset resins with bio-derived ECH-IA polymers in both chloroform and THF, proving that high molecular weight polymeric material can be created by ROCOP from entirely bio-derived sources.

However, such testing does not give any information on the degree of crosslinking, and the insolubility of the products makes them impossible to analyse by ^1H NMR spectroscopy. As a result, the crosslinked materials were analysed by a range of techniques such as IR spectrometry, TGA, DSC and elemental analysis in order to gather evidence on their purity and physical properties; solid state ^{13}C NMR spectroscopy was unavailable due to non-functional equipment.

The percentage yields of insoluble polymeric resin produced suggests that in general, diamines are more effective at performing this reaction than thiols. This runs contrary to expectations in that thiols tend to be more reactive than amines; despite N_2 -purging of the reaction system, oxidation of thiol crosslinkers could be occurring either during the reaction or during preparation to render them inactive. It also suggests that crosslinking in solution was more effective than reaction in bulk, which is unsurprising since as viscosity increases, the decreasing solubility of reactants in the reaction mixture slows the rate of reaction.

TGA analysis was performed on the starting ECH-IA polymer which showed a $T_{\text{D}10}$ of 286 °C, suggesting that thermal properties of crosslinked materials are inferior compared to those of the starting copolymer, with most TGAs of crosslinked resins showing a thermal degradation curve with two phases (Fig. 19). This could either show that the polymer is only partially crosslinked, and the unreacted polymer degrades in the first phase with the crosslinked material degrading subsequently, or that the first phase of degradation consists of retro-Michael addition of reacted crosslinkers with subsequent degradation of the polymer and crosslinks reacted *via* nucleophilic substitution at higher temperatures. This theory is supported by the fact that the most thermally stable of the crosslinkers by a large margin (100 °C) was the tetrathiol, which

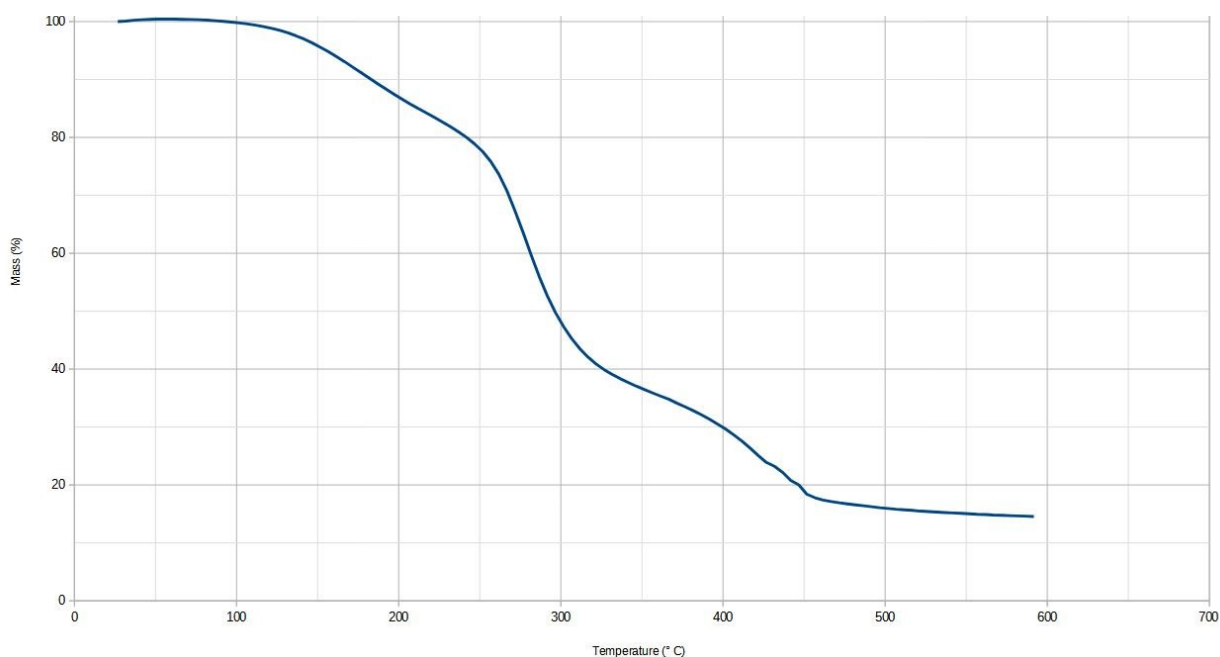


Figure 19 –Thermal degradation curve of CLDA15 – piperazine cross-linked in solution

as well as possessing the extra degree of crosslinking afforded by a crosslinker with four active sites rather than two, is also bonded by thio-Michael rather than aza-Michael addition, which requires more thermal input to reverse as well as any large unreacted crosslinker molecule requiring more energy to remove.

Elemental analysis was performed to gain evidence on whether insoluble yield is an accurate representation of cross-linking based on the percentage of nitrogen or sulphur incorporated from crosslinkers, and the results are shown in Table 5. However to complicate matters, the theoretical amounts of each element present in the material differ depending on which PPM target the crosslinkers attack. These amounts have been calculated based on both nucleophilic substitution through pendant Cl and Michael addition onto double bonds and are presented in Table 6.

Table 5: Elemental analysis of crosslinked material

Entry	Cross-Linker	Medium	C (%)	H (%)	N (%)	S (%)	Rest (%)
CLDA12	MMAPA	bulk	46.4	7.2	6.6	-	39.8
CLDA13	MMAPA	solution	47.4	7.0	7.2	-	38.4
CLDA16	piperazine	bulk	41.9	4.2	2.5	-	51.4
CLDA15	piperazine	solution	41.3	5.5	5.0	-	48.2
CLDT9	EDDET	bulk	44.7	5.1	0	7.3	42.9
CLDT10	EDDET	solution	45.2	5.5	0.3	3.5	45.5
CLDT11	PETMP	bulk	44.3	4.7	0	3.1	47.9
CLDT12	PETMP	solution	42.5	4.8	0	5.2	47.5

Elemental composition determined by CHN(S) analysis, averaged between two runs.

Table 6: Ideal elemental composition assuming 100% crosslinking

Cross-Linker	Target	C (%)	H (%)	N (%)	S (%)	Rest (%)
MMAPA	Cl	58.9	7.7	8.3	0	25.1
MMAPA	d.b.	51.6	7.1	7.2	0	34.1
piperazine	Cl	56.9	6.2	6.6	0	30.3
piperazine	d.b.	48.5	5.7	5.7	0	40.1
EDDET	Cl	50.6	6.5	0	12.3	30.6
EDDET	d.b.	44.4	6.1	0	10.8	38.7
PETMP	Cl	50.3	5.8	0	11.0	32.9
PETMP	d.b.	44.8	5.5	0	9.8	39.9

Ideal elemental composition calculated assuming a perfect reaction of one crosslinker to two polymer repeat units *via* either nucleophilic substitution onto pendant Cl or Michael addition onto double bond on polymer backbone.

None of the crosslinked material showed nitrogen or sulphur incorporation at percentages expected with full conversion of active sites into crosslinks, with the closest to ideal being the linear diamine MMAPA. This supports the hypothesis that only partial crosslinking was achieved, as suggested by TGA data. The percentage of nitrogen compared to sulphur incorporated also supports our theory that diamines are more effective at performing these crosslinking reactions, though minimal amounts of nitrogen could have been incorporated from initiators present in starting polymers; several batches were tested, and a maximum contribution of 1% was found from this source. In order to try and determine which method of crosslinking was dominant, all samples with enough material were analysed by IR spectroscopy.

The IR spectrum of the starting material showed a characteristic peak corresponding to the itaconate double bond at 1651 cm^{-1} and its presence, or lack of it, was the main piece of evidence to determine which crosslinking method was dominant. Unfortunately the equipment for ^{13}C solid state NMR spectroscopy was out of order for several months at the conclusion of the research period but had it been available, we would have used it to check for any vinylic environments detectable, as well as any unreacted thiol or amine peaks to determine if either unreacted or mono-reacted cross-linker was present in the product.

IR analysis for all insoluble materials crosslinked using diamines showed a large peak in the $1620\text{-}1625\text{ cm}^{-1}$ range corresponding to the itaconate double bond in the polymer backbone (Fig. 20) which suggests that at longer reaction times such as those used in our experiments, they end up irreversibly reacted *via* nucleophilic substitution of the pendant Cl group rather than Michael addition at the itaconate double bond. EDDET reacted in solution does show a C=C peak around 1659 cm^{-1} whereas in the other thiol

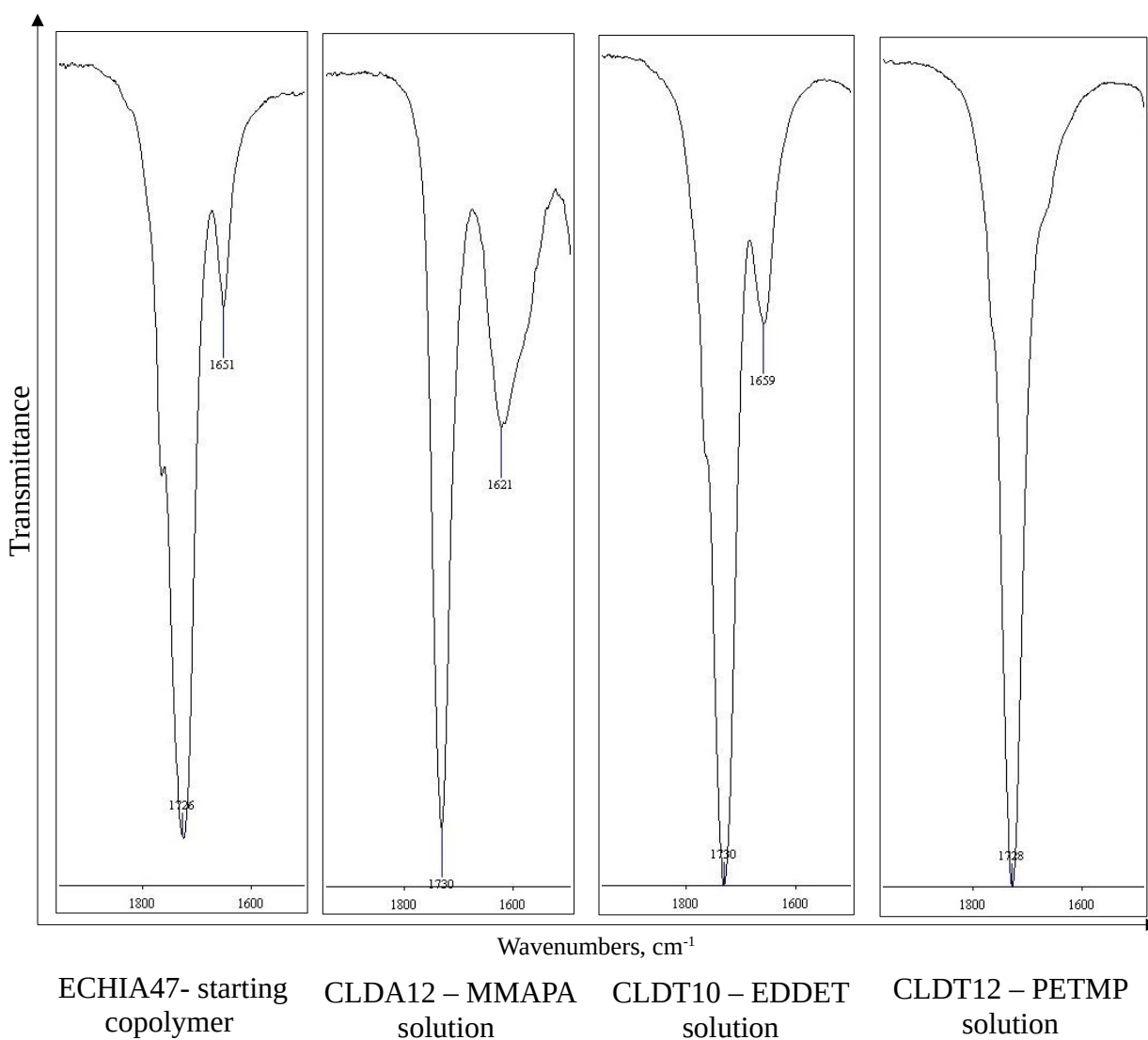


Figure 20 – IR spectra of crosslinked materials comparing the carbonyl and double bond peaks in the 1500-1900 cm^{-1} range

materials it is absent. As the yields and elemental analysis suggest that thiol crosslinkers are slower-reacting and that reactions in solution are faster than those in bulk, this could indicate that as the reaction proceeds it initially reacts with Michael addition *via* the double bond and since Michael reactions are reversible, the faster the rate of reaction of the crosslinkers is the greater the proportion of them we would find irreversibly reacted by nucleophilic substitution. Additionally, since citraconate isomers are present in significant quantities in our itaconate starting materials and they are unreactive to PPM by Michael addition⁶⁴ due to steric hindrance at the double bond but the pendant Cl in

the isomer is still available as a target, preferential nucleophilic substitution could occur leaving the double bond intact to be detected by IR spectroscopy.

4. Conclusion

ROCOP is a promising method of synthesising polyesters under mild conditions compared to traditional polycondensation, with a wide variety of functionalisation available on demand, but its industrial utility has been limited by the rigorously anhydrous conditions it has been tested in. Our aims were to prove that it can be undertaken without extreme water-removal techniques with a range of initiators and monomers, to discover if polyesters could be synthesised via ROCOP using entirely bio-derived materials, and to investigate methods to improve their properties. These aims have been achieved; a wide range of monomers have been effectively copolymerised in bench-top conditions, including an entirely bio-derived copolymer of ECH and IA, with cheap, widely available organoinitiator DCU showing comparable activity to an Al salophen complex commonly used in ROCOP^{29,33}, making it a promising candidate for greener polyester synthesis. We have also shown that using bio-derived monomers with multiple reaction sites with this reaction method can create high molecular weight, crosslinked products from two separate polyunsaturated oils. The properties of the bio-derived copolymer of ECH and IA have also been modified after the fact, showing that polymers created from small-molecule, bio-derived widely available monomers can be used as starting materials to create crosslinked polymeric resins by PPM with a range of amines and thiols. Due to time constraints, a comprehensive range of testing was not able to be completed, with no physical testing taking place. As a result, there was no clear conclusion as to which crosslinker was the most effective, with diamines reacting most completely according to elemental analysis but with a less thermally stable material as a product compared to the tetrathiol. Nonetheless, we have proved that a range of crosslinkers are effective at improving the properties of bio-derived polymers

created using ROCOP, and that high molecular weight polymeric materials can be created from bio-derived sources without the costs, restrictions and waste associated with extreme water removal.

5. Future Work

Further work is necessary to determine how scaleable the ECH-IA copolymerisation reaction is as many attempts ended in an insoluble material being formed, either because the polymer was of a sufficiently high molecular weight or more likely polymer chains were being crosslinked during the polymerisation reaction due to spontaneous radical cross-linking at extended periods of elevated temperature. This is not necessarily a negative result as high molecular weight materials were created in either case, but solubility is necessary for most PPM and desired for ease of characterisation. Future work could determine the properties of this insoluble material and its suitability for industrial purposes, as well as how well the ECH-IA reaction scales beyond the gram scale and whether the addition of a radical scavenger could improve its scaleability.

Further work is also necessary to properly elucidate which of the crosslinkers creates the material with the most favourable properties for industrial applications. The answer is not conclusive from data that was able to be collected, but time pressures did not allow, for example, physical properties to be tested.

Finally, none of the crosslinkers used was bio-derived. A potential bio-derived crosslinker, L-cystine dimethyl ester, was acquired and tested but no reactivity was observed, so another focus of future work could be comparing the effectiveness of a range of bio-derived crosslinkers.

6. References

1. P. B. Weisz, *Physics Today*, 2004, **57**, 47–52.
2. M. Eriksen, L. C. M. Lebreton, H. S. Carson, M. Thiel, C. J. Moore, J. C. Borerro, F. Galgani, P. G. Ryan and J. Reisser, *PLOS ONE*, 2014, **9**, e111913.
3. E. van Sebille, C. Wilcox, L. Lebreton, N. Maximenko, B. D. Hardesty, J. A. van Franeker, M. Eriksen, D. Siegel, F. Galgani and K. L. Law, *Environ. Res. Lett.*, 2015, **10**, 124006.
4. J. R. Jambeck, R. Geyer, C. Wilcox, T. R. Siegler, M. Perryman, A. Andrady, R. Narayan and K. L. Law, *Science*, 2015, **347**, 768–771.
5. O. Hoegh-Guldberg, D. Jacob, M. Taylor, M. Bindi, S. Brown, I. Camilloni, A. Diedhiou, R. Djalante, K. L. Ebi, F. Engelbrecht, J. Guiot, Y. Hijikata, S. Mehrotra, A. Payne, S. I. Seneviratne, A. Thomas, R. Warren and G. Zhou, in *An IPCC Special Report on the impacts of global warming of 1.5°C above pre-industrial levels and related global greenhouse gas emission pathways, in the context of strengthening the global response to the threat of climate change, sustainable development, and efforts to eradicate poverty*, IPCC, Geneva, 2018.
6. C. K. Williams and M. A. Hillmyer, *Polym. Rev.*, 2008, **48**, 1–10.
7. M. Vert, *Biomacromolecules*, 2005, **6**, 538–546.
8. F. H. Isikgor and C. R. Becer, *Polym. Chem.*, 2015, **6**, 4497–4559.
9. M. J.-L. Tschan, E. Brulé, P. Haquette and C. M. Thomas, *Polym. Chem.*, 2012, **3**, 836–851.
10. R. H. Platel, L. M. Hodgson and C. K. Williams, *Polym. Rev.*, 2008, **48**, 11–63.
11. S. Philip, T. Keshavarz and I. Roy, *J. Chem. Technol. Biotechnol.*, 2007, **82**, 233–247.
12. G.-Q. Chen and Q. Wu, *Biomaterials*, 2005, **26**, 6565–6578.

13. J. H. Park, J. Y. Jeon, J. J. Lee, Y. Jang, J. K. Varghese and B. Y. Lee, *Macromolecules*, 2013, **46**, 3301–3308.
14. C. K. Williams, *Chem. Soc. Rev.*, 2007, **36**, 1573–1580.
15. R. A. Gross, A. Kumar and B. Kalra, *Chem. Rev.*, 2001, **101**, 2097–2124.
16. S. Paul, Y. Zhu, C. Romain, R. Brooks, P. K. Saini and C. K. Williams, *Chem. Commun.*, 2015, **51**, 6459–6479.
17. R. F. Fischer, *J. Polym. Sci.*, 1960, **44**, 155–172.
18. T. Tsuruta, K. Matsuura and S. Inoue, *Die Makromol. Chem.*, 1964, **75**, 211–214.
19. M. E. Fieser, M. J. Sanford, L. A. Mitchell, C. R. Dunbar, M. Mandal, N. J. Van Zee, D. M. Urness, C. J. Cramer, G. W. Coates and W. B. Tolman, *J. Am. Chem. Soc.*, 2017, **139**, 15222–15231.
20. T. Aida and S. Inoue, *J. Am. Chem. Soc.*, 1985, **107**, 1358–1364.
21. T. Aida, K. Sanuki and S. Inoue, *Macromolecules*, 1985, **18**, 1049–1055.
22. R. C. Jeske, A. M. DiCiccio and G. W. Coates, *J. Am. Chem. Soc.*, 2007, **129**, 11330–11331.
23. A. L. Borgne, V. Vincens, M. Jouglard and N. Spassky, *Makromol. Chem. Macromol. Symp.*, 1993, **73**, 37–46.
24. L. E. Martinez, J. L. Leighton, D. H. Carsten and E. N. Jacobsen, *J. Am. Chem. Soc.*, 1995, **117**, 5897–5898.
25. D. J. Darensbourg and J. C. Yarbrough, *J. Am. Chem. Soc.*, 2002, **124**, 6335–6342.
26. S. Huijser, E. Hosseini Nejad, R. Sablong, C. de Jong, C. E. Koning and R. Duchateau, *Macromolecules*, 2011, **44**, 1132–1139.
27. A. M. DiCiccio and G. W. Coates, *J. Am. Chem. Soc.*, 2011, **133**, 10724–10727.
28. C. Robert, F. de Montigny and C. M. Thomas, *Nat. Commun.*, 2011, **2**, 586.

29. N. J. Van Zee, M. J. Sanford and G. W. Coates, *J. Am. Chem. Soc.*, 2016, **138**, 2755–2761.
30. E. H. Nejad, C. G. W. van Melis, T. J. Vermeer, C. E. Koning and R. Duchateau, *Macromolecules*, 2012, **45**, 1770–1776.
31. J. Y. Jeon, S. C. Eo, J. K. Varghese and B. Y. Lee, *Beilstein J. Org. Chem.*, 2014, **10**, 1787–1795.
32. E. H. Nejad, A. Paoniasari, C. G. W. van Melis, C. E. Koning and R. Duchateau, *Macromolecules*, 2013, **46**, 631–637.
33. M. Proverbio, N. G. Galotto, S. Losio, I. Tritto and L. Boggioni, *Polymers*, 2019, **11**, 1222.
34. R. Mundil, Z. Hošťálek, I. Šeděnková and J. Merna, *Macromol. Res.*, 2015, **23**, 161–166.
35. D. J. Darensbourg, R. M. Mackiewicz, J. L. Rodgers, C. C. Fang, D. R. Billodeaux and J. H. Reibenspies, *Inorg. Chem.*, 2004, **43**, 6024–6034.
36. E. H. Nejad, A. Paoniasari, C. E. Koning and R. Duchateau, *Polym. Chem.*, 2012, **3**, 1308–1313.
37. D. Ryzhakov, G. Printz, B. Jacques, S. Messaoudi, F. Dumas, S. Dagorne and F. L. Bideau, *Polym. Chem.*, 2021, **12**, 2932–2946.
38. B. Han, L. Zhang, B. Liu, X. Dong, I. Kim, Z. Duan and P. Theato, *Macromolecules*, 2015, **48**, 3431–3437.
39. Z. Hošťálek, O. Trhlíková, Z. Walterová, T. Martinez, F. Peruch, H. Cramail and J. Merna, *Eur. Polym. J.*, 2017, **88**, 433–447.
40. H.-Y. Ji, X.-L. Chen, B. Wang, L. Pan and Y.-S. Li, *Green Chem.*, 2018, **20**, 3963–3973.

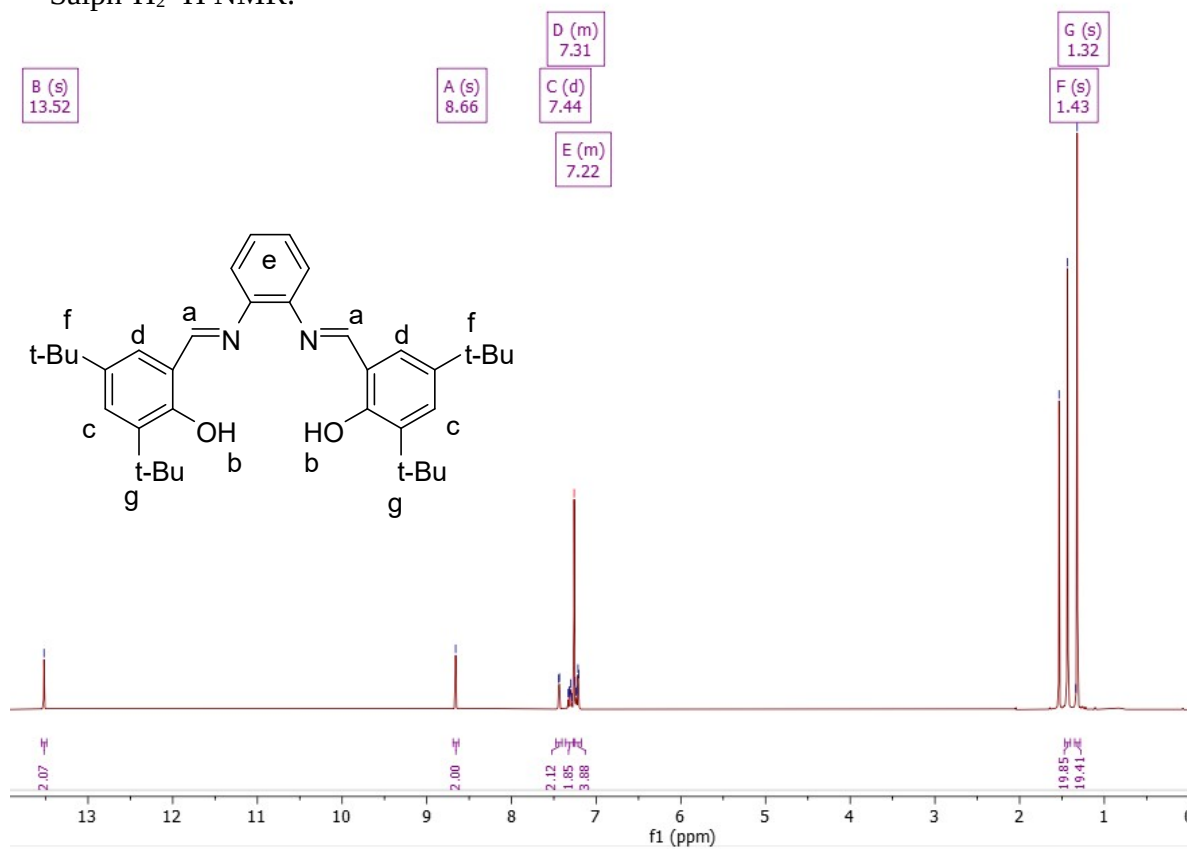
41. L.-F. Hu, C.-J. Zhang, H.-L. Wu, J.-L. Yang, B. Liu, H.-Y. Duan and X.-H. Zhang, *Macromolecules*, 2018, **51**, 3126–3134.
42. B. Zhang, H. Li, H. Luo and J. Zhao, *Eur. Polym. J.*, 2020, **134**, 109820.
43. L. Lin, J. Liang, Y. Xu, S. Wang, M. Xiao, L. Sun and Y. Meng, *Green Chem.*, 2019, **21**, 2469–2477.
44. B. Neises and W. Steglich, *Angew. Chem. Int. Ed. Engl.*, 1978, **17**, 522–524.
45. N. L. Benoiton, *Chemistry of Peptide Synthesis*, CRC Press, Boca Raton, FL, 2016.
46. B. Lin and R. M. Waymouth, *J. Am. Chem. Soc.*, 2017, **139**, 1645–1652.
47. A. J. D. Silvestre and A. Gandini, in *Monomers, Polymers and Composites from Renewable Resources*, eds. M. N. Belgacem and A. Gandini, Elsevier, Amsterdam, 2008, pp. 17–38.
48. L. Peña Carrodeguas, C. Martín and A. W. Kleij, *Macromolecules*, 2017, **50**, 5337–5345.
49. A. Behr, J. Eilting, K. Irawadi, J. Leschinski and F. Lindner, *Green Chem.*, 2008, **10**, 13–30.
50. B. M. Bell, J. R. Briggs, R. M. Campbell, S. M. Chambers, P. D. Gaarenstroom, J. G. Hippler, B. D. Hook, K. Kearns, J. M. Kenney, W. J. Kruper, D. J. Schreck, C. N. Theriault and C. P. Wolfe, *CLEAN – Soil, Air, Water*, 2008, **36**, 657–661.
51. B. Liu, J. Chen, N. Liu, H. Ding, X. Wu, B. Dai and I. Kim, *Green Chem.*, 2020, **22**, 5742–5750.
52. Y. Liu, H. Tüysüz, C.-J. Jia, M. Schwickardi, R. Rinaldi, A.-H. Lu, W. Schmidt and F. Schüth, *Chem. Commun.*, 2010, **46**, 1238–1240.
53. A. Takasu, T. Bando, Y. Morimoto, Y. Shibata and T. Hirabayashi, *Biomacromolecules*, 2005, **6**, 1707–1712.

54. M. Winkler, C. Romain, M. A. R. Meier and C. K. Williams, *Green Chem.*, 2014, **17**, 300–306.
55. C. Wang, A. Thygesen, Y. Liu, Q. Li, M. Yang, D. Dang, Z. Wang, Y. Wan, W. Lin and J. Xing, *Biotechnol. Biofuels*, 2013, **6**, 74.
56. M. G. Steiger, M. L. Blumhoff, D. Mattanovich and M. Sauer, *Front. Microbiol.*, 2013, **4**, 23.
57. M. Okabe, D. Lies, S. Kanamasa and E. Y. Park, *Appl. Microbiol. Biotechnol.*, 2009, **84**, 597–606.
58. N. J. Van Zee and G. W. Coates, *Angew. Chem. Int. Ed.*, 2015, **54**, 2665–2668.
59. F. D. Monica and A. W. Kleij, *Polym. Chem.*, 2020, **11**, 5109–5127.
60. T. J. Farmer, J. W. Comerford, A. Pellis and T. Robert, *Polym. Int.*, 2018, **67**, 775–789.
61. R. Baumgartner, Z. Song, Y. Zhang and J. Cheng, *Polym. Chem.*, 2015, **6**, 3586–3590.
62. G. Si, L. Zhang, B. Han, Z. Duan, B. Li, J. Dong, X. Li and B. Liu, *Polym. Chem.*, 2015, **6**, 6372–6377.
63. S. Chanda and S. Ramakrishnan, *Polym. Chem.*, 2015, **6**, 2108–2114.
64. T. J. Farmer, D. J. Macquarrie, J. W. Comerford, A. Pellis and J. H. Clark, *J. Polym. Sci. A Polym. Chem.*, 2018, **56**, 1935–1945.
65. O. Daglar, B. Ozcan, U. S. Gunay, G. Hizal, U. Tunca and H. Durmaz, *Polymer*, 2019, **182**, 121844.
66. L. Fournier, C. Robert, S. Pourchet, A. Gonzalez, L. Williams, J. Prunet and C. M. Thomas, *Polym. Chem.*, 2016, **7**, 3700–3704.
67. A. Lv, Z.-L. Li, F.-S. Du and Z.-C. Li, *Macromolecules*, 2014, **47**, 7707–7716.

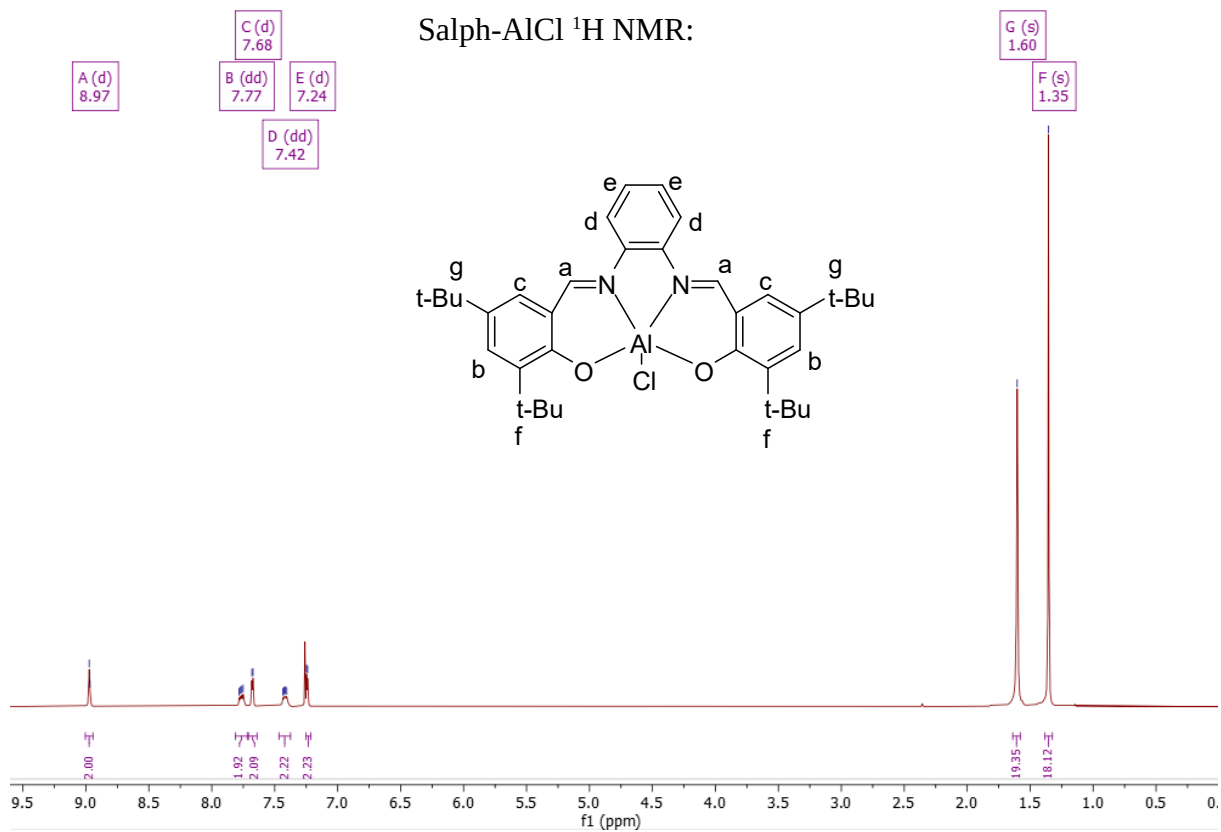
68. C. Hoffmann, M. C. Stuparu, A. Daugaard and A. Khan, *J. Polym. Sci. A Polym. Chem.*, 2015, **53**, 745–749.
69. T. Mehtiö, A. Anghelescu-Hakala, J. Hartman, V. Kunnari and A. Harlin, *J. Appl. Polym. Sci.*, 2017, **134**, 1–8.
70. N. R. James and A. Jayakrishnan, *Biomaterials*, 2003, **24**, 2205–2212.
71. S. Lakshmi and A. Jayakrishnan, *Biomaterials*, 2002, **23**, 4855–4862.
72. R. T. Alarcon, C. Gaglieri, K. J. Lamb, M. North and G. Bannach, *Ind. Crop. Prod.*, 2020, **154**, 112585.
73. K. Bester, A. Bukowska, B. Myśliwiec, K. Hus, D. Tomczyk, P. Urbaniak and W. Bukowski, *Polym. Chem.*, 2018, **9**, 2147–2156.
74. D. Rutherford and D. A. Atwood, *Organometallics*, 1996, **15**, 4417–4422.
75. A. M. DiCiccio, J. M. Longo, G. G. Rodríguez-Calero and G. W. Coates, *J. Am. Chem. Soc.*, 2016, **138**, 7107–7113.
76. R. L. Paddock and S. T. Nguyen, *J. Am. Chem. Soc.*, 2001, **123**, 11498–11499.
77. J. Liu, Y.-Y. Bao, Y. Liu, W.-M. Ren and X.-B. Lu, *Polym. Chem.*, 2013, **4**, 1439–1444.
78. A. Takasu, M. Ito, Y. Inai, T. Hirabayashi and Y. Nishimura, *Polym. J.*, 1999, **31**, 961–969.
79. I. Schoon, M. Kluge, S. Eschig and T. Robert, *Polymers*, 2017, **9**, 693.
80. M. Bernasconi, M.-A. Müller and A. Pfaltz, *Angew. Chem.*, 2014, **126**, 5489–5492.
81. R. Greco and L. Nicolais, *Polymer*, 1976, **17**, 1049–1053.
82. A. Kummari, S. Pappuru and D. Chakraborty, *Polym. Chem.*, 2018, **9**, 4052–4062.

7. Appendices

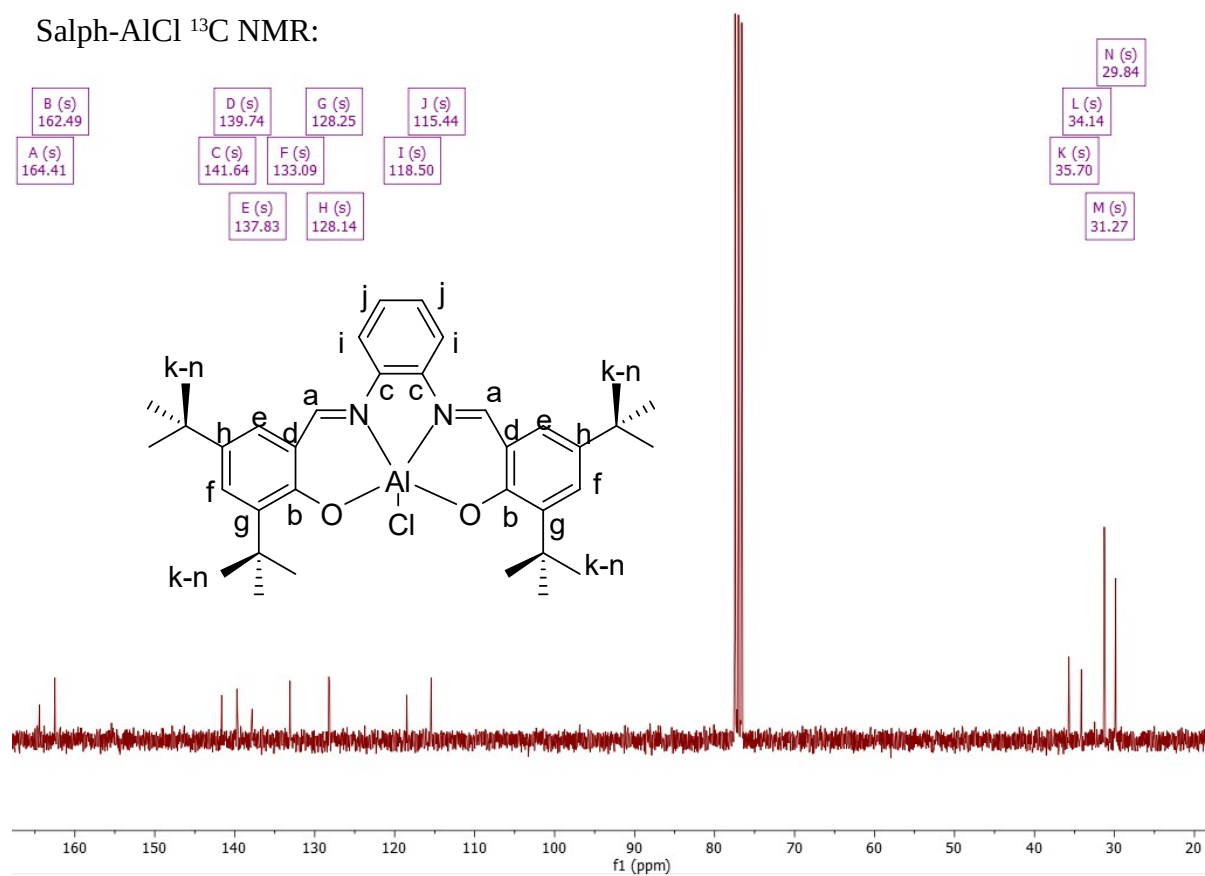
Salph-H₂ ¹H NMR:



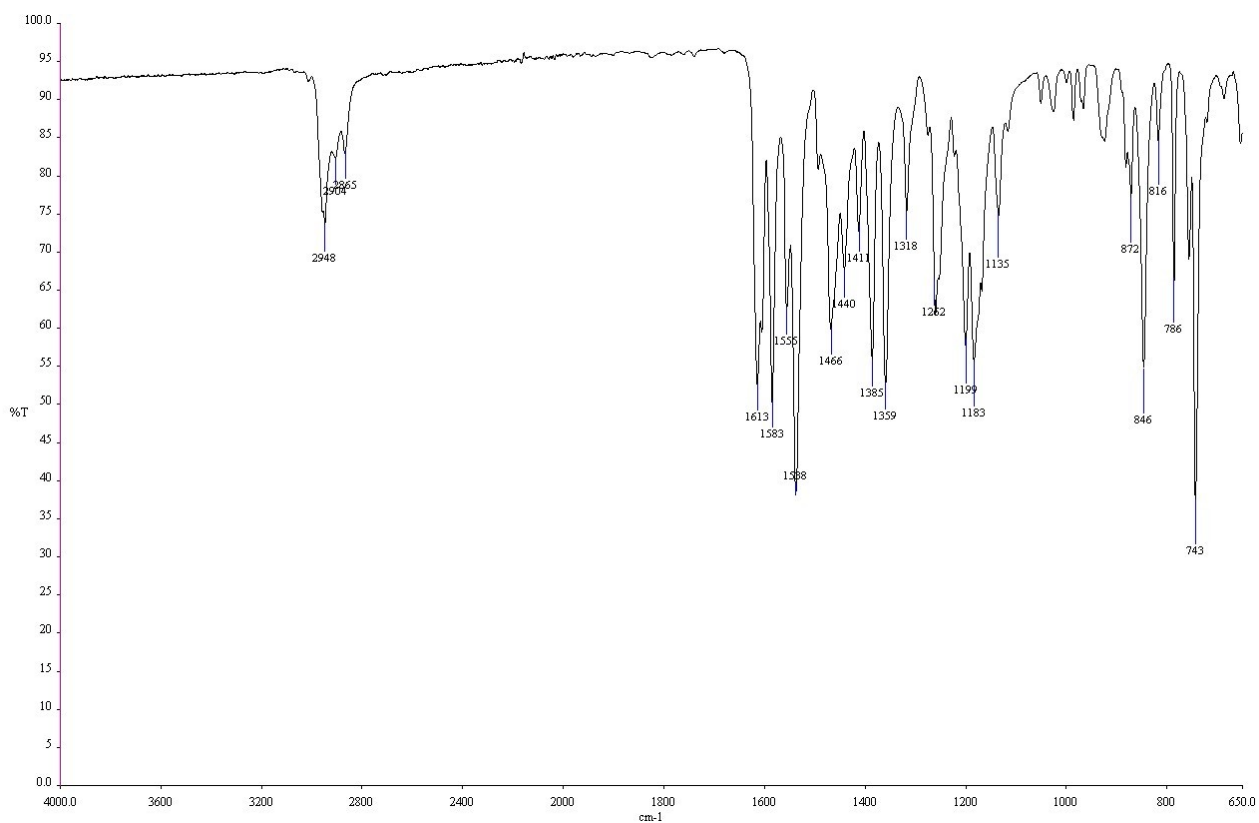
Salph-AlCl ¹H NMR:



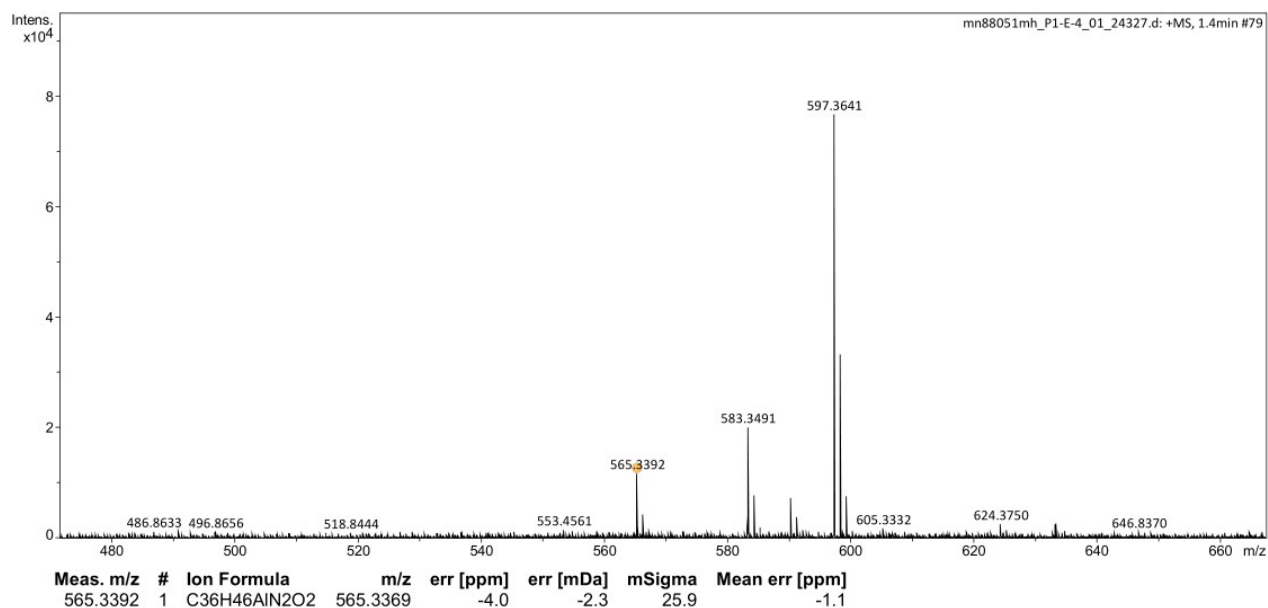
Salph-AlCl ¹³C NMR:



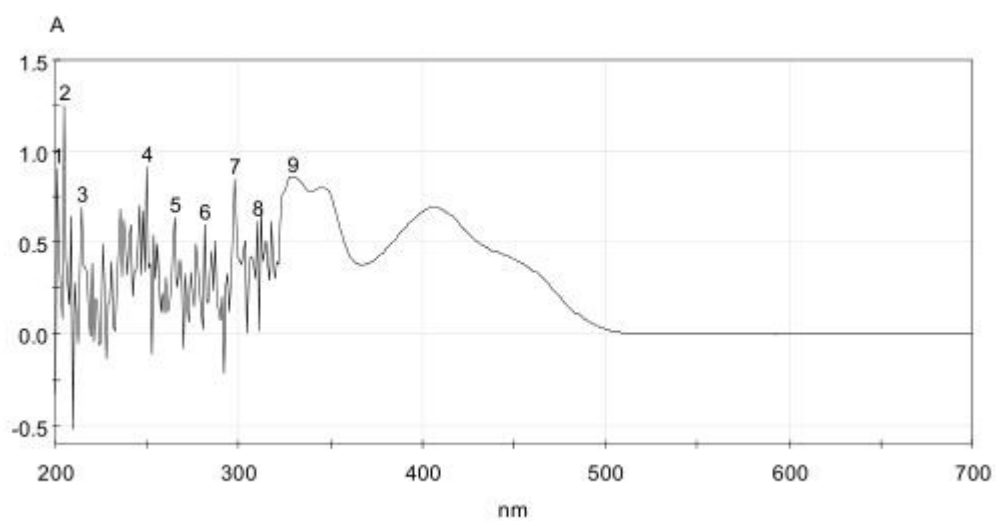
Salph-AlCl IR:



Salph-AlCl ESI-MS:

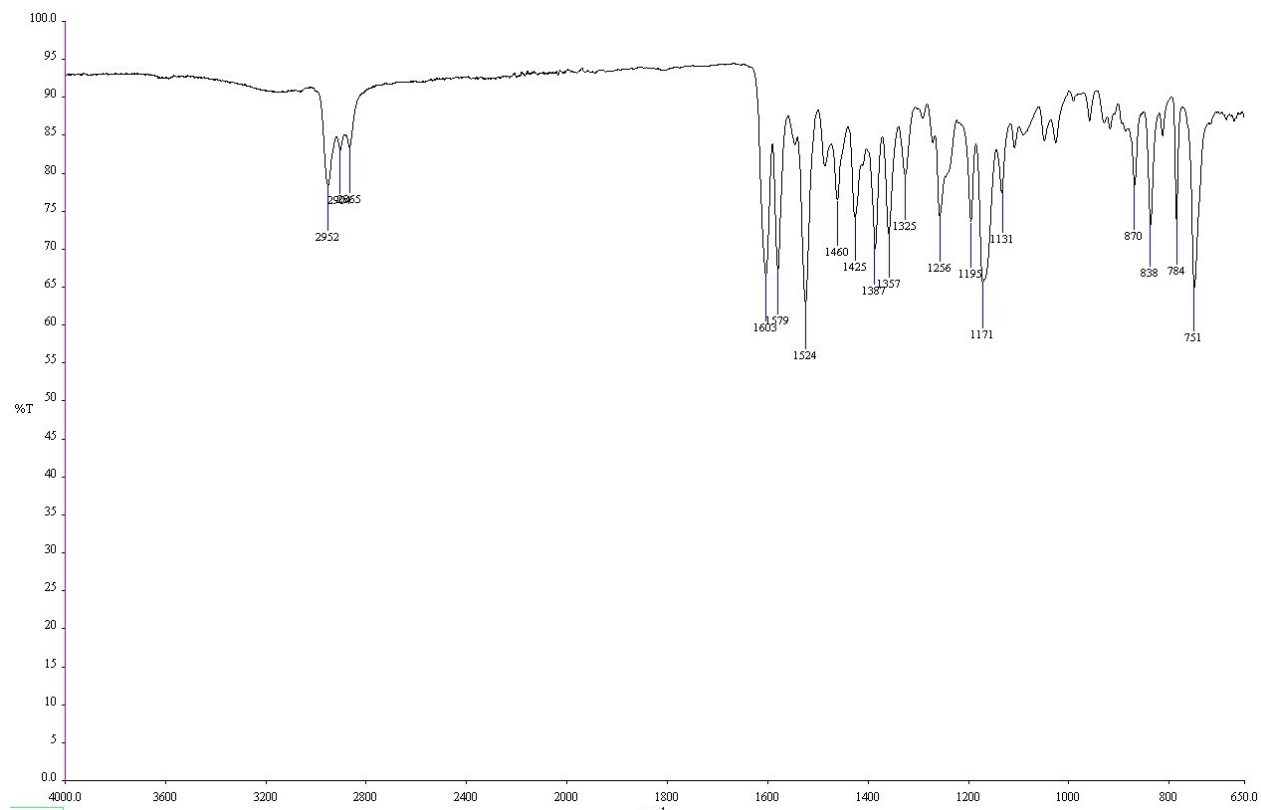


Salph-AlCl UV/Vis:

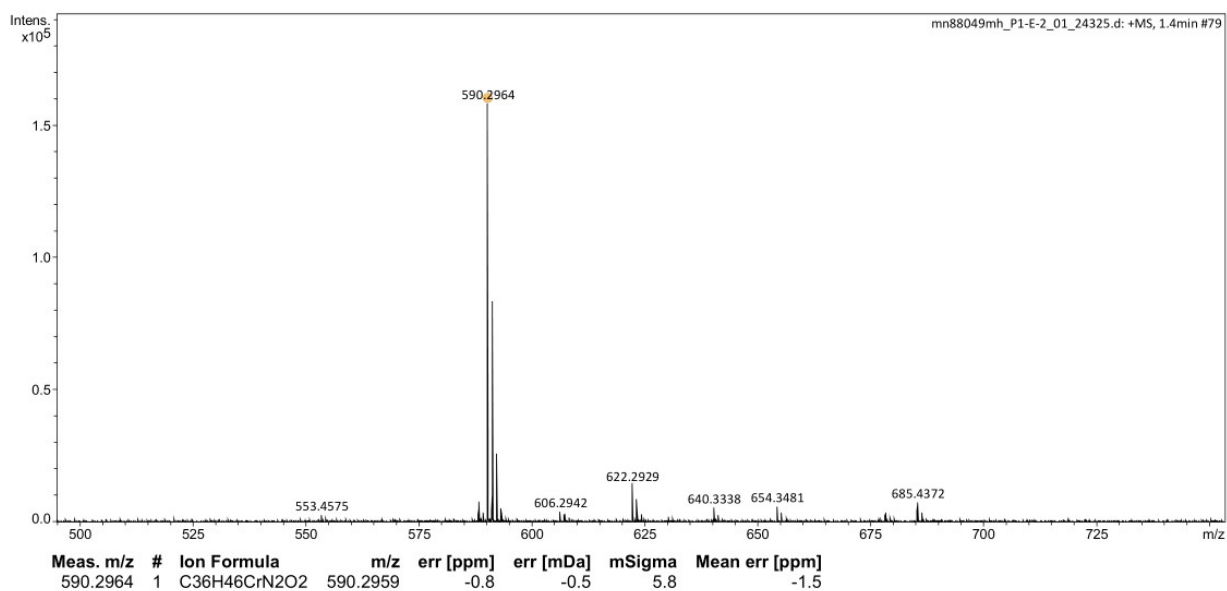


Relevant peaks: 346-353 nm, 395-419 nm

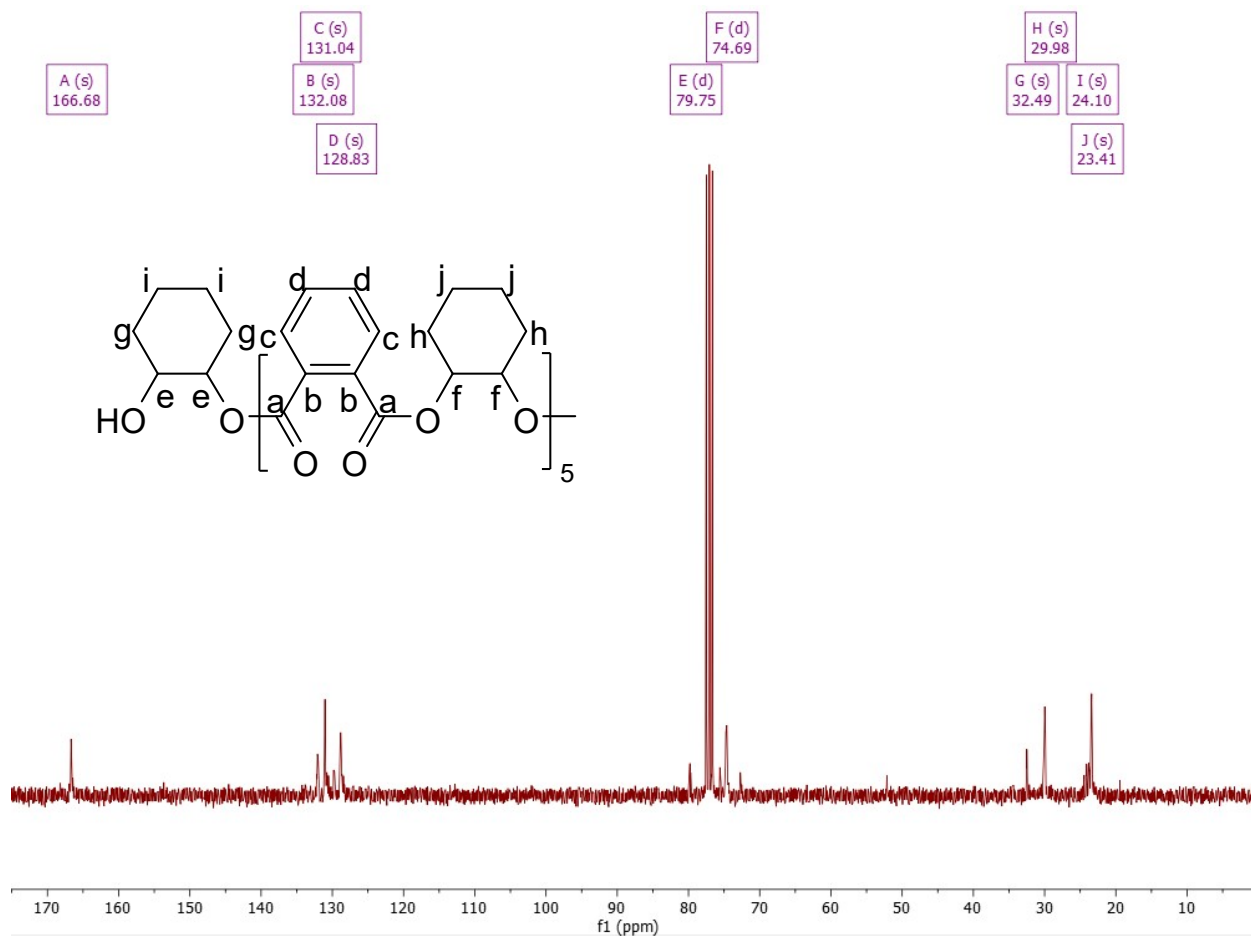
Salph-CrCl IR:



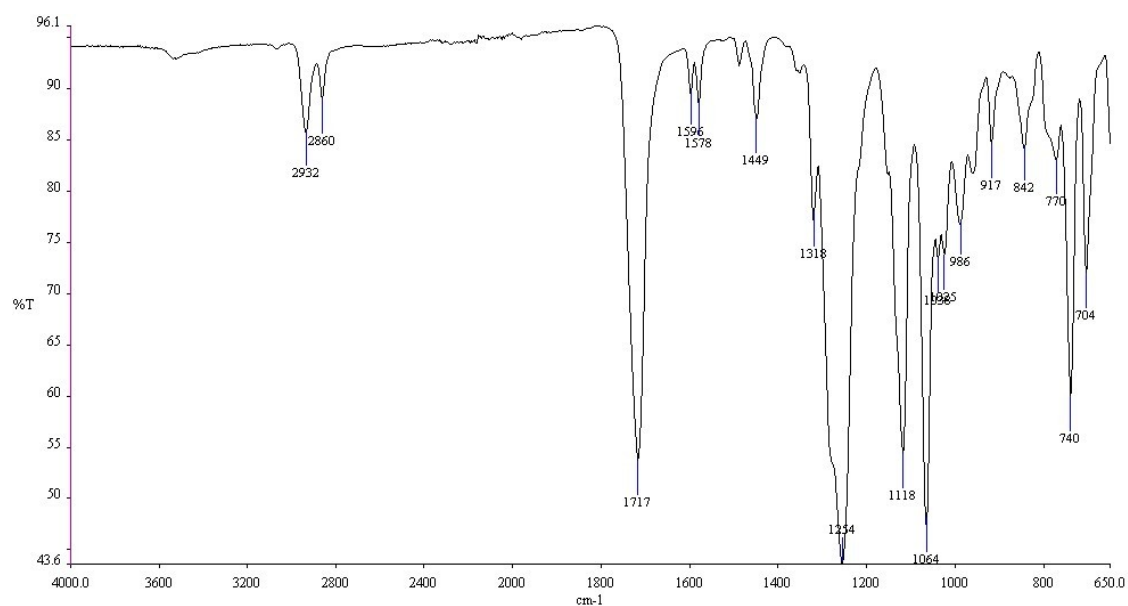
Salph-CrCl ESI-MS:



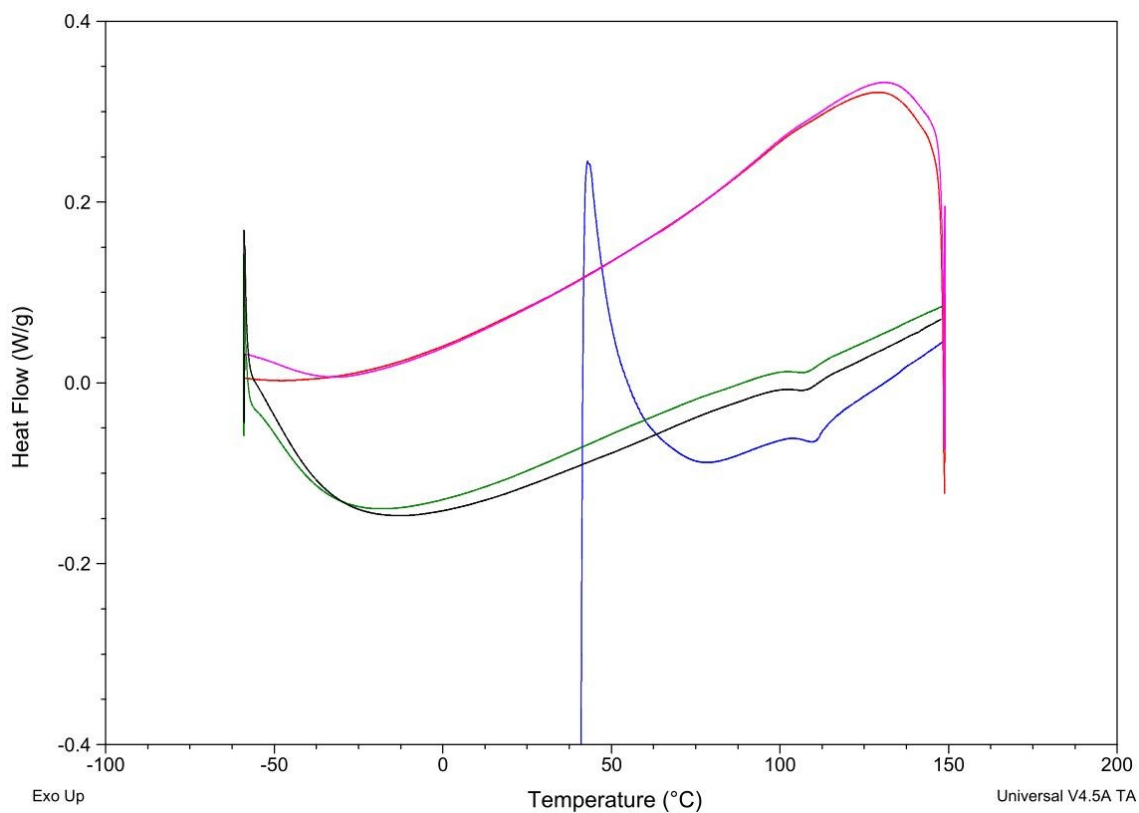
CHO-PA copolymer ¹³C NMR:



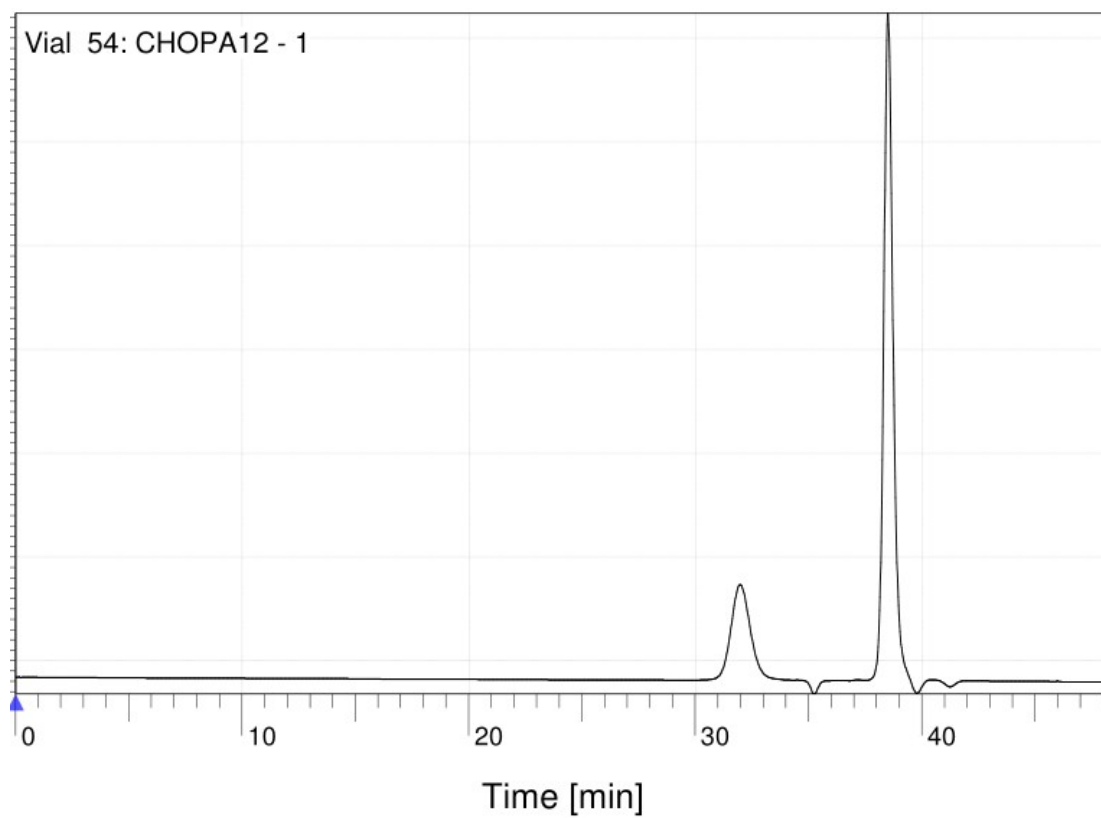
CHO-PA copolymer IR:



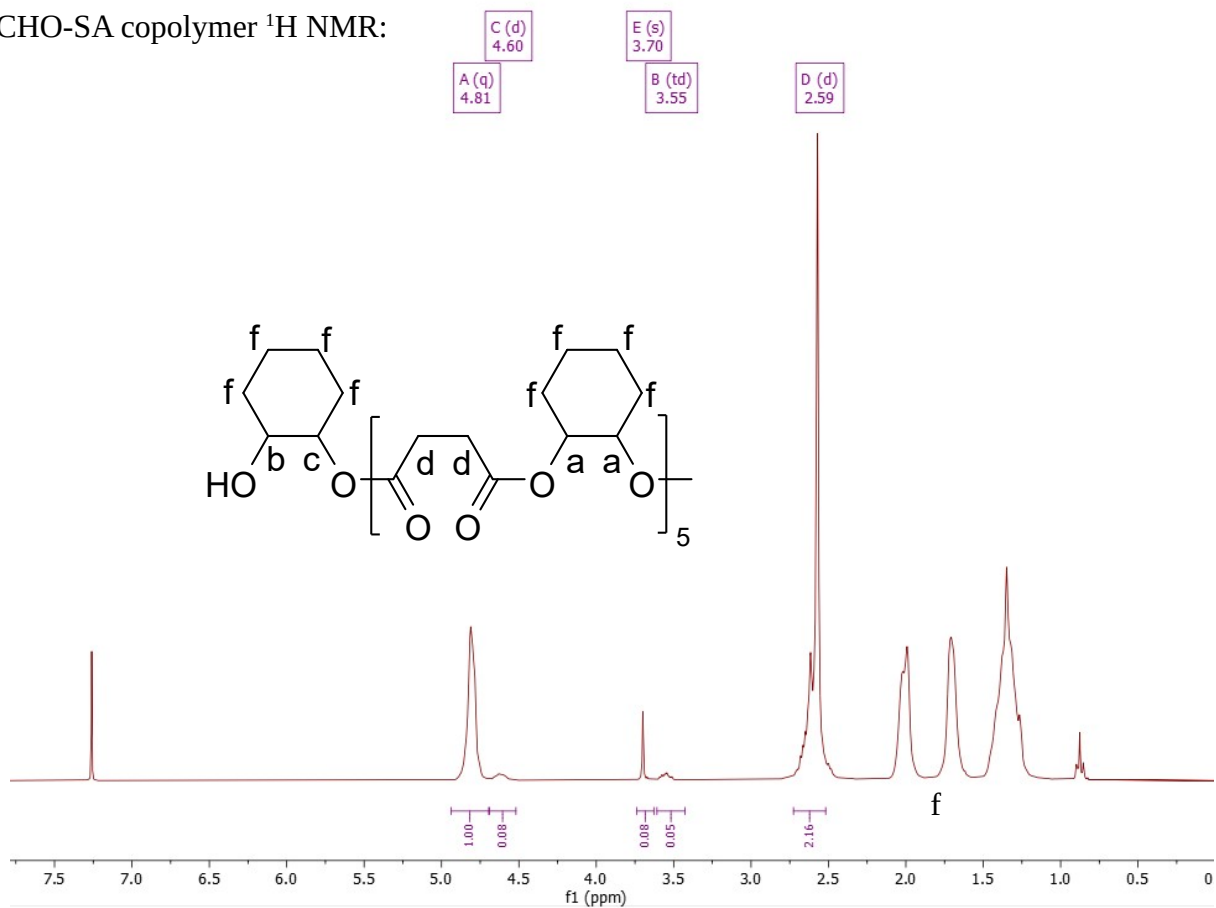
CHO-PA copolymer DSC:



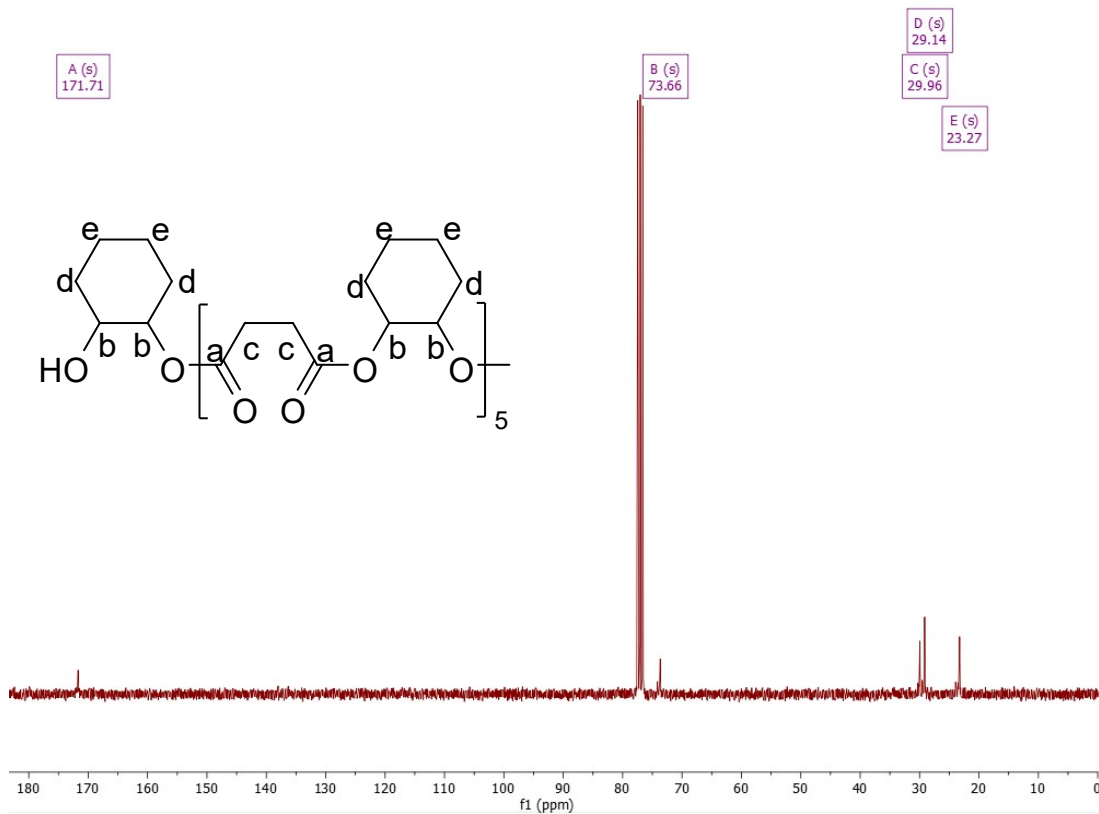
CHO-PA copolymer GPC:



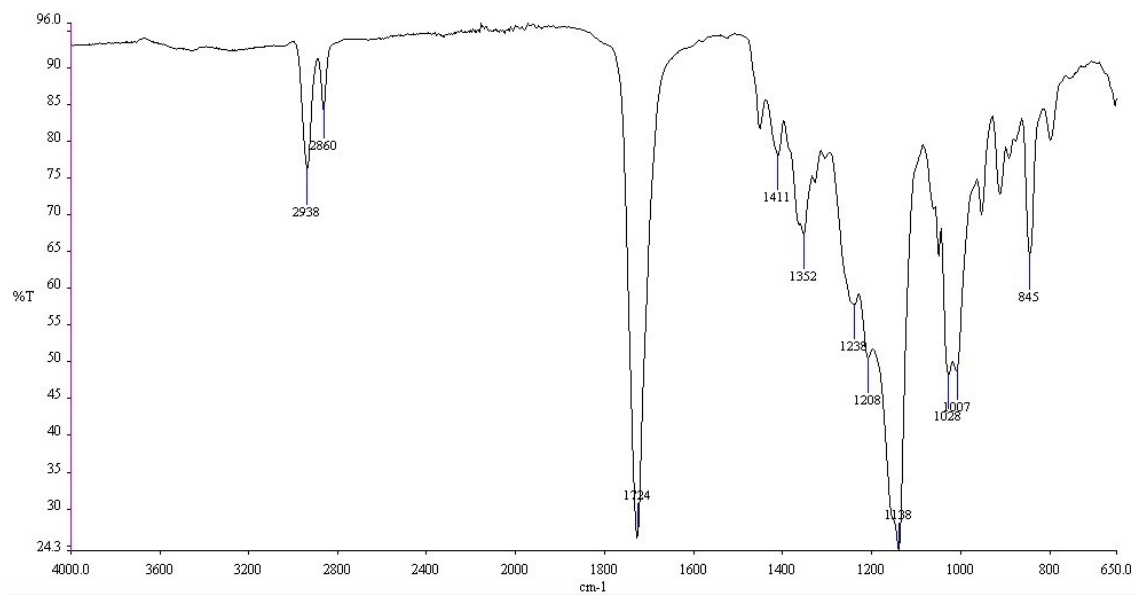
CHO-SA copolymer ^1H NMR:



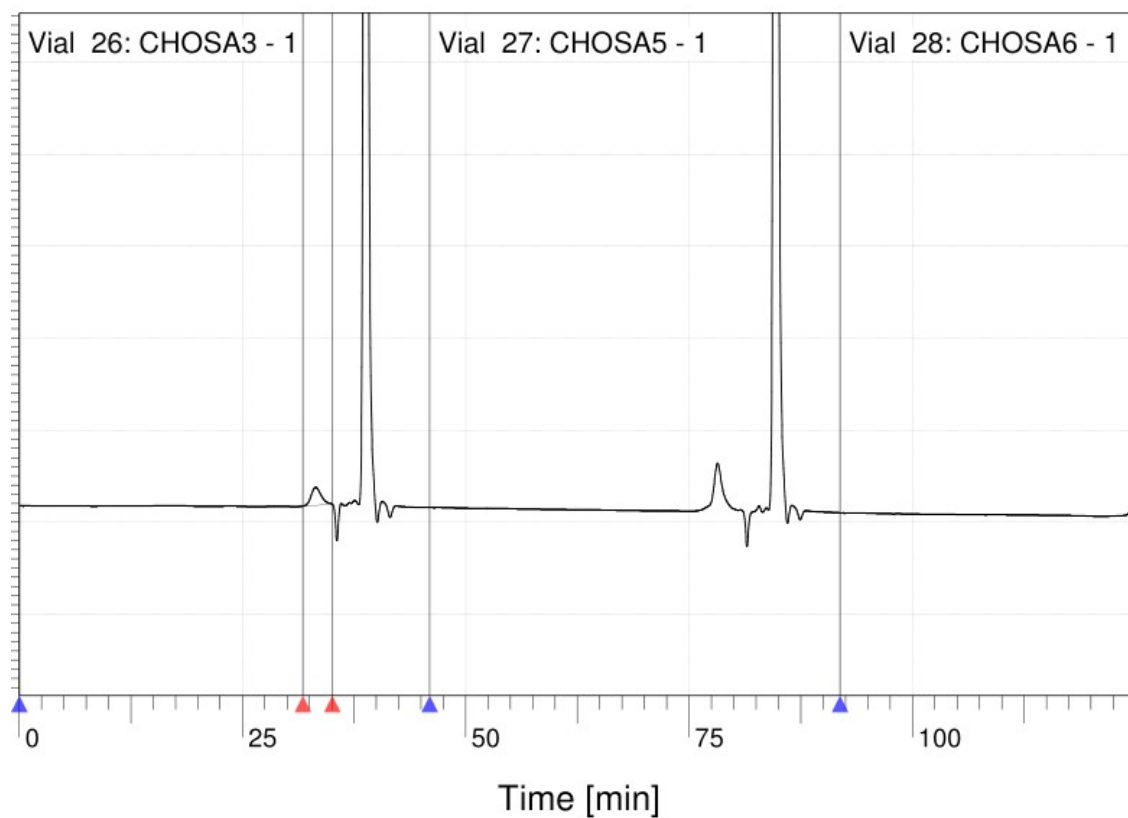
CHO-SA copolymer ^{13}C NMR:



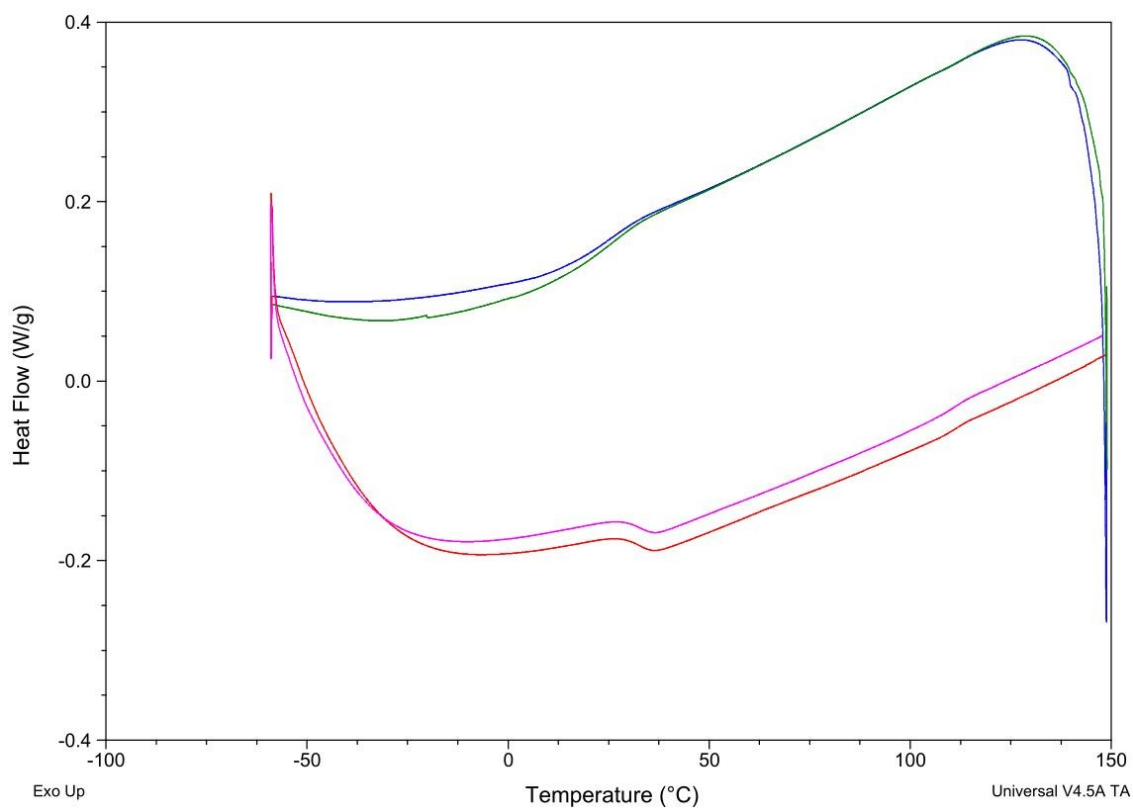
CHO-SA copolymer IR:



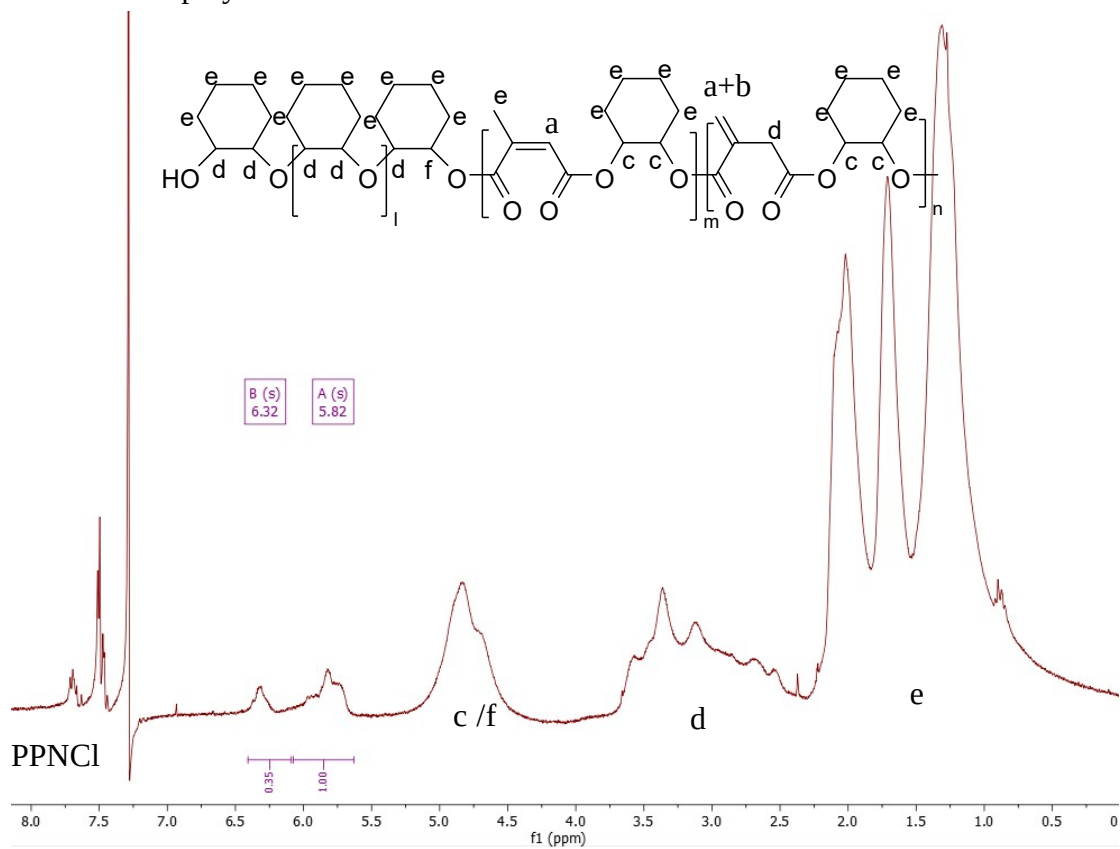
CHO-SA copolymer GPC:



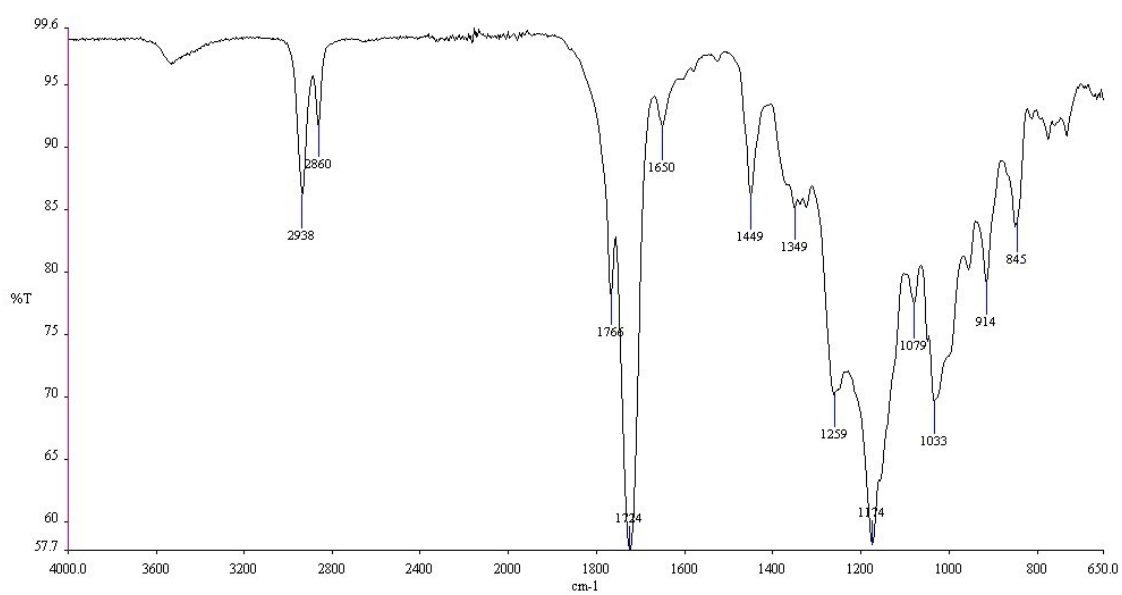
CHO-SA copolymer DSC:



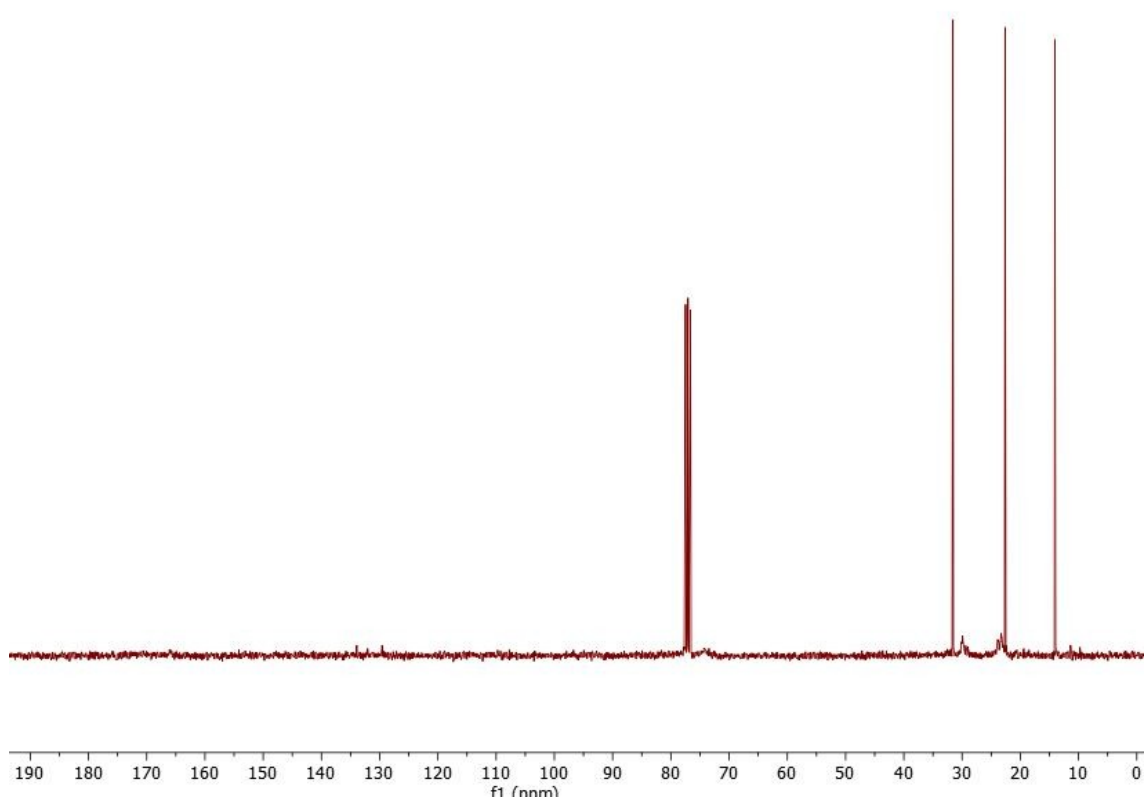
CHO-IA copolymer ¹H NMR:



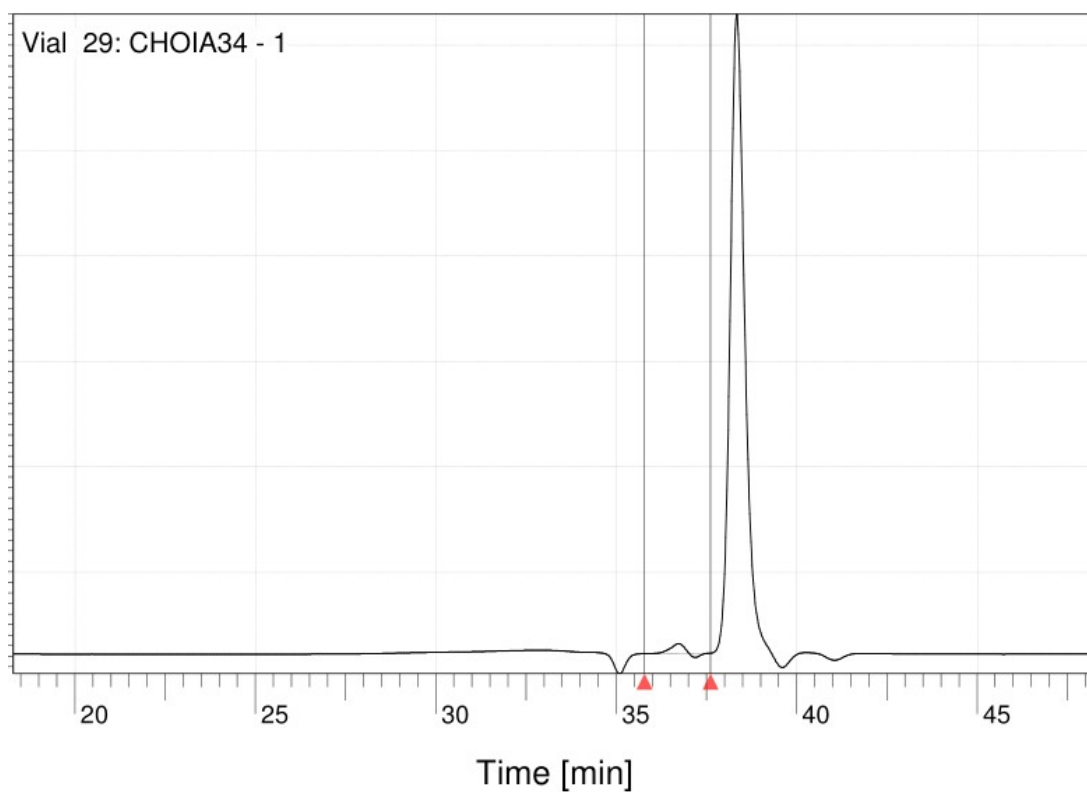
CHO-IA copolymer IR:



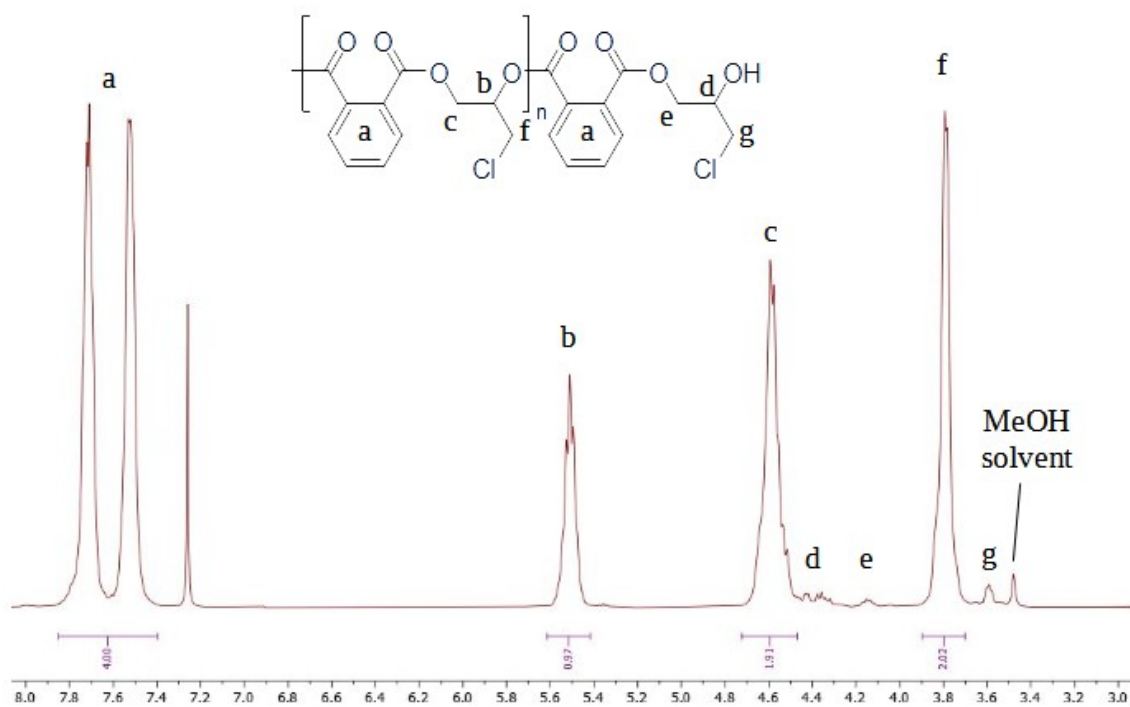
CHO-IA ¹³C NMR:



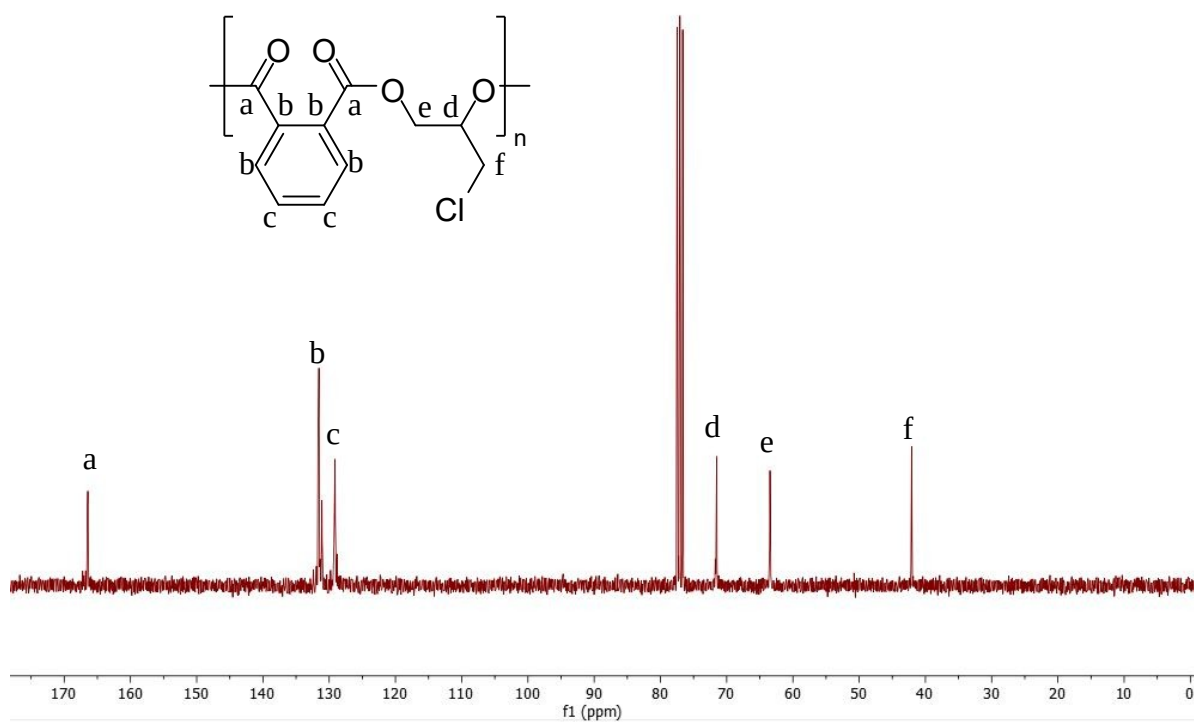
CHO-IA copolymer GPC:



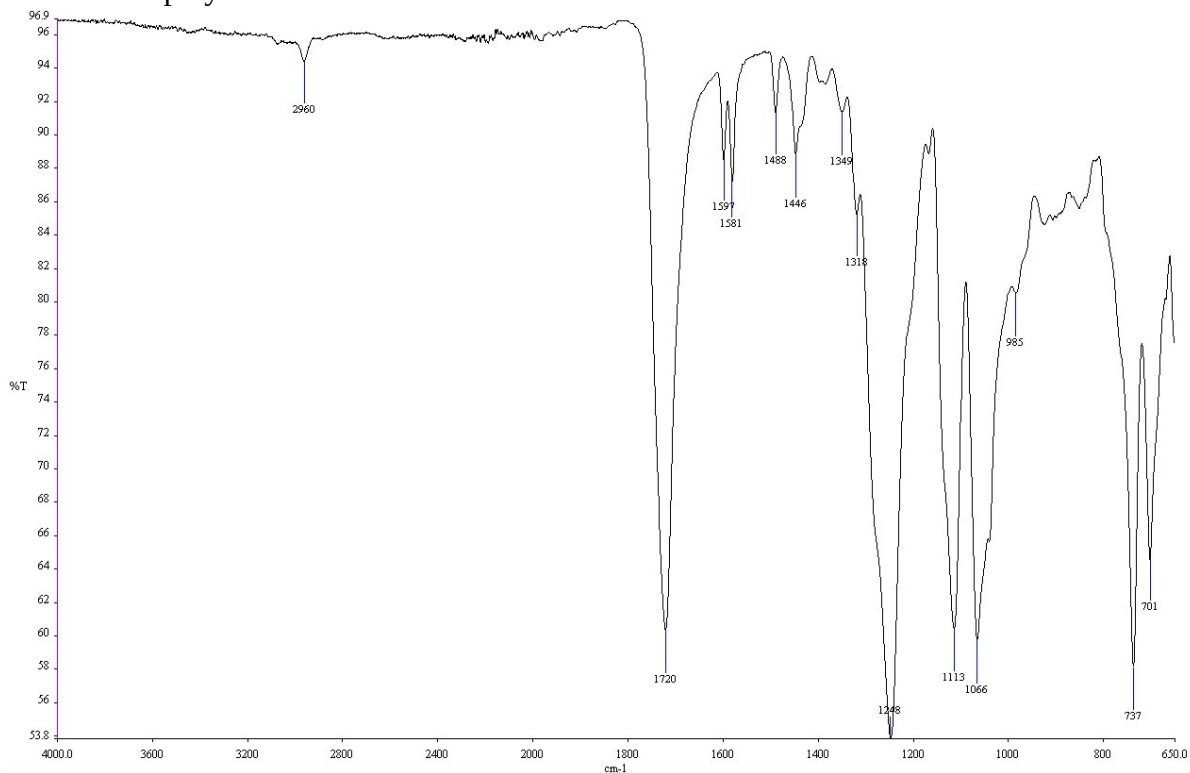
ECH-PA copolymer ^1H NMR



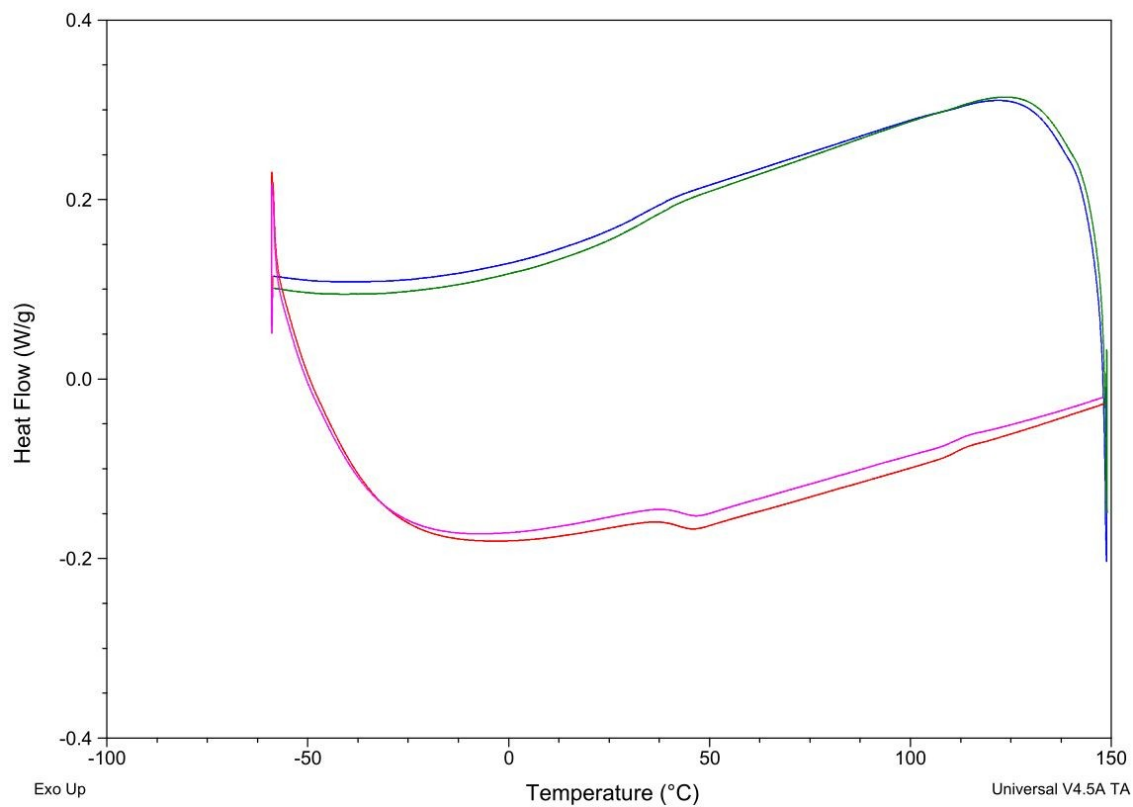
ECH-PA copolymer ^{13}C NMR:



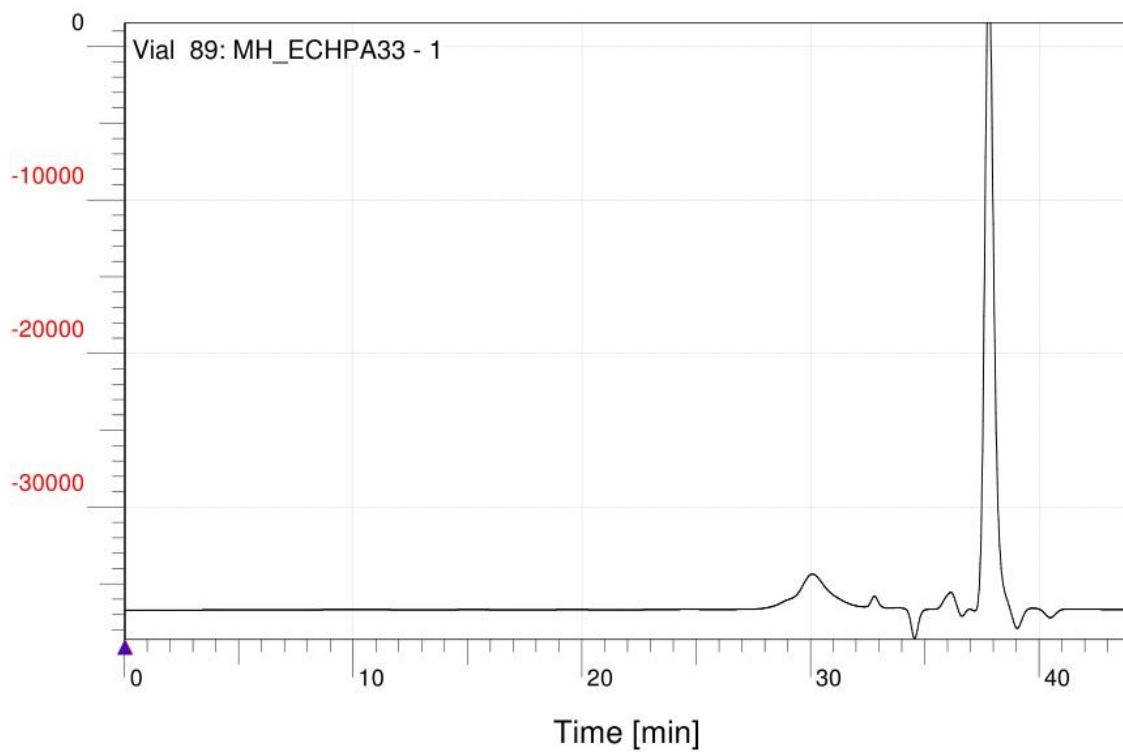
ECH-PA copolymer IR:



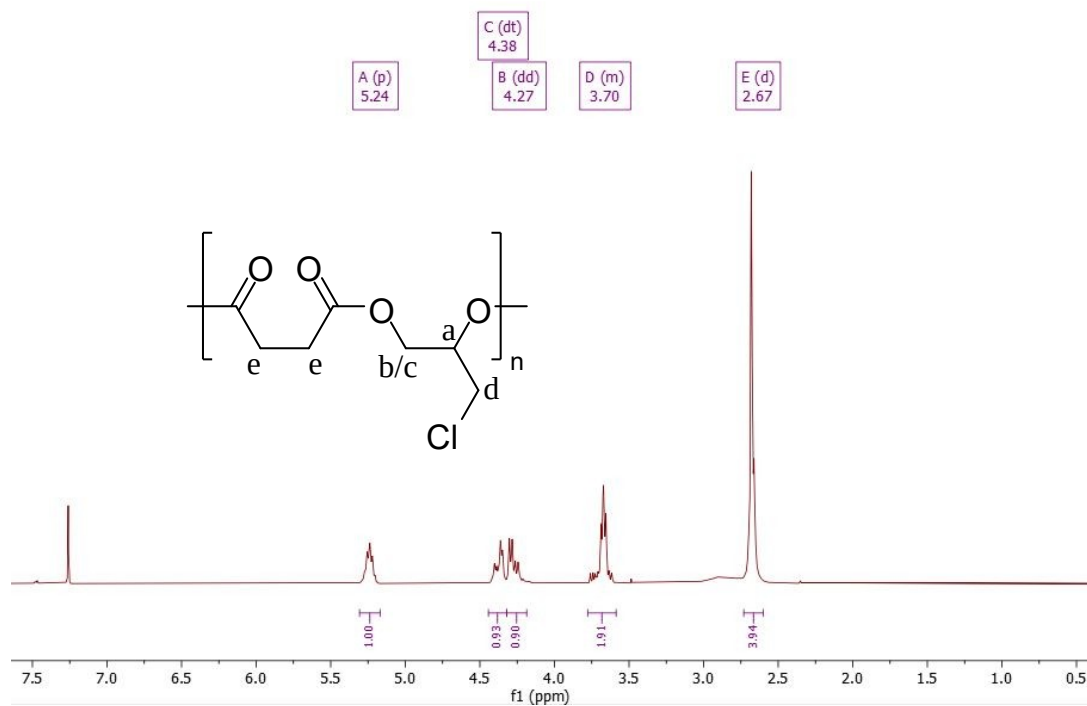
ECH-PA copolymer DSC:



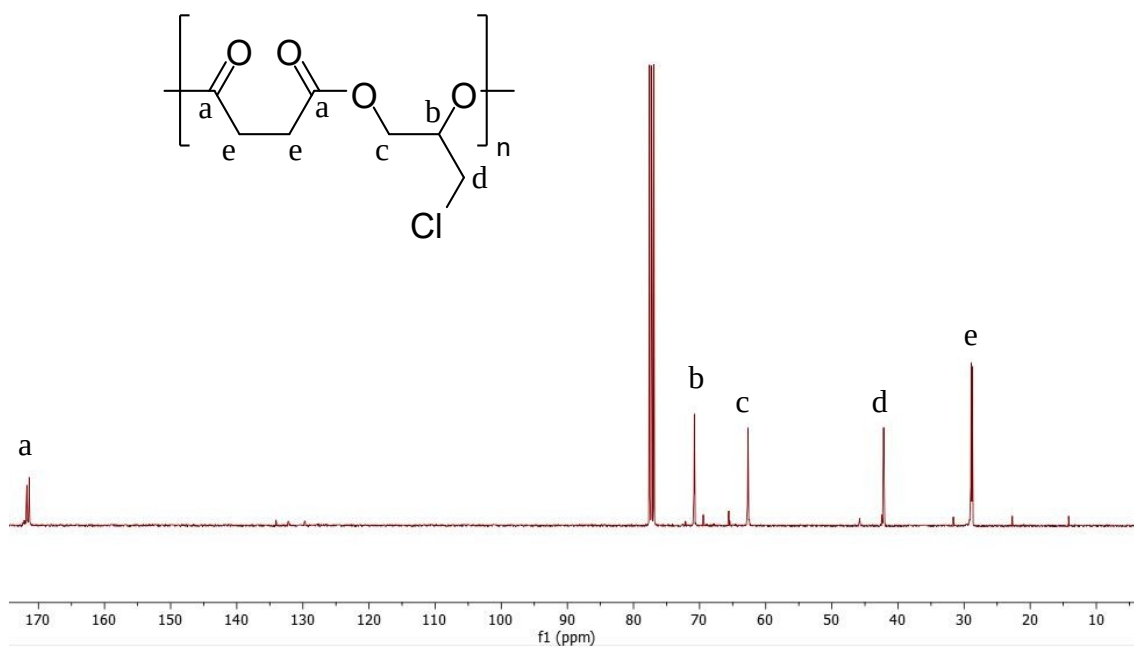
ECH-PA copolymer GPC:



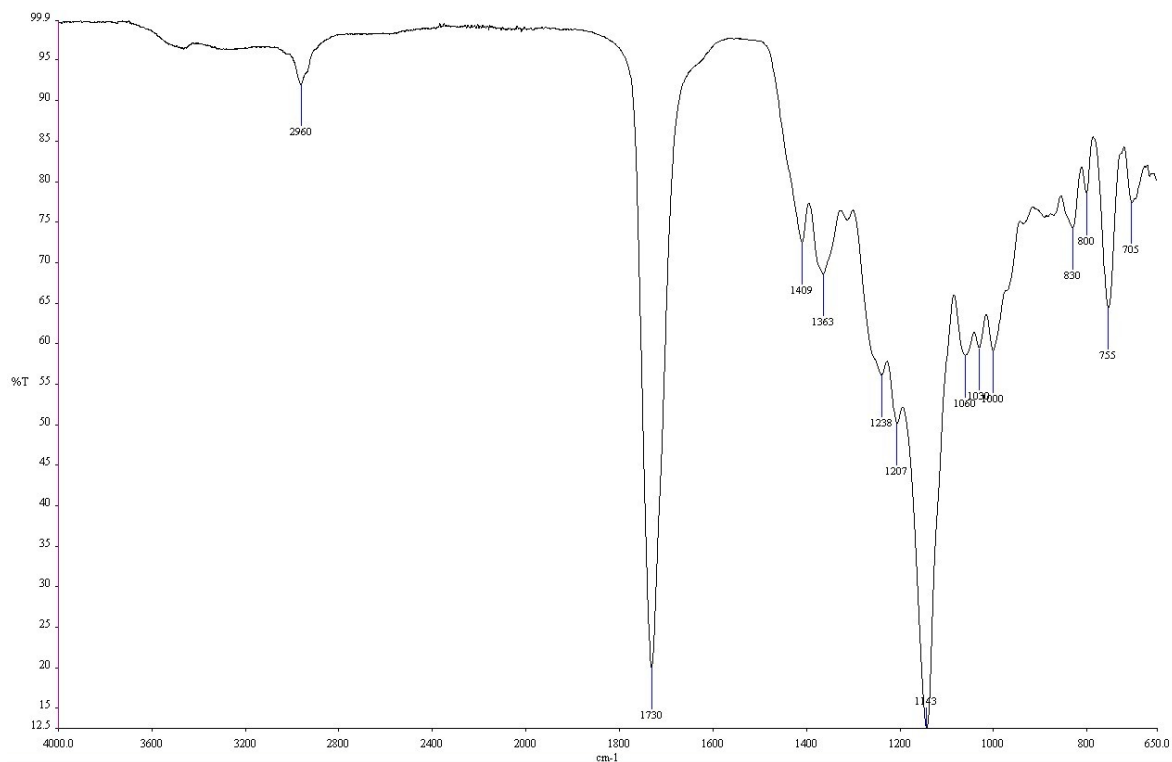
ECH-SA copolymer ^1H NMR:



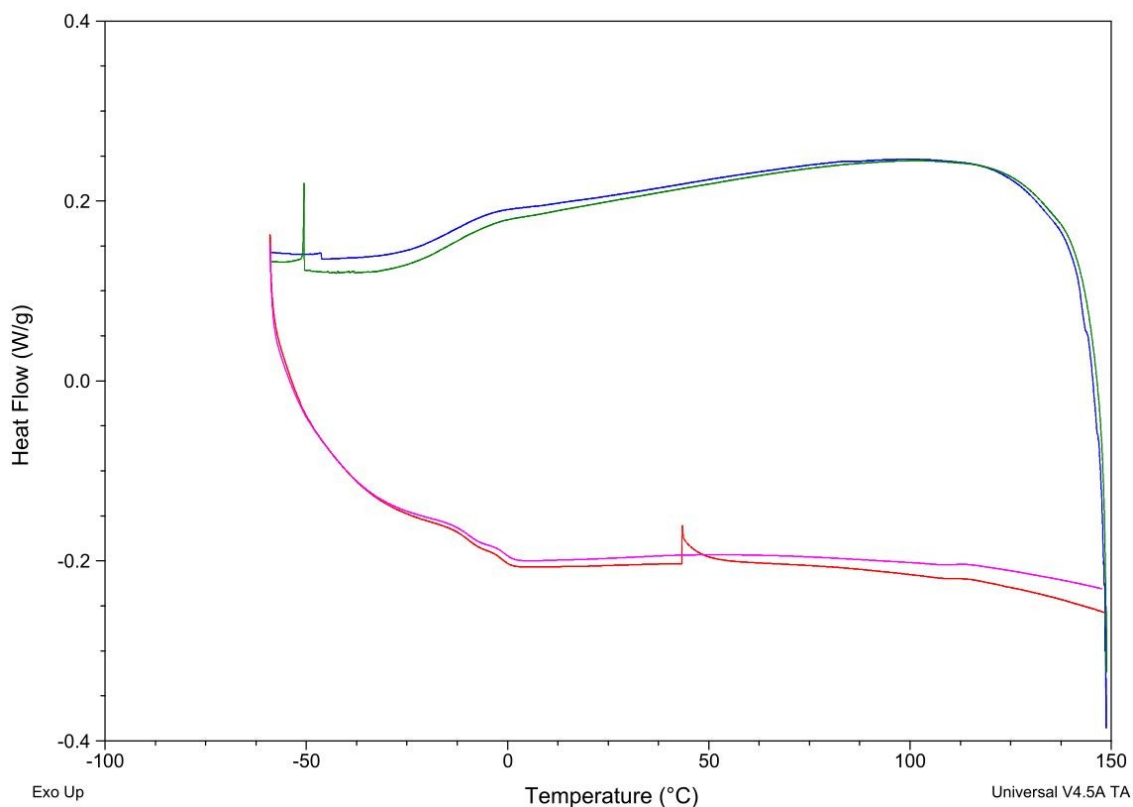
ECH-SA copolymer ^{13}C NMR:



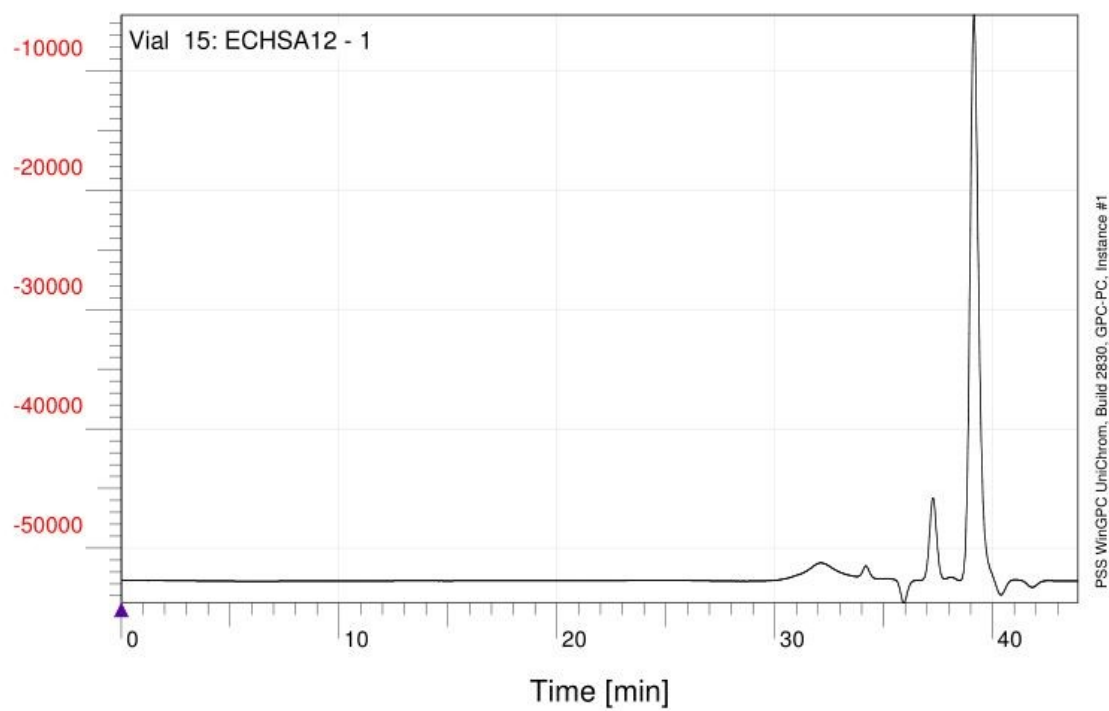
ECH-SA copolymer IR:



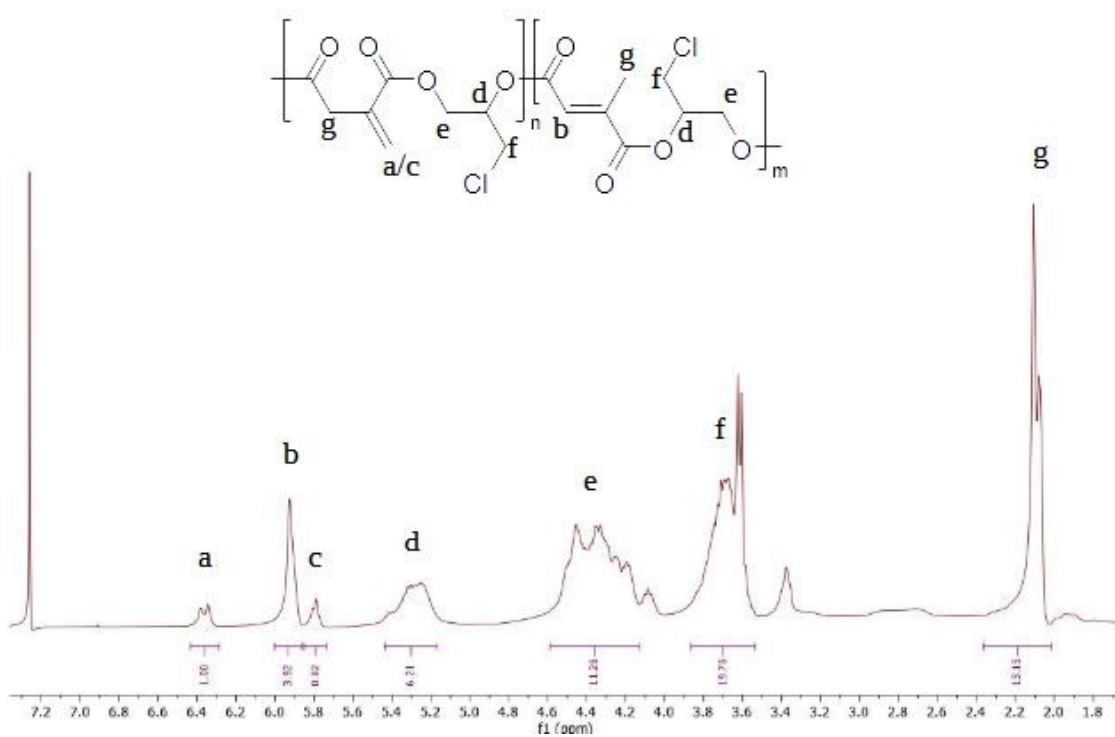
ECH-SA copolymer DSC:



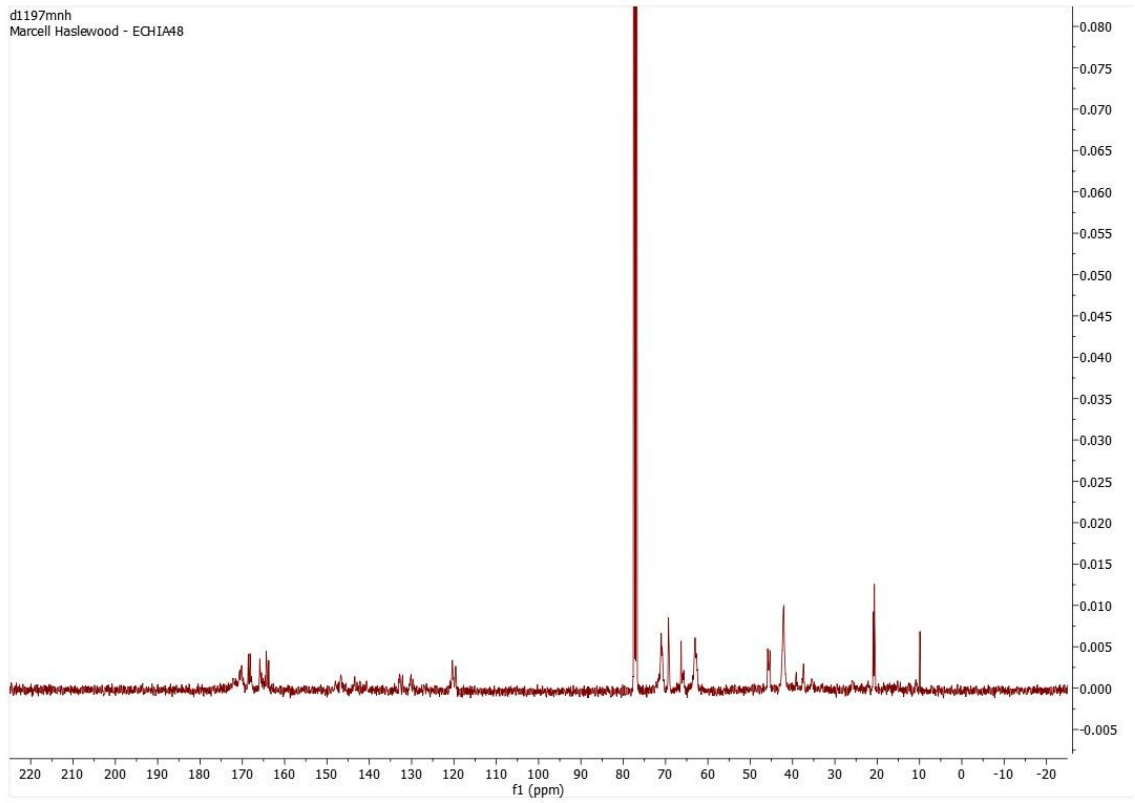
ECH-SA copolymer GPC:



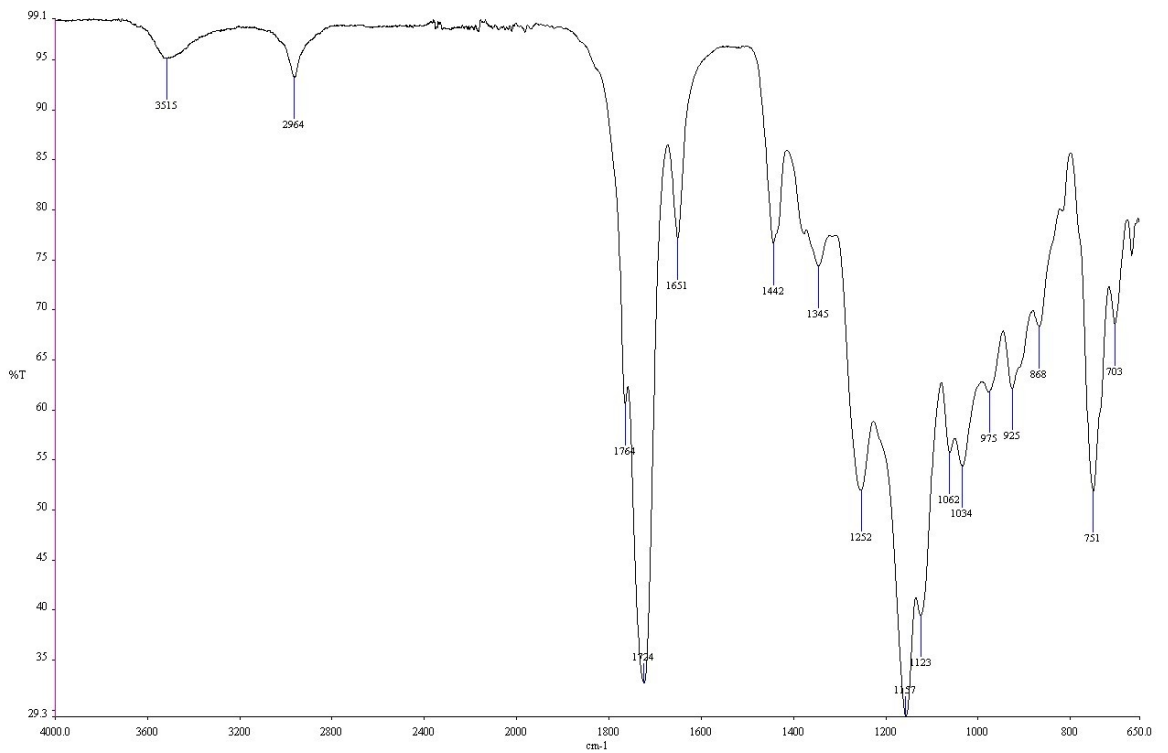
ECH-IA copolymer ^1H NMR:



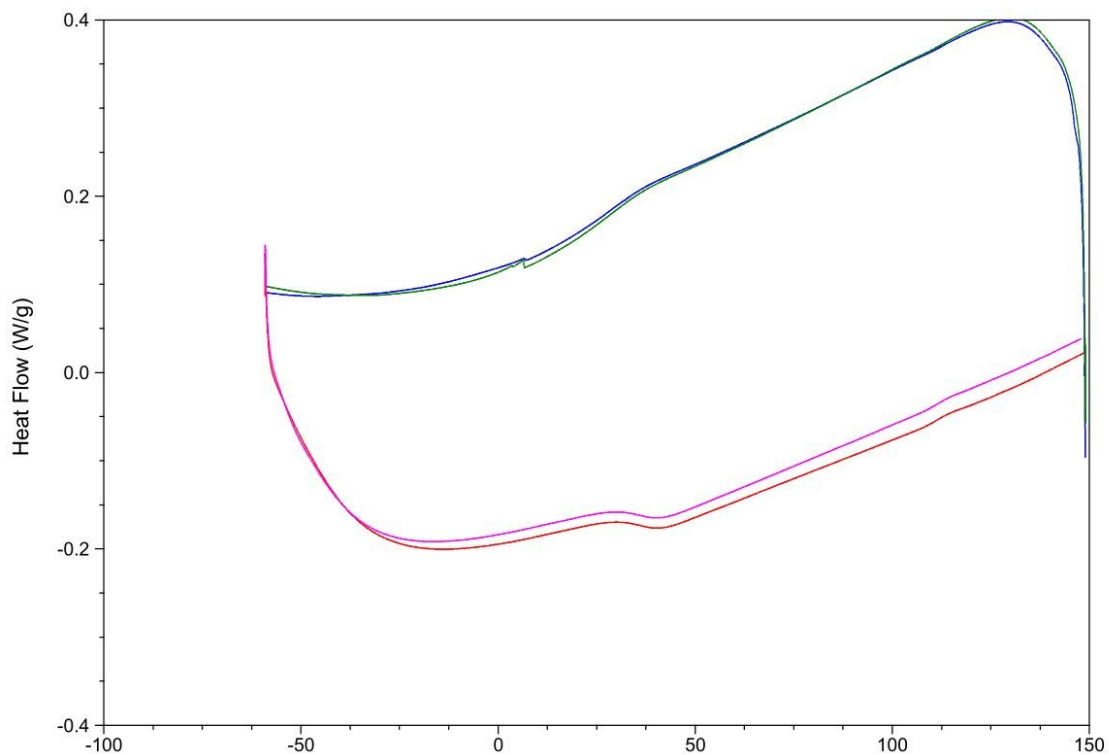
ECH-IA copolymer ^{13}C NMR:



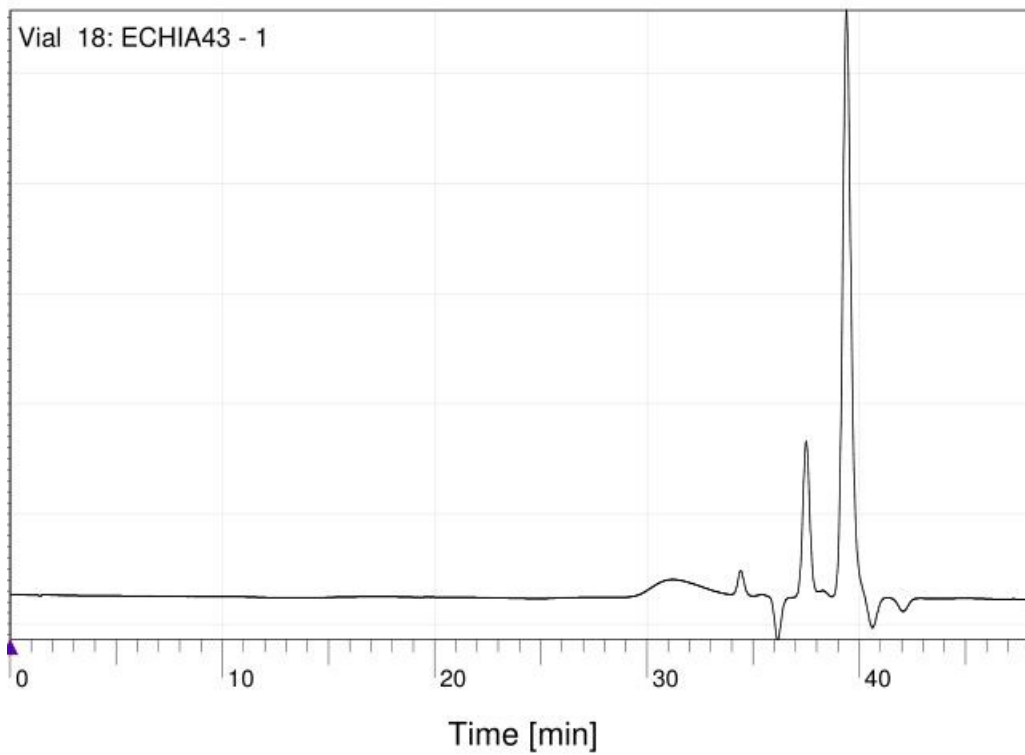
ECH-IA copolymer IR:



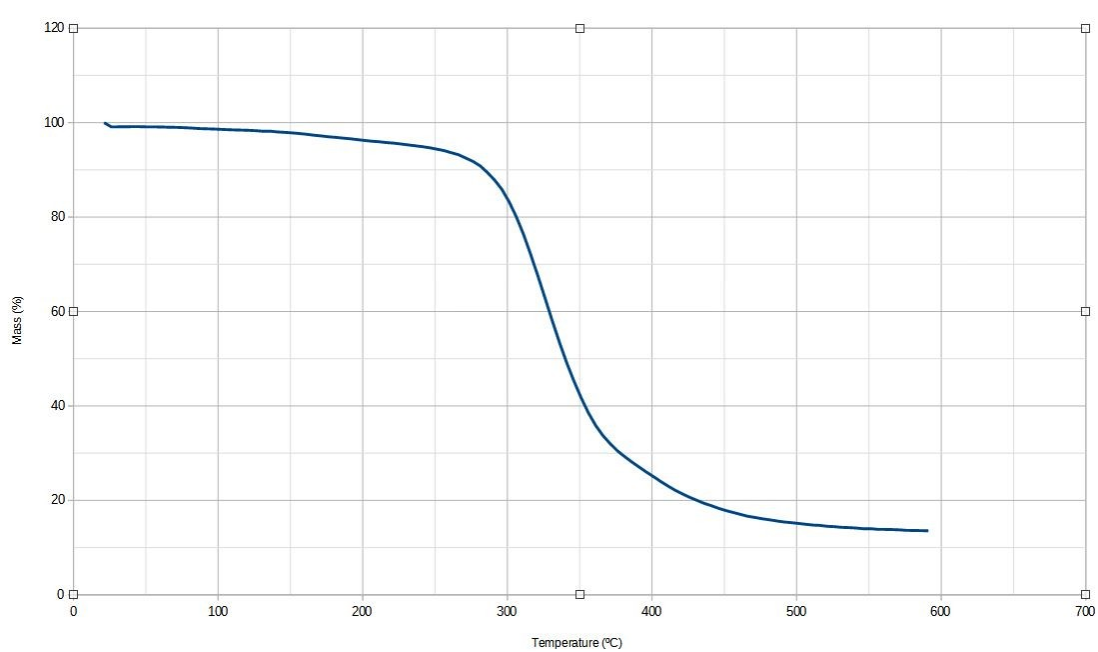
ECH-IA copolymer DSC:



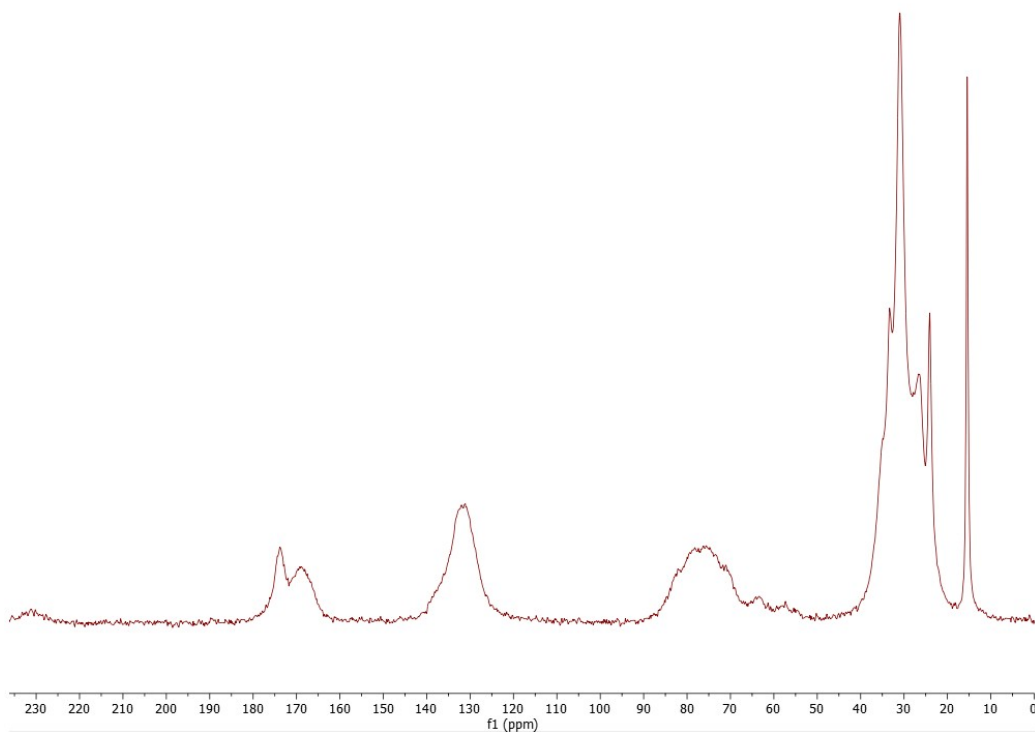
ECH-IA copolymer GPC:



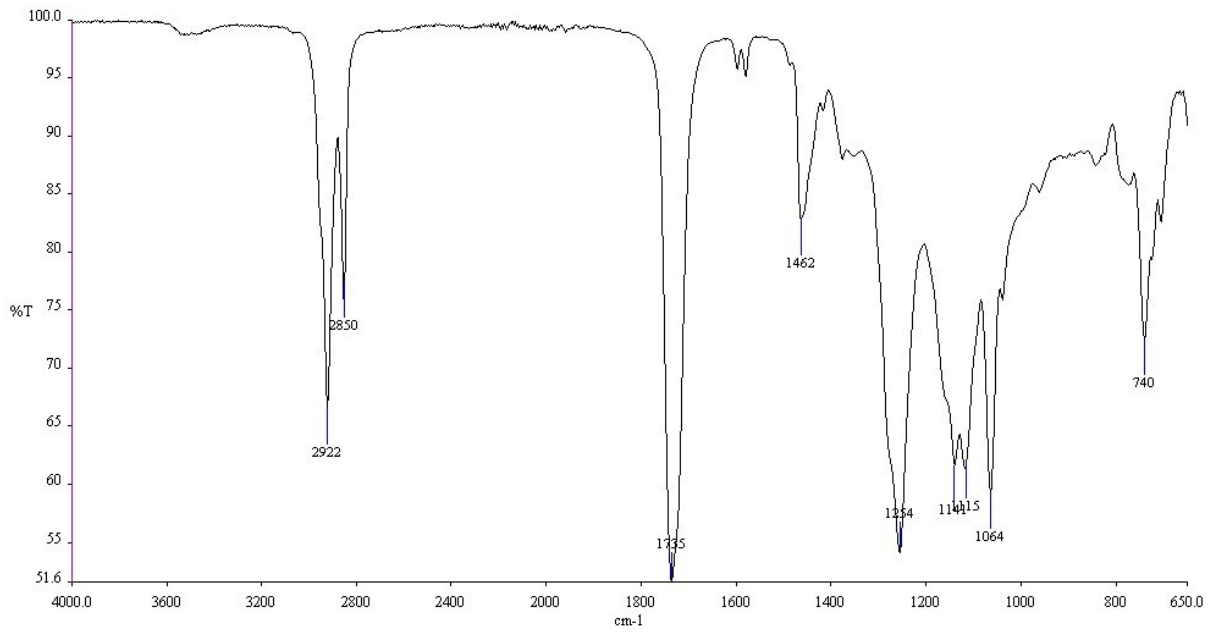
ECH-IA copolymer TGA:



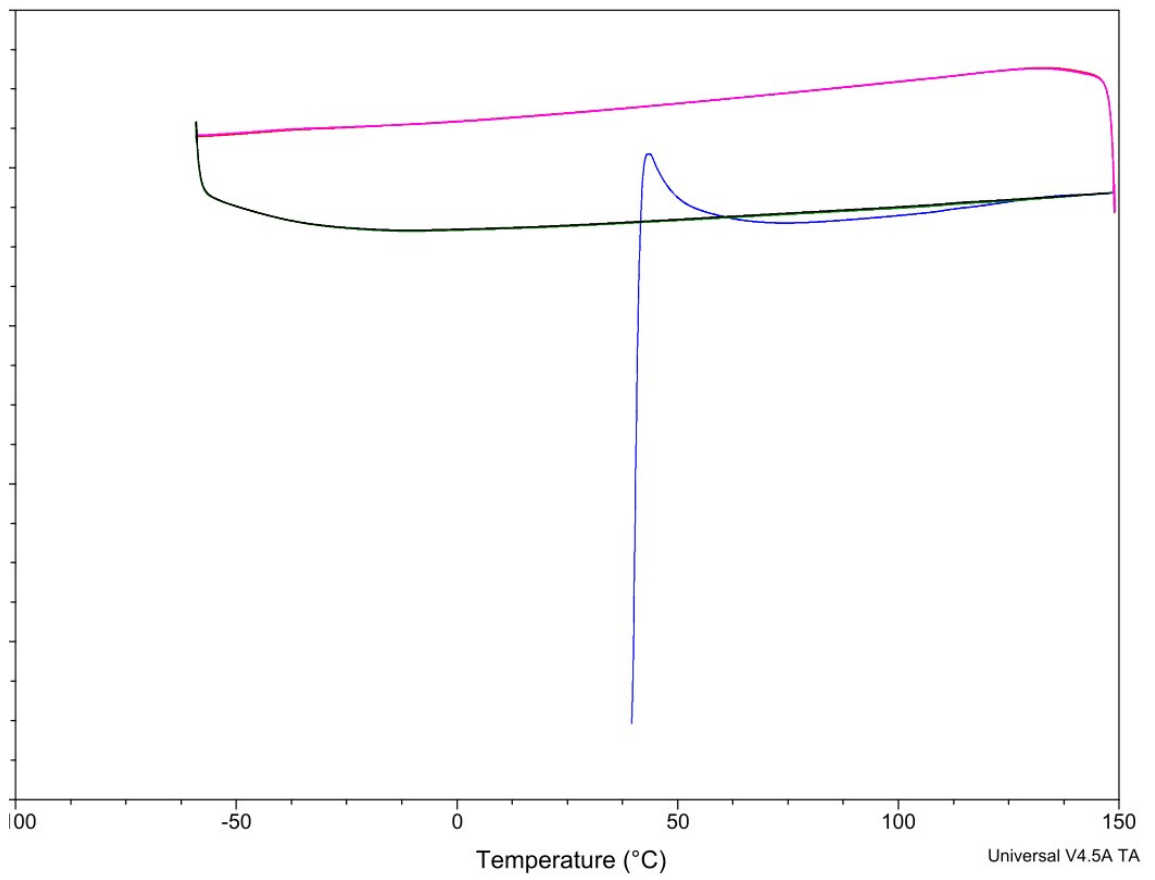
BME-PA copolymer solid state ^{13}C NMR:



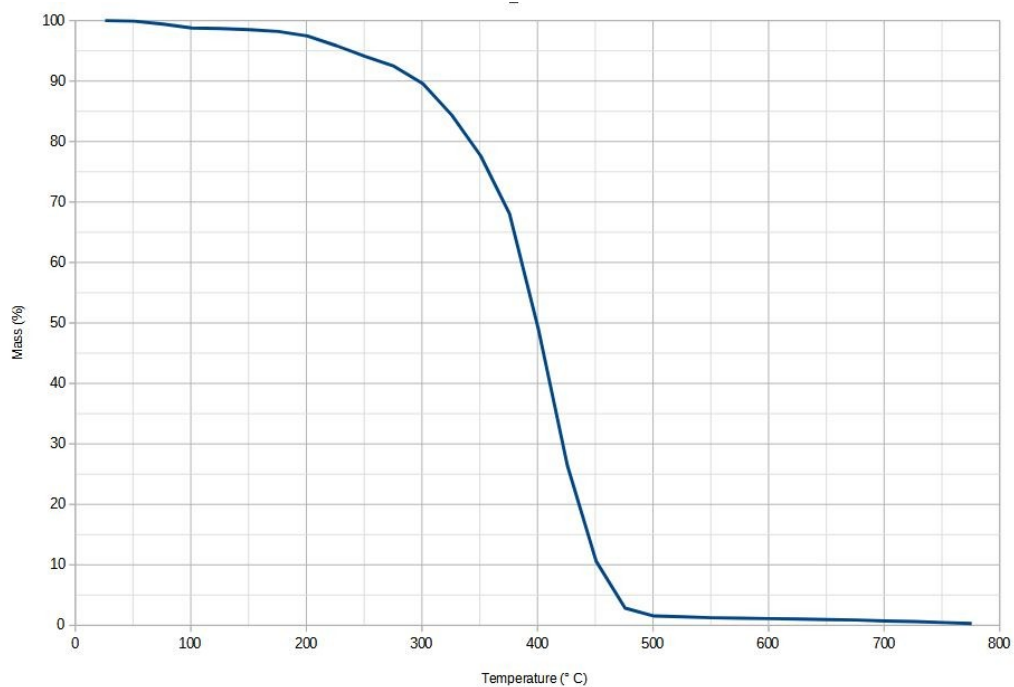
BME-PA copolymer IR



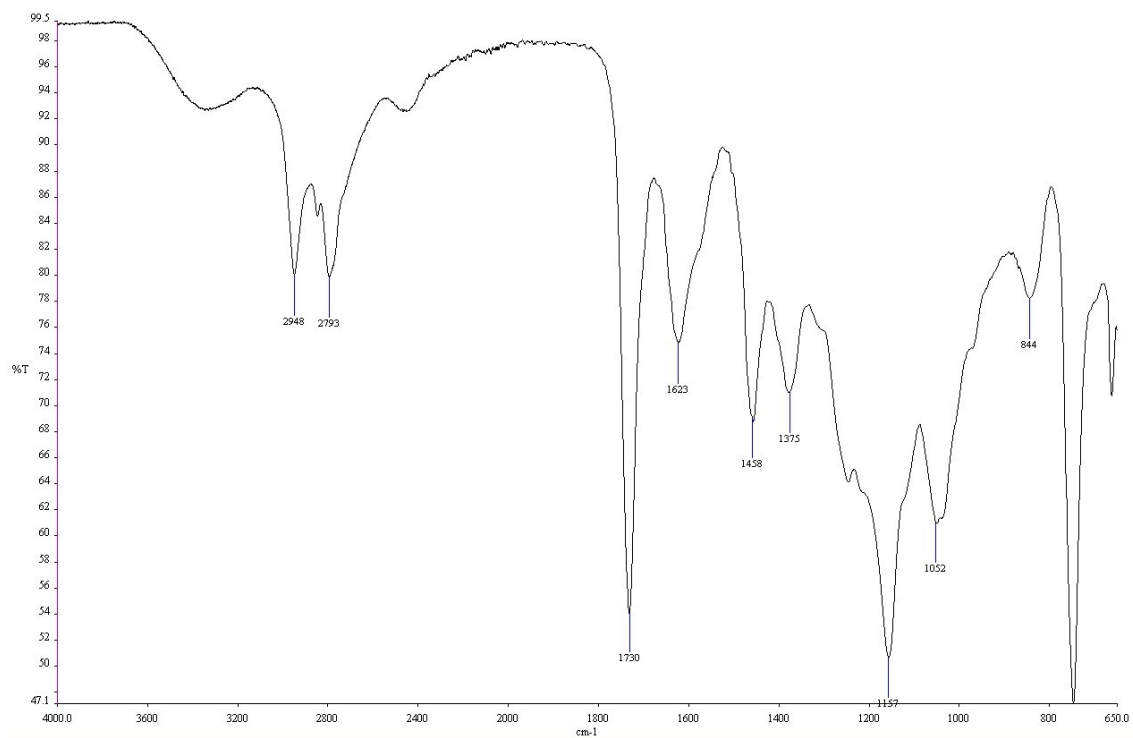
BME-PA copolymer DSC



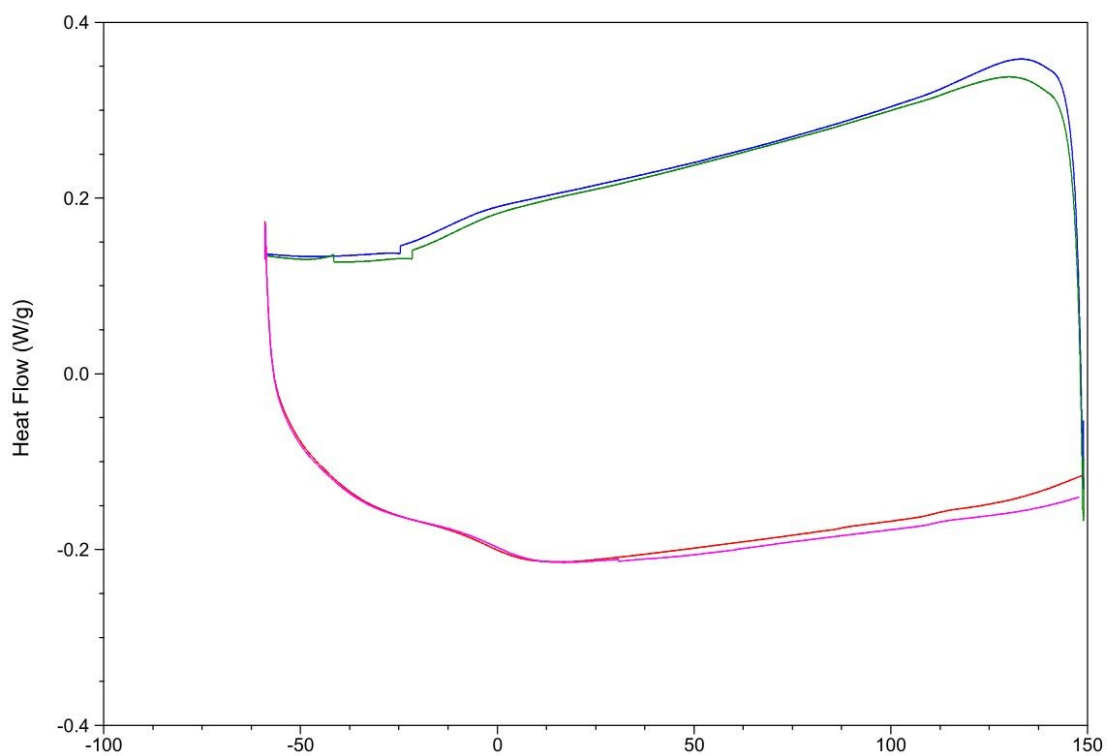
BME-PA copolymer TGA:



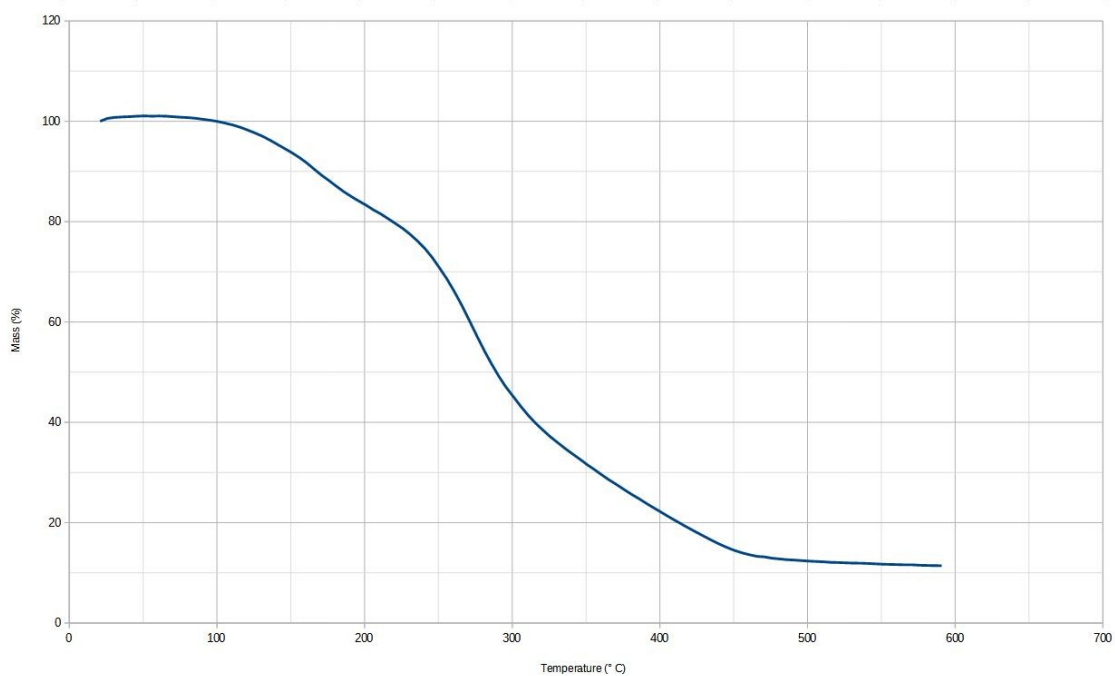
MMAPA cross-linked material – IR:



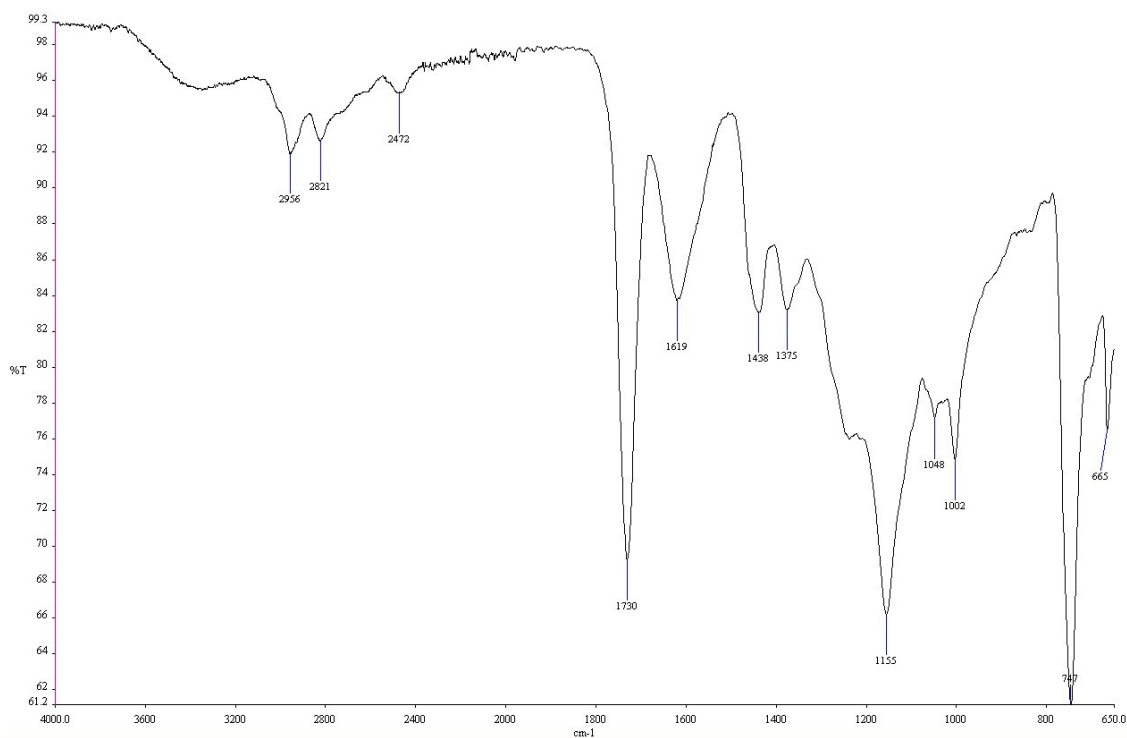
MMAPA cross-linked material – DSC:



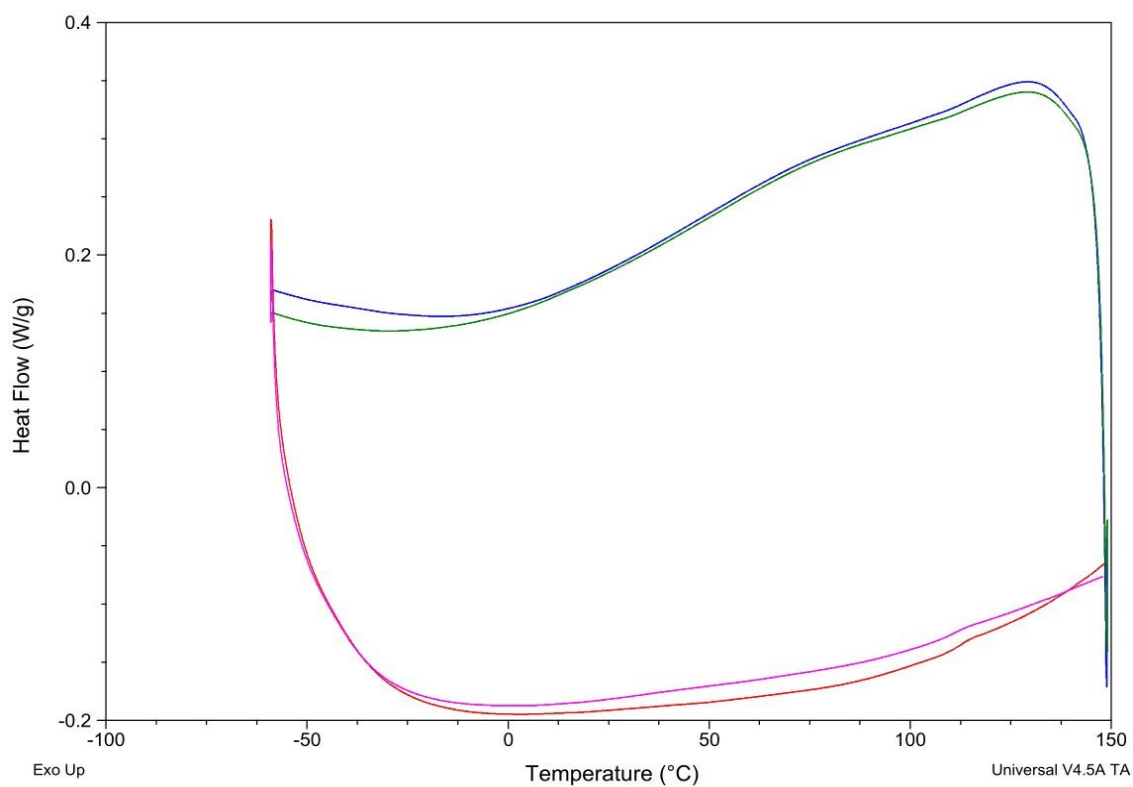
MMAPA cross-linked material – TGA:



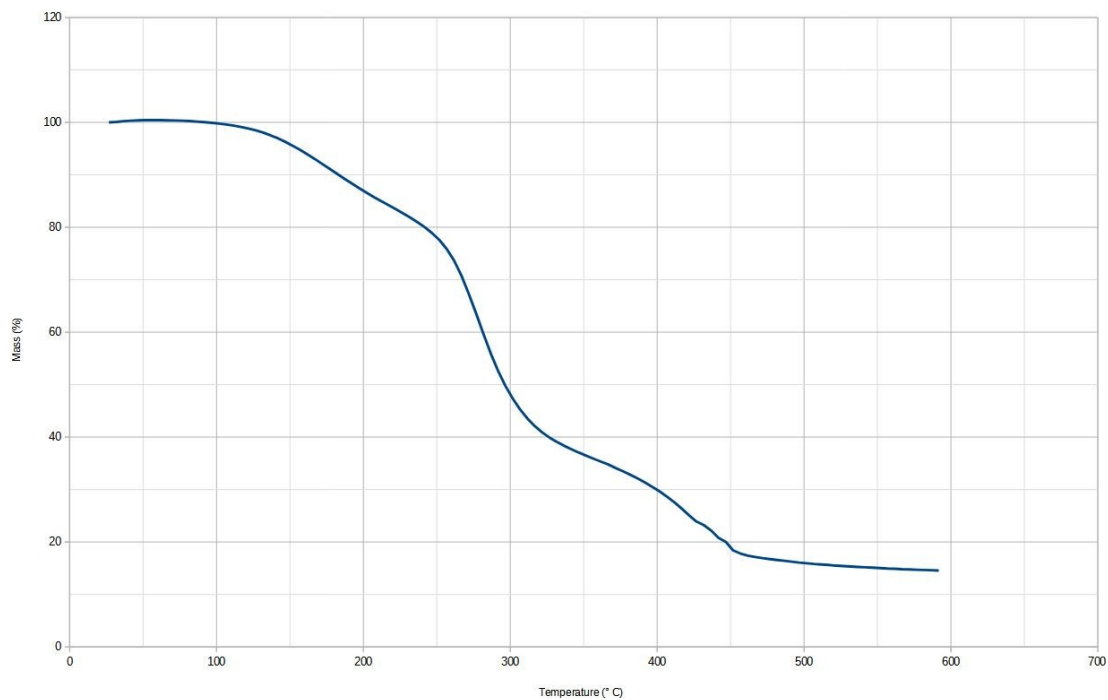
Piperazine cross-linked material – IR:



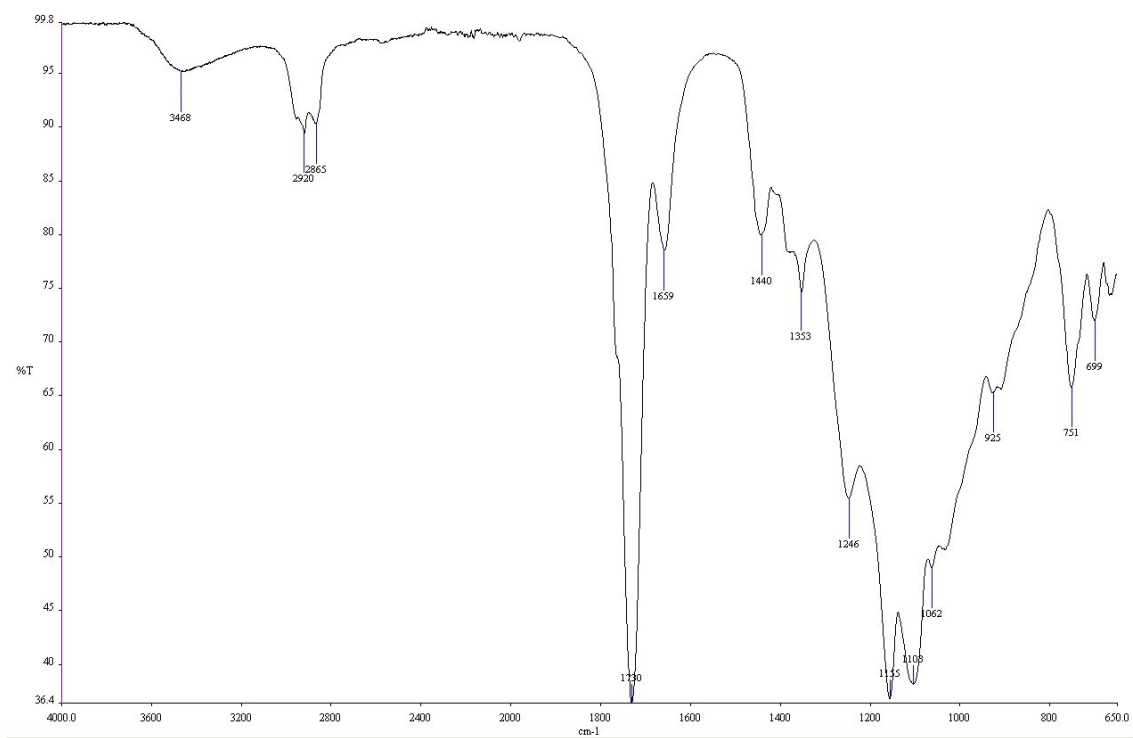
Piperazine cross-linked material – DSC:



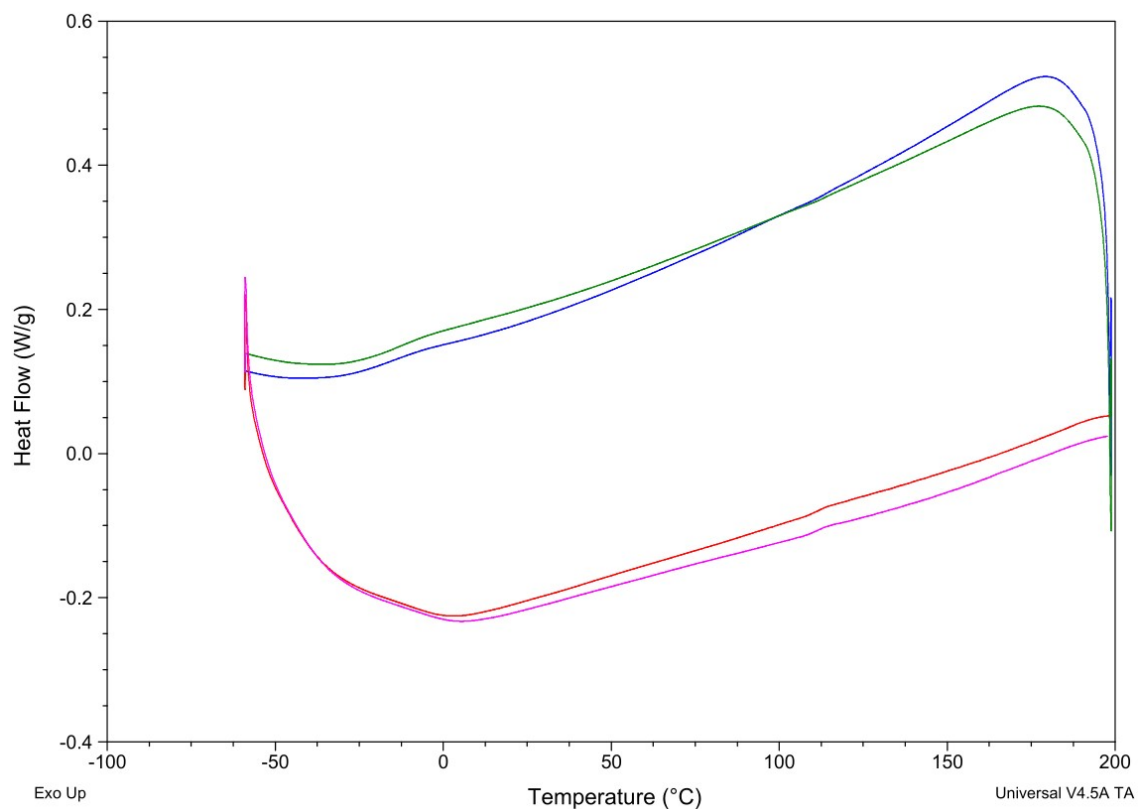
Piperazine cross-linked material – TGA:



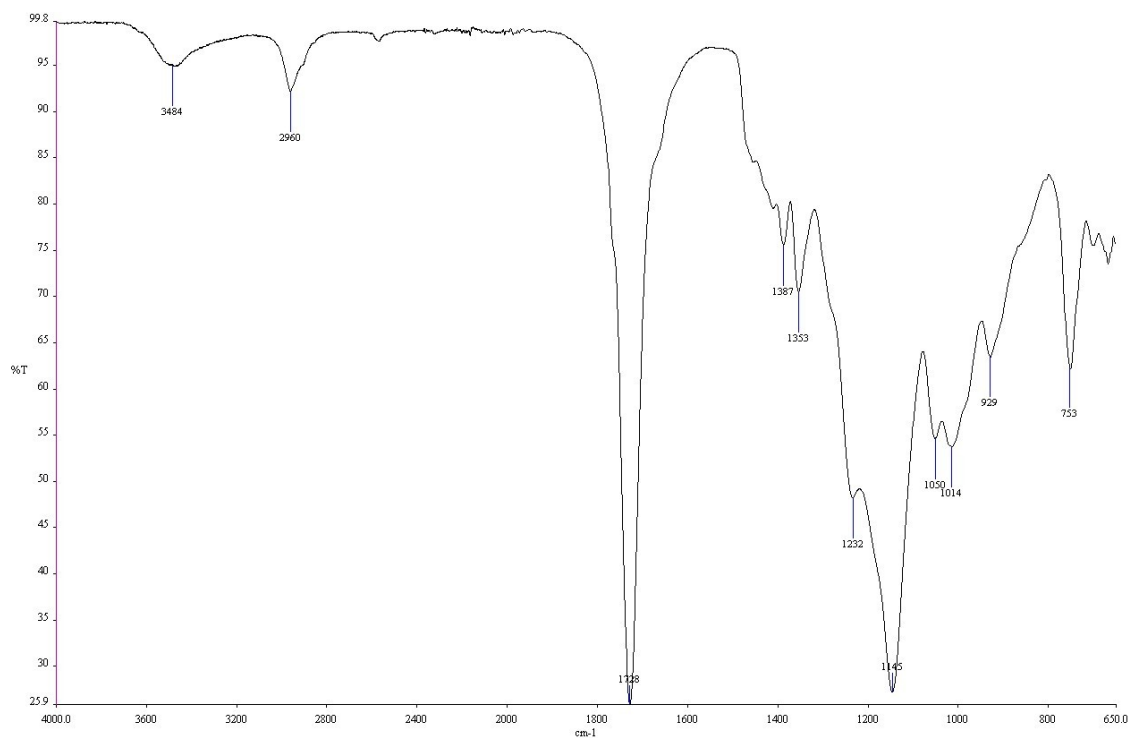
EDDET cross-linked material – IR:



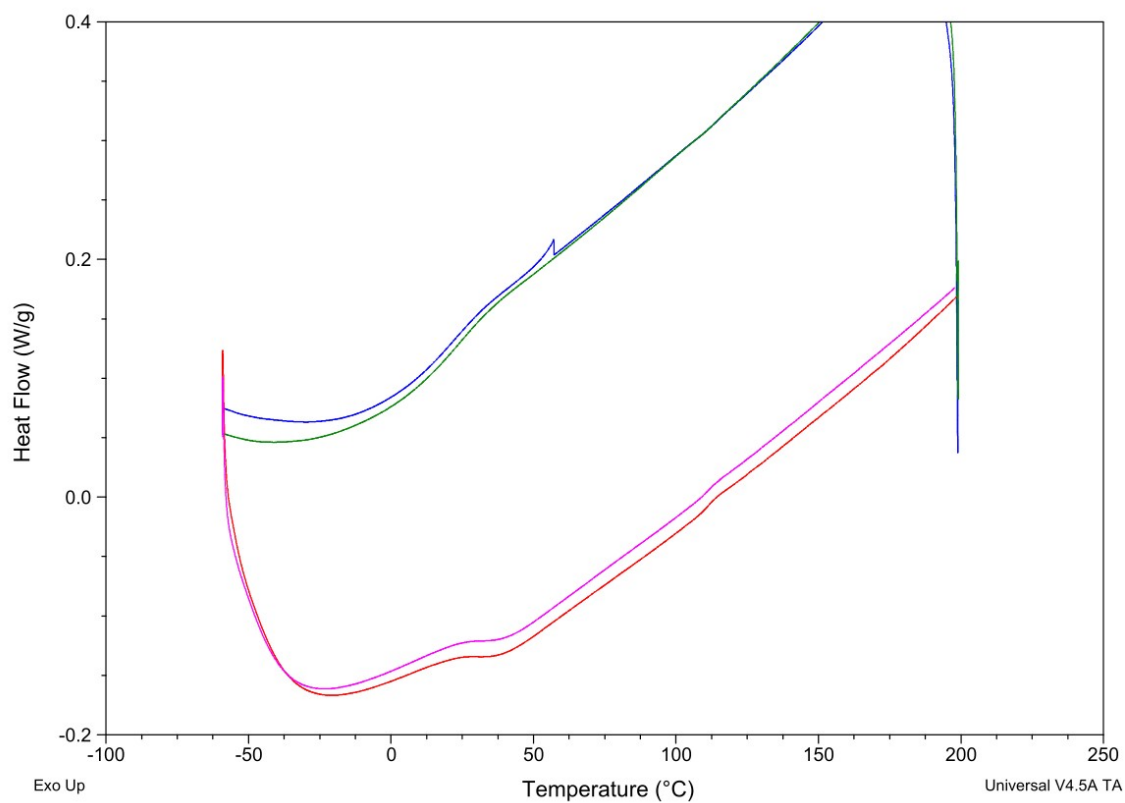
EDDET cross-linked material – DSC:



PETMP cross-linked material – IR:



PETMP cross-linked material – DSC:



PETMP cross-linked material – TGA:

